ELSEVIER

Earth-Science Reviews 53 (2001) 35–93

EARTH-SCIENCE REVIEWS

www.elsevier.com/locate/earscirev

The geology of aluminium phosphates and sulphates of the alunite group minerals: a review

Harald G. Dill *

Bundesanstalt für Geowissenschaften und Rohstoffe, P.O. Box 510153, D-30631 Hannover, Germany

Accepted 24 October 2000

Abstract

Aluminium phosphates and sulphates of the alunite supergroup (APS minerals) occur in a wide range of environments of formation covering the metamorphic, igneous and sedimentary realms. Supergene processes, including mineral dressing and dumping when sulphide ores are mined, as well as hypogene alteration are also responsible for the precipitation of APS minerals. In these environments, complex solid solution series (s.s.s.) can form. The general formula of these alunite minerals is $AB_3(XO_4)_2(OH)_6$, where A is a large cation (Na, U, K, Ag, NH_4, Pb, Ca, Ba, Sr, REE). B sites are occupied by cations of the elements Al, Fe, Cu and Zn. In nature, the anion $(XO_4)^{x-}$ is dominated by P and S. Mineral dressing and identification of APS minerals often needs a combination of highly sophisticated measures including Atterberg settling methods, XRD, DTA, TGA, TEM-EDX, SEM, EMPA and XRF.

In sedimentary rocks APS minerals occur in various rocks and environments of deposition: calcareous, phosphorite-bearing, argillaceous–carbonaceous, arenaceous, coal-bearing environments, in soils and paleosols, in saprolite (bauxites, laterites) and in calcareous–argillaceous sequences hosting Carlin-type SHDG deposits.

In igneous rocks, APS minerals may be encountered mainly in acidic through intermediate pyroclastic, volcanic and subvolcanic rocks. They occur in barren volcanic rocks and porphyry-type intrusions that have sparked epithermal Au–Ag-base metal deposits, Au–Sb mineralization, APS-bearing argillite and alunite deposits in their immediate surroundings. Granitic and pegmatitic rocks are rarely host of supergene APS mineralization. During low-grade stage regional metamorphism, peraluminous parent rocks originating from a sedimentary or igneous protolith may also give rise to APS mineralization.

Peraluminous parent rocks enriched in S and/or P are a prerequisite for the formation of APS minerals that are stable up to a temperature of 400°C at moderately high fluid pressure of up to 1 kbar. The various APS mineralizations in nature occur in three zones; a fourth zone may be singled out when the enrichment of APS compounds in waste dumps, in acid mine drainage and during alum production is considered as part of the story.

Zone I encompasses APS mineralization observed in metamorphic rocks of lowermost greenschist facies and igneous rocks that have undergone advanced argillic alteration with or without hydrothermal ore and non-metal mineralizations. Zone II following vertically upward in the earth crust is characterised by steam-heated, connate water- and ground water-related APS mineralization. This sort of APS mineralization forms close to the boundary between the vadose and phreatic hydraulic

* Tel.: +49-511-643-0; fax: +49-643-2686.
E-mail address: dill@bgr.de (H.G. Dill).

PII: S0012-8252(00)00035-0

stockwork. The overlying zone III is confined to the topmost part of the vadose or infiltration zone. Its mineralization originated from meteoric waters and may be called supergene in the strict sense. Results obtained from the study of this kind of mineralization can directly be applied to artificial accumulation of APS compounds at the present-day surface.

A combination of chemical measures such as S–O–H isotopes and REE variation together with experimentally based mineralogical data may be instrumental in the distinction of supergene and hypogene APS mineralization. This set of data may also assist in the assignment of APS mineralization either to hydrothermal magmatic or to steam-heated acid sulphate mineralizations. The K-bearing end members of the APS s.s.s. have proven to be an efficient tool to determine the age of formation of magmatic, weathering, diagenetic and alteration processes. APS minerals, however, can locally provide much more information to the origin of host and parent rocks than the rock-forming minerals themselves, which make up the host rocks of APS mineralization.

Keywords: alunite supergroup; sediments; igneous rocks; metamorphic rocks; geology; mineralogy

1. Introduction

Aluminium-phosphate–sulphate minerals of the alunite supergroup (APS minerals) do not belong to the generally accepted suite of rock-forming minerals, which geologists encounter when studying metamorphic, igneous and sedimentological processes. The various members of this sort of minerals can hardly be identified by geologists who carry out their field work only armed with a hand lens or a hammer

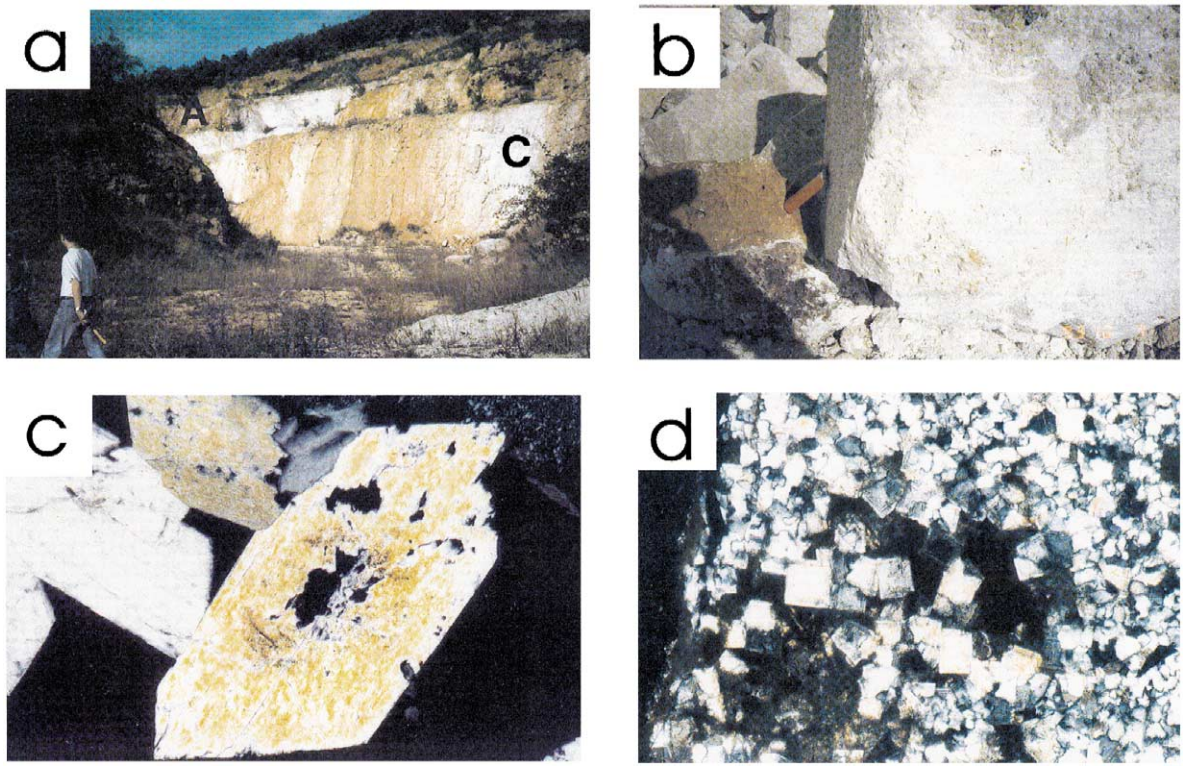

Fig. 1. Alunite at various scales: (a) Open cast mine at Mad Kiralhegy, Hungary exposes the various zones of hydrothermal mineralization: (A) silica-alunite zone (C) smectite–kaolinite zone. The steeply dipping boundaries are accentuated by coatings of hydrohematite and goethite originating from supergene alteration of Fe sulphides, (b) fresh (right) and altered (left) boulders of alunite ore from the above mine, (c) micrograph of thin sections from Mad Kiral Hegy, Hungary, showing an open space filling of individual crystals of alunite growing in a cavity of massive alunite—crossed polars, XX size 100 μm, (d) micrograph of thin sections from Cosuño, Bolivia, showing pseudocubic crystals of alunite–crossed polars, XX size 30 μm.

as the outward appearance of this minerals is often not very much distinctive (Fig. 1) (Dill, 1996).

The APS minerals contain more than 40 mineral species (Jambor, 1999). Their attribution to various groups and their naming is still under debate as it is the case with the type of nomenclature scheme (Strunz and Tennyson, 1982; Scott, 1987a; Jambor, 1999). Such mineralogical classification schemes in their attempt to accommodate the structural variation of mineral groups used to cover all species irrespective of their abundance in nature, whether they form deposits on their own or occur only sporadically among other rock-forming minerals. Therefore, this review focused on the origin and occurrence of APS minerals in various lithologies takes a somewhat different approach based on a simple chemical classification scheme (Table 1).

APS minerals occur in the metamorphic, igneous and sedimentary realms (Stoffregen and Alpers, 1987). Supergene as well as hypogene processes are held responsible for the precipitation of APS minerals that form complex solid solution series (s.s.s.) (for details see Section 2) encompassing prevalently earth alkaline and alkaline elements as cations and phosphate-, sulphate- and arsenate complexes as anions (Strunz and Tennyson, 1982; Scott, 1987a; Jambor, 1999). The chemical composition of APS minerals is controlled by the physico-chemical formation conditions (Eh, pH, activities) (Herold, 1987; Stoffregen et al., 1990; Stoffregen et al., 1994).

Stable isotope data can be extracted from hydrogen of the hydroxide, oxygen and sulphur from the sulphate complexes of APS minerals (Wasserman et al., 1990). Radiometric age data can be determined from K and Ar in the K-bearing end members of the APS s.s.s. (Morrison and Parry, 1988; Bird et al., 1990; Sillitoe and McKee, 1996; Gilg and Frei, 1997; Polyak et al., 1998). The APS minerals offer the potential clue to disentangle the geochronological evolution of an environment of formation and help to constrain the physico-chemical formation conditions.

In the following paragraphs, emphasis is placed on the environment of formation of APS minerals. Results obtained from such geological investigations may be useful in the field of extractive geology (APS minerals as ore guide vs. ore proper) and environmental geology (e.g. ground water pollution).

2. APS minerals from the crystallographic and mineralogical point of view

APS minerals are members of the alunite–jarosite family. The general formula of the APS minerals, the name has been coined based on the major elements in the supergroup, is $AB_3(XO_4)_2(OH)_6$, where A is a large cation (Na, U, K, Ag, NH_4, Pb, Ca, Ba, Sr, REE) in 12-fold coordination. B sites are occupied by cations of the elements Al, Fe, Cu and Zn in octahedral coordination. In nature, the anion $(XO_4)^{x-}$ is dominated by P and S (Strunz and Tennyson, 1982; Scott, 1987a,b). In the XO_4 complex P^{5+} may also be substituted for by the bigger As^{5+}. Locally, CO_3^{2-}, SbO_4^{3-}, CrO_4^{2-} and SiO_4^{2-} may replace the more common phosphate and sulphate complexes in the APS minerals (Scott, 1987a,b). APS minerals like the widespread crandallite (Table 1) are built from sheets of aluminium octahedra, each of them sharing four corners with other octahedra. In this way, large hexagonal and small trigonal rings perpendicular to the *c*-axis are formed (Radoslovich and Slade, 1980). The metal cations are located in a large cavity formed by a hexagonal ring with six OH^- groups.

The wide range of elements accommodated in the lattice of alunite-type minerals makes this s.s.s. very attractive for mineralogist and mineral hunters alike in search of rare and new minerals. The reader is referred among others to Hak et al. (1969), Pring et al. (1995), Birch et al. (1992), Li et al. (1992) and the textbook by Strunz and Tennyson (1982).

In nature, however, only some minerals out of the broad spectrum of APS minerals play a major part in rock- and ore-forming processes (Table 1). A complete solid solution between Al and Fe in B sites may be expected in the more phosphate-rich members of these APS minerals. There is, however, little evidence for this s.s.s. in nature (Rattray et al., 1996). A separation into alunite and jarosite supergroups, according to the greater Al or Fe occupancy, is considered appropriate (Scott, 1987a,b). Following the proposals by Strunz and Tennyson (1982), APS minerals may be subdivided into the alunite-, woodhouseite-, crandallite- and wardite-s.s.s.. This approach to subdivide this group of minerals may not fully accord with the present-day mineralogical–

Table 1
Classification scheme and formulae of aluminium-phosphate–sulphate (APS), aluminium-phosphate (AP), aluminium-sulphate (AS) and iron-phosphate minerals (FS) referred to in the text

Most common APS minerals		
Alunite series		
Alunite	$KAl_3(SO_4)_2(OH)_6$	Strunz (1970)
Natroalunite	$NaAl_3(SO_4)_2(OH)_6$	Strunz (1970)
Natrojarosite	$NaFe_3(SO_4)_2(OH)_6$	Strunz (1970)
Jarosite	$KFe_3(SO_4)_2(OH)_6$	Michel and Van Everding (1987)
Ammoniumjarosite	$(NH_4)Fe_3(SO_4)_2(OH)_6$	Strunz (1970)
Hydronium alunite	$(H_3O)Al_3(SO_4)_2(OH)_6$	Strunz (1970)
Minamiite	$Ca_{0.5}Al_3(SO_4)_2(OH)_6$	Ossaka et al. (1982, 1987)
Woodhouseite series		
Woodhouseite	$CaAl_3(PO_4/SO_4)(OH)_6$	Pabst (1947)
Svanbergite	$SrAl_3(PO_4/SO_4)(OH)_6$	Switzer (1949)
Hinsdalite	$PbAl_3(PO_4/SO_4)(OH)_6$	Scott (1990)
Corkite	$PbFe(PO_4/SO_4)(OH)_6$	Strunz (1970)
Kemmlitzite	$SrAl_3(AsO_4/SO_4)(OH)_6$	Hak et al. (1969)
Crandallite series		
Crandallite	$CaHAl(PO_4)_2(OH)_6$	Scott (1987a,b)
Goyazite	$SrHAl_3(PO_4)_2(OH)_6$	Kato and Radoslovich (1968)
Gorceixite	$BaHAl_3(PO_4)_2(OH)_6$	Kato and Radoslovich (1968)
Plumbogummite	$PbHAl_3(PO_4)_2(OH)_6$	Palache et al. (1951)
Florencite	$(REE)Al_3(PO_4)_2(OH)_6$	Pouliot and Hofmann (1981)
Arsenocrandallite	$CaHAl_3(AsO_4)_2(OH)_6$	Walenta (1981)
Philipsbornite	$PbHAl_3(AsO_4)_2(OH)_6$	Schmetzer et al. (1982)
Dussertite	$BaHFe_3(AsO_4)_2(OH)_6$	Walenta (1966)
Segnitite	$PbHFe_3(AsO_4)_2(OH)_6$	Bird et al. (1990)
Wardite series		
Wardite	$NaAl_3(PO_4)_2(OH)_4 \cdot 2H_2O$	Strunz (1970)
Millisite	$(Na, Ca)Al_3(PO_4)_2(OH, O)_4 \cdot 2H_2O$	Strunz (1970)
Rare species of phosphate minerals referred to in the text		
Wyllieite	$Na_2Fe_2Al(PO_4)_3$	Strunz (1970)
Cacoxenite	$AlFe_{24}(OH)_{12}O_6(PO_4)_7(H_2O)_{24} \cdot 51H_2O$	Strunz (1970)
Vivianite	$Fe_3(PO_4)_2 \cdot 8H_2O$	Strunz (1970)
Beraunite	$Fe_6(OH)_5(H_2O)_4(PO_4)_4 \cdot 2H_2O$	Strunz (1970)
Montgomeryite	$Ca_4MgAl_4(PO_4)_6(OH)_4 \cdot 12H_2O$	Strunz (1970)
Souzalite	$(Al, Mg, Fe)_6Al(PO_4)_4(OH)_6 \cdot 2H_2O$	Strunz (1970)
Taranakaite	$H_6K_3Al_5(PO_4)_8 \cdot 18H_2O$	Nriagu and Moore (1984)
Turquoise	$CuAl_6(PO_4)_4(OH)_8 \cdot 4H_2O$	Nriagu and Moore (1984)
Palermonite	$(Li, Na)_2(Sr, Ca)Al_4(PO_4)_4(OH)_4$	Strunz (1970)
Lazulite	$(Mg, Fe)Al_2(PO_4)_2(OH)_2$	Strunz (1970)
Diadochite	$Fe_2(PO_4)(SO_4)(OH) \cdot 5H_2O$	Strunz (1970)
Brazilianite	$NaAl_3(PO_4)_2(OH)_4$	Strunz (1970)
Most common AP minerals referred to in the text		
Berlinite	$AlPO_4$	Strunz (1970)
Augelite	$Al_2PO_4(OH)_3$	Strunz (1970)
Variscite	$AlPO_4 \cdot 2H_2O$	Strunz (1970)
Wavellite	$Al_3(OH)_3(PO_4)_2 \cdot 5H_2O$	Strunz (1970)
Most common FS and AS minerals referred to in the text		
Melanterite	$FeSO_4 \cdot 7H_2O$	Strunz (1970)
Szomolnokite	$FeSO_4 \cdot H_2O$	Strunz (1970)

Table 1 (*continued*)

Most common APS minerals		
Most common FS and AS minerals referred to in the text		
Rhomboclase	$FeH(SO_4)_2 \cdot 4H_2O$	Strunz (1970)
Paracoquimbite	$Fe_2(SO_4)_3 \cdot 9H_2O$	Strunz (1970)
Coquimbite	$Fe_2(SO_4)_3 \cdot 9H_2O$	Strunz (1970)
Jurbanite	$AlOHSO_4$	Courchesne and Henderschot (1990)
Aluminite	$Al_2SO_4(OH)_4 \cdot 7H_2O$	Strunz (1970)
Alunogene	$Al_2(SO_4)_3 \cdot 17H_2O$	Strunz (1970)

crystallographic classification schemes but rather matches the occurrence of APS minerals in nature (Jambor, 1999).

Mineral dressing and identification of APS minerals is often difficult as APS minerals are dispersed in the matrix of rocks (Dill et al., 1995a,b,c,d, 1997a).

The powdered samples that comprise the size fractions < 2 μm, 2 to 6.3 μm, 6.3 to 20 μm, 20 to 63 μm, and > 63 μm and whole-rock samples were prepared for XRD determination involving oriented slides and random samples. The XRD measures were backed up by concurrent differential thermoanalysis (DTA) including differential gravitational analysis (TGA).

Advanced studies into the mineralogical composition of APS-bearing argillaceous rocks involved a combination of scanning electron microscopy (SEM) and transmission electron microscopy (TEM-EDX). As no investigations so far exist on the homogeneity of APS minerals, microtome-sections (thickness: approximately 120 to 150 Å) have been made prior to microscopic analyses.

Optical microscopy supplemented by electronmicroprobe analysis (EMPA) is a useful tool for those samples that by their outward appearance show that they contain APS minerals in significant amounts. This approach is prevalently taken when APS minerals in metamorphic rocks are targeted (Schreyer, 1987; Morteani and Ackermand, 1996). Thin sections, however, are less useful when the true nature of the APS minerals is to be unravelled, because the optical properties of transparent minerals are not distinctive within the group (Girault, 1980).

The various steps of determination of APS minerals are depicted in detail in Störr et al. (1991) and in Kassbohm et al. (1998), where EMP, SEM and TEM methods applied to APS mineral analysis were discussed with micrographs and XRD spectra.

3. APS minerals in sedimentary rocks

3.1. APS minerals in calcareous environments

3.1.1. Results

In the Carlsbad Cavern, SW USA, various phyllosilicates, gypsum and native sulphur are found together with alunite and natroalunite in pockets, wall residues, floor deposits and solution cavities of Cretaceous limestones and dolostones (Polyak and Guven, 1996; Polyak et al., 1998) (Table 2). In the Rhenish Slate Mts., Germany, near Lohrheim, phosphates developed where Devonian limestones, graywackes, keratophyres, slates are overlain by a thick blanket of late Cretaceous to early Tertiary saprolite (Dill et al., 1995b). In cavities of the calcareous host-rocks, only earthy, nodular and concretionary lumps containing predominantly carbonate–fluorapatite were encountered (Germann et al., 1981), whereas in the saprolite of the surrounding siliciclastic rocks gorceixite, florencite and goyazite-rich phosphate minerals formed instead (Dill et al., 1995b). They are disseminated in an argillaceous substrate made up of kaolinite, muscovite and quartz (Fig. 2).

3.1.2. Interpretation

Karstification and the argillitisation are processes common to both occurrences under consideration, yet the mineral assemblages are contrasting. In the Carlsbad Cavern, sheetsilicates and various types of alunite derived from cave-forming waters. Sulphuric waters, when exposed to clay-rich sediments converted clay minerals to alunite and natroalunite. Smectitic clay was converted into hydrated halloysite by interaction with H_2SO_4 (reaction (1)). Karstifica-

Table 2
APS mineralization in various types of sedimentary environments of deposition (m.l. = mixed layer phyllosilicates)

Locality	References in the literature and in text	Host rocks/parent material	
		Lithology	Age of formation
Carlsbad and Lechuguilla Cavern (New Mexico, USA)	Polyak and Guven (1996)—Section 3.1	limestone, dolostones	Cretaceous
Lohrheim (Rheinisches Schiefergebirge, Germany)	Dill et al. (1991)—Section 3.1	altered basic volcanics, limestones, bituminous shales	Late Devonian
Thies Plateau, Western Senegal	Flicoteaux (1982), Nriagu and Moore (1984)—Section 3.2	phosphorite, limestone, claystones, chert	Tertiary
Variscan Mts. Range, Northern Portugal and Central Europe; Nuba Mountains, Sudan; Carpathian Mts., Slovakia	Dill (1986), Meireles et al. (1987), Dill et al. (1991), Rojkovič et al. (1999)—Section 3.3	black shales, graphite schists, chert, metaargillites, black phyllites, lydites	Early Paleozoic, Upper Precambrian
Cook Inlet-Alaska, USA	Reinink-Smith (1990), Bohor and Triplehorn (1993), Rao and Walsh (1999)—Section 3.4	subbituminous coal	Tertiary
Bobov Dol coal field, Bulgaria	Stanislav et al. (1994)—Section 3.4	high ash coal	data not available
Coal fields in the Coal Measures and brown coal basins, Germany	Dill and Pöllmann (1999)—Section 3.4	lignitic to anthracitic coal	Tertiary, Cretaceous, Upper Carboniferous
Modern soils and peat bogs, Malaysia	Courchesne and Henderschot (1990), Shamshuddin and Auxtero (1991), Van Breemen (1993), Shamshuddin et al. (1995)—Section 3.5	hydromorphic soils	Recent
Paleosols and duricrust, W Portugal	Meyer and Pena Dos Reis (1985)—Section 3.5	silcretes	Tertiary
Saprolites, laterites and bauxites (Hungary, Russia, Brazil, Germany, France, Peru)	Yasychenko et al. (1989), Störr et al. (1991), Wipki et al. (1993), Walter et al. (1995), Schwab et al. (1996), Gilg and Frei (1997), Mordberg (1999)—Section 3.6	carbonatite, basic volcanics, pegmatite, leucogranite, dolostone, siliciclastics	Precambrian–Tertiary
Arenacoeus rocks (Austria, Australia, Jordan, Kuwait, Gabon)	Khoury (1987), Spötl (1990), Khalaf (1990), Birger et al. (1998)—Section 3.7	claystones, siltstone, fine- to coarse-grained sandstone	Permian–Quaternary
Carbonate–argillite sequences hosting micron gold deposits (USA, Macedonia, Malaysia)	Ilchik (1990), Arehart (1996), Percival et al. (1990, 1993), Dill and Horn (1996)—Section 3.8	silty carbonates, limey siltsones, calcareous shales, dolostones	Cambrian through Tertiary

tion and the formation of APS mineralization was a single-phase process that obviously took place at higher temperatures than in Lohrheim. Dickite may have produced from hydrothermal solutions in the temperature range of 100–400°C (Dill et al., 1997a) (Table 2). In Lohrheim, APS mineralization is part

APS mineralization			
Associated non-APS minerals	APS mineral assemblage	Age of formation	Origin
halloysite, smectite, illite, palygorskite, dickite, kaolinite	alunite, Na alunite	Quaternary	speleothems and karst cavities produced by hot brines
kaolinite, Fe–Mn-oxide-hydrates, muscovite–illite, alkali feldspar, apatite	gorceixite, florencite, goyazite	Cretaceous to Tertiary	karst cavities and kaolinite saprolite (“residual kaolin”) produced by meteoric waters
attapulgite, smectite, illite, kaolinite, goethite, mixed-layer phyllosilicates, quartz, chalcedony, wavellite, apatite	crandallite, Ca-millisite	Tertiary	pervasive chemical weathering of phosphorite-bearing rocks caused by meteoric waters
apatite, quartz, illite, goethite, kaolinite, variscite, zincian-turquoise (faustite), wavellite, xenotime, allanite, monazite, U minerals	U-REE-bearing woodhouseite–crandallite, goyazite, plumbogummite	Tertiary to Quaternary	bulk of vein-like deposits formed by meteoric waters; in parts hot brines may have contributed to the formation of APS mineralization
siderite, apatite, volcanic glass	crandallite, goyazite	Tertiary	diagenetically altered phosphate-bearing coal
quartz, kaolinite, illite, plagioclase, K-feldspar, Fe–Pb sulfides, siderite, calcite, dolomite, gypsum, muscovite, smectite, volcanic glass, Fe oxides, rutile, anatase, corundum, gibbsite, biotite, chlorite, zircon, barite, polyhalite, aragonite, ankerite, witherite, apatite, halite, sylvite.	jarosite, alunite	data not available	phosphate-bearing coal overprinted by diagenetic and epigenetic mineralizing processes associated with hydrothermal and volcanic activities
rhomboclase, szomolnokite, poorly crystallised Fe oxide-sulfate, Zn–Pb–Fe sulfides, Mg calcite, Fe dolomite, siderite, dolomite, bassanite, gypsum, dickite, muscovite, talc, smectite, illite, illite–smectite m.l., kaolinite, sylvite, thenardite, halite, feldspar, quartz	jarosite (?), Na alunite	Tertiary to Recent	phosphate-bearing coal overprinted by diagenetic and epigenetic mineralizing processes which subsequently underwent supergene alteration
illite–smectite m.l., kaolinite, illite, chlorite, feldspar, Fe oxide-hydrates, Fe sulfides, quartz	jarosite, Na jarosite, alunite (poorly crystallised)	Recent	pedologic processes in hydromorphic soils
kaolinite, opal CT, quartz, illite, Fe oxides, pyrite, palygorskite	alunite	Tertiary	paleopedologic processes in hydromorphic soils
diaspore, berthierine, sericite, kaolinite, goethite, apatites, calcite, Mn-oxyhydroxides, smectite, hornblende, quartz, hematite, gibbsite, halloysite, wavellite, wardite	crandallite, svanbergite, gorceixite, alunite, goyazite, florencite, kemmlitzite	Devonian through Recent	bauxite deposit, phosphate laterite, kaolinite saprolite (“residual kaolin”) caused by pervasive chemical weathering
quartz, gypsum, K-feldspar, xenotime, apatite, Fe–Mn oxide-hydrates, kaolinite, illite, smectite–illite m.l., gibbsite, pyrite, organic matter	alunite, hydronium-alunite, Na-alunite, florencite, goyacite, crandallite, gorceixite, hinsdalite	data not available	lacustrine and shallow-marine clastic sediments that underwent diagenetic alteration
baryte, stibnite, gold, quartz, Fe sulfides, native As, kaolinite, realgar/ orpiment, calcite, As–Sb oxides, complex As–Hg–Tl–Sb-sulfides/oxides	alunite, jarosite	data not available	fault-related replacement deposits in limey argillites and silty carbonates (Carlin-type) overprinted by supergene processes

of a two-phase process. During an incipient stage, low-temperature karstification provided the pockets and cavities that accommodate the residual minerals. In a subsequent stage, various phosphates precipitated in the weathering loam according to which position they have formed in the host/source rocks.

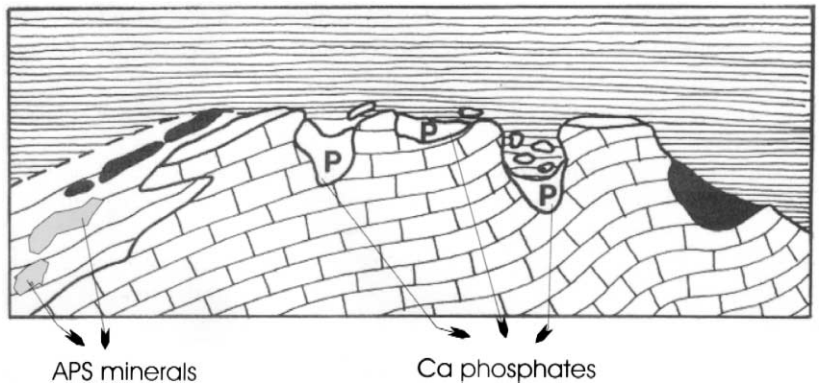

Fig. 2. APS mineralization in Palaeozoic limestones subject to Tertiary weathering processes in the Rhenish Slate Mts. (Dill et al., 1995b). Idealised cross-section through a karst cavity filling in the Palaeozoic limestones underneath the Tertiary saprolite (not to scale).

Pure calcareous rocks have brought about apatite. The Ba and Sr contents of APS minerals were provided by the supergene alteration of barite-bearing bituminous slates and basic volcanics nearby, whereas the REE derived from alteration of keratophyres (Dill et al., 1995b).

$$6\,\text{smectite} + 12H^{+} + 2H_4SiO_4 + 2Al(OH)_4 \Rightarrow 12\,\text{halloysite} + Ca^{2+}. \quad (1)$$

3.2. APS minerals in phosphorite-bearing environments

3.2.1. Results

Apatite-bearing phosphate accumulations of marine origin are very widespread in calcareous–argillaceous host rocks of different ages (Föllmi, 1996; Dill and Kantor, 1997). In some places, apatite enrichment is of economic grade and has given rise to renowned phosphate deposits such as Ruseifa, Jordan (Abed and Kraishan, 1991), Khouribga, Morocco (Boujo, 1976; Trappe, 1991), Gafsa, Tunisia (Slansky, 1986), Mazidagi-Mardin, Turkey (Lucas et al., 1980a) and Arat, Israel (Zohar and Moshkovitz, 1984). In their topstratum, these phosphorite deposits are altered, resulting, in places, in the formation of APS mineralizations.

The phosphate deposits on the Thies Plateau in western Senegal have been studied in detail by Flicoteaux (1982) and Nriagu and Moore (1984)—see also Fig. 3. In a Tertiary series of alternating argillaceous and calcareous phosphorite deposits, carbonate-fluor apatite weathers to a polyphase mineralization with Ca-millisite and various generations of crandallite and wavellite. Subsequently, calcite is leached (Lucas et al., 1980b). When calcite is destroyed, the Ca apatite begins to transfer into the above-mentioned sequence of APS minerals (Table 2).

Further examples of phosphorites subject to alteration leading to APS minerals were reported from Ivory Coast (Parron and Nahon, 1980). A summary of the secondary phosphates produced throughout alteration of marine phosphorites was given in Nriagu and Moore (1984) who listed among others the following minerals: augelite, beraunite, cacoxenite crandallite, goyazite, Ca-millisite, turquoise, variscite, vivianite, wardite, wavellite.

3.2.2. Interpretation

Supergene alteration of phosphorites in argillaceous–calcareous host lithologies leads to two different types of products according to the intensity of weathering.

Less intensive weathering causes the phosphorites to turn their rock colour red and trigger intracrystalline changes in the parent phosphate. The CO_2 in the lattice decreases from as much as 5.5 wt.% to a minimum content of 0.5 wt.% along with a concomitant increase in the lattice constant [a] as was re-

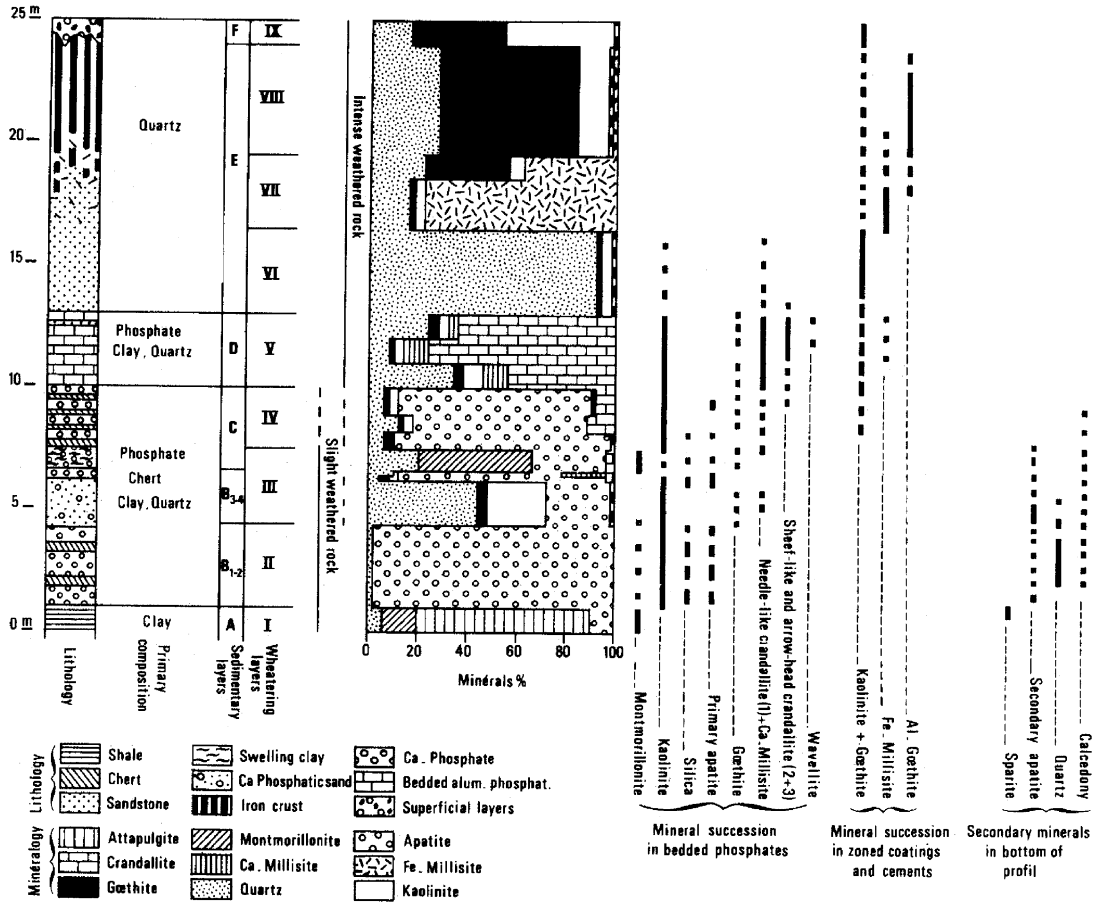

Fig. 3. Mineral succession in the two first stages of aluminous phosphate genesis in Western Senegal (Flicoteaux and Lucas, 1984).

ported from Sidi Dauoi, Morocco (El Mountassir, 1977). Along with that transformation the apatite becomes depleted in F, Ca, Na and Sr. The original association of clay minerals, quartz, calcareous minerals and apatite is stable under near neutral conditions.

During a more intensive stage of weathering when the lithology is depleted of Ca, the meteoric fluids become more acidic, apatite is totally removed. Various APS minerals originate from this alteration. Low phosphate concentration result in the formation of crandallite and wavellite, higher concentration in the precipitation of montgomeryite (Nriagu, 1976). The amount of amorphous $Al(OH)_3$ available in the weathering system plays a decisive role as to what type of APS mineral eventually comes into being. Phosphatization of phosphorites rich in argillaceous material will invariably lead to the formation of millisite and taranakite. The presence of abnormally high trace element contents in the parent rocks may alter the mineralogical composition of the resulting APS minerals.

Elevated contents of Cu may give rise to turquoise and given abnormally high values of Zn in the source rock may modify its chemical composition and provoke the precipitation of faustite (Zn-bearing turquoise) (Dill et al., 1991). Sulphur-bearing species among the APS minerals and members of the alunite s.s.s. are rare or absent in a calcareous environment due to the buffering effect of CO_2^{2-} released from the ubiquitous carbonate minerals present in the parent rock of phosphorites and due to the low total sulphur content (TS), which lies in the range of 0.07–3.90 wt.% SO_3 (Slansky, 1980).

3.3. APS minerals in argillaceous–carbonaceous environments

3.3.1. Results

In the Silurian and lower Devonian Graptolite Shales, across the European Variscides such as in Germany (Dill, 1986) and in Portugal (Meireles et al., 1987), in early Palaeozoic black phyllites and lydites of the Carpathian Mts. Range (Rojkovič et al., 1999), in Precambrian graphite schists in the Nuba Mts., Sudan (Dill et al., 1991), well-crystallised APS minerals may be observed in pockets and hairline cracks. APS minerals form earthy, botryoidal and rhythmically banded vein-like phosphate mineralizations, which fade out at a depth of a few meters below the present-day surface. The APS minerals observed in fracture zones cutting through the carbonaceous argillites mainly belong to the U-REE-bearing woodhouseite–crandallite series. They are less widespread than wavellite, variscite and minerals of the turquoise group (Table 2). The enclosing wall rocks are abundant in Fe disulphides and organic matter. In places, the argillaceous rocks contain base metal sulphides and low grade U concentrations. Phosphate nodules and lenses scattered throughout the black shales are rich in F apatite. The maximum TS analysed in samples from the black shale under consideration was 24.07 wt.%, their P_2O_5 contents run up to as much as 7.75 wt.% (Dill, 1986).

3.3.2. Interpretation

Despite the widespread occurrence of pyrite and marcasite in the unaltered carbonaceous parent material, the SO_4^{2+} released during oxidation of sulphides was insufficient to form alunite. There was only a limited substitution of SO_4^{2+} for PO_4^{3+} in the crandallite–woodhouseite s.s.s. Fe disulphide was oxidised resulting in the precipitation of goethite and hydrosulphuric acid, which provoked a drastic lowering of the pH of the mineralising fluids (reaction (2)).

$$2FeS_2 + 7.5O_2 + 7H_2O \Rightarrow \text{goethite} + 8H^+ + 4SO_4^{2-} \quad (2)$$

$$Al(OH)_3 + HPO_4^{2-} + 2H^+ \Rightarrow \text{variscite} + H_2O. \quad (3)$$

Amorphous $Al(OH)_3$ and HPO_4^{2-} from decomposition of sheetsilicates and phosphates, respectively, provide the basis to form variscite (reaction (3))—the chemical composition of phosphate minerals reported in the reaction is given in Table 1. When the fluids become more acidic and the quantities in $Al(OH)_3$ and HPO_4^{2-} increase, wavellite may also come into existence (reaction (4)).

$$\text{variscite} + 2Al(OH)_3 + 4H^+ + HPO_4^{2-} \Rightarrow \text{wavellite} + 2H_2O. \quad (4)$$

The argillaceous host rocks are poor in Ca. Not surprisingly, Ca-bearing APS minerals are only present in subordinate amounts. In the mineral assemblage that comes into being when black shales are subject to oxidising processes in nature, alunite is not a common constituent either. In course of manmade oxidation of black shales to produce alum, however, the pH value is significantly lowered so that even alunite becomes stable (see Section 6) (Fig. 4).

The base metals and REE are accommodated in the crystal lattice of APS minerals, whereas U is only loosely bound to the secondary phosphates, which have derived from the enclosing black shales.

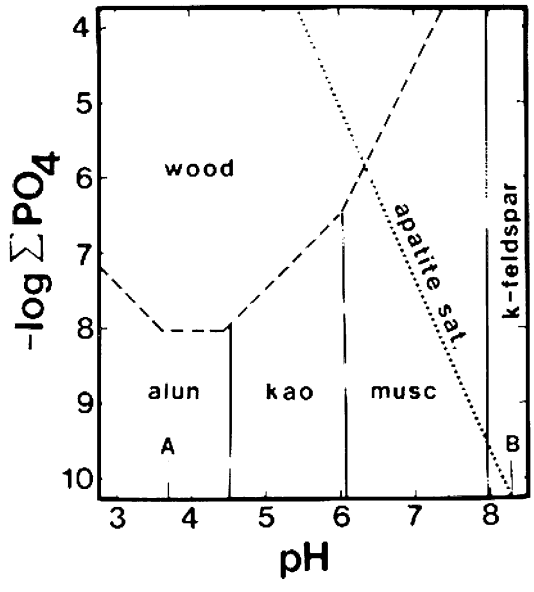

Fig. 4. Stability fields of some silicates, phosphates and APS minerals that occur together in alteration zones. Line B denotes the pH for equal activities of $H_2PO_4^-$ and HPO_4^{2-}, line A represents the pH value for equal activities of H_3PO_4 and $H_2PO_4^-$ (Stoffregen and Alpers, 1987).

The chemical composition of the non-mineralised carbonaceous sediments is not very much distinct from that of the vein structures (Dill, 1986; Dill et al., 1991; Rojkovič et al., 1999) and the sulphur isotopes demonstrate that sulphur in the APS minerals is likely to have derived from oxidation of sulphides in the bedrock (Dill et al., 1991).

In the vein-like deposits from Sudan, a meteoric low-temperature solution is likely to have brought about the APS mineralization. There exists a precursor stage to the APS mineralization characterised by secondary apatite, which resembles this sort of low-intensity weathering of phosphorites reported from Sidi Dauoi, Morocco by El Mountassir (1977)—see Section 3.2. Due to the lack of accompanying minerals typical of high-temperature origin and the U disequilibria determined in the U–P mineral association, a supergene process of Quaternary age is held responsible for this mineralization that evolved within four phases. Phase I saw the precipitation of secondary apatite in association with illite under neutral to moderately alkaline conditions (Fig. 5a). During phase II, crandallite replaced apatite and kaolinite substituted for illite. To demonstrate the occurrence of goethite relative to strengite, the phase boundary has been calculated using the data given by Lindsay (1979) and Ruppert (1980). The assemblage in the shaded area of Fig. 5b indicates that the pH may have decreased to 5.8 at log $a\ (HPO_4^{2-}) = -7$. Phase III differs from phase II by the appearance of variscite. Apart from lowering of Fe concentration, H^+ and HPO_4^2-concentrations increase. During this phosphatization, pH values below 5.8 may, locally, be achieved (Fig. 5b, stippled area). The most decisive factor to postulate a phase IV is a strong increase in Cu^{2+} in the pore fluid that triggered turquoise to gradually develop at the expense of Ca–Al and Al phosphates towards shallower depth in the saprolite profile.

3.4. APS minerals in coal-bearing environments

3.4.1. Results

Coal-forming environments are not only well suited for the preservation of organic matter but, locally, also are abundant in phosphorus. Ward (1978), Reinink-Smith (1990), Bohor and Triplehorn (1993), and Rao and Walsh (1997) reported abnormally high P_2O_5 contents from Alaskan coals of the Cook Inlet interbedded with tonsteins. P contents in

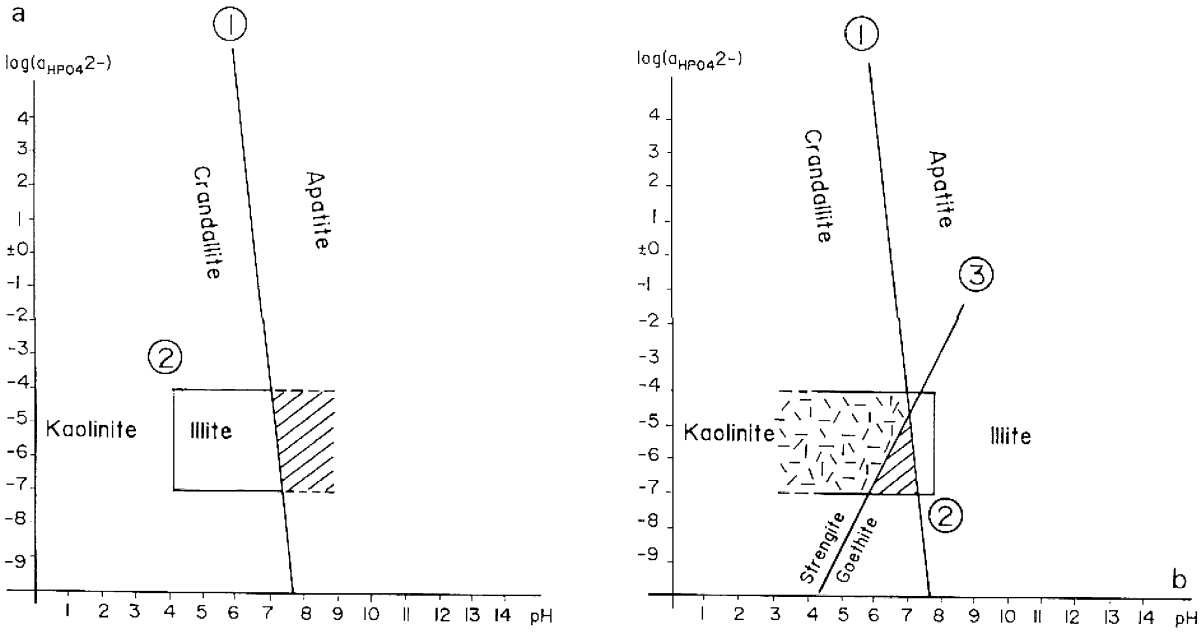

Fig. 5. Stability fields of some coexisting minerals in the APS mineralization at the Nuba Mts., Sudan (Dill et al., 1991).

coal range from 0.001 to 0.229 wt.% in raw material (Rao and Walsh, 1997). In subbituminous coal from the Beluga coalfield, Alaska, certain increments showed of as much as 17.03% P_2O_5 in the coal ash and 1.01% P on a moisture-free coal basis. Apatite occurs in trace amounts only rarely in tonsteins. Most of the P contents were ascribed to APS minerals of the goyazite–crandallite s.s.s., which form pseudomorphs after glass shards and bubble junctions and observed as colloidal precipitates and as concretions in coal. In other seams, crandallite is associated with structured vitrinite and as cell fillings in fusinite (Triplehorn and Bohor, 1983; Rao and Walsh, 1999). The S content in the coal under consideration is rather low ranging from 0.21% to 0.25% S (Rao and Walsh, 1999). From the Bobov Dol high ash coal, Bulgaria, a wide variety of oxides, sulphides, sulphates, carbonates, chlorides, and silicates were reported by Stanislav et al. (1994) (see Table 2). The sole APS minerals spotted in the coal are jarosite and alunite. In samples taken from coal seams of limnic and paralic origin in Germany, which cover the entire rank of coal from the lignite to the anthracite stages, APS minerals make up only a small deal of the mineral assemblage. In German coal, Fe sulphates (AS) running the gamut from melanterite to szomolnokite are more abundant than APS minerals the only representative of which is poorly crystallised Na alunite (Dill and Pöllmann, 1999).

3.4.2. Interpretation

Sulphur is primarily concentrated in sulphides, predominantly Fe disulphides and in chemical compounds closely linked to organic matter. Provided there is no introduction of S into the coal-forming system by, e.g. hydrothermal processes, the presence of S-enriched or S-poor APS species reflect the original S content and furnish compelling evidence on whether there was a marine flooding of the peat swamp or not.

A late-stage S influx may have played a significant part in the Bobov Dol coals, Bulgaria, which have undergone complex syngenetic, diagenetic and epigenetic mineralization processes associated with hydrothermal and volcanic activities. They gave rise to a couple of uncommon base metal sulphides. Not surprisingly, alunite and jarosite are the sole representative of APS minerals when these sulphides become decomposed or the mineralising fluids become more oxidising. While alunite may easily be accounted for by such hypogene processes (a detailed description of alunite formation from hydrothermal solutions is given in Sections 4.2–4.5), jarosite is mostly considered as a product of supergene alteration. Alunite and jarosite although occurring in the same deposit, they seldom have the same age (Rye et al., 1993). As jarosite requires parent solutions with a lower pH than those for alunite, it is highly unlikely that these minerals can form simultaneously (Stoffregen, 1993) (reaction (5)).

$$6\,\text{goethite} + 2K^+ + 2H^+ + 4HSO_4^- \Rightarrow 2\,\text{jarosite}. \quad (5)$$

Even at this moderate temperature, a relatively high S molality is required. At near ambient conditions with temperatures of 25°C, the values are less extreme (Van Breeman, 1972).

$$3\,\text{kaolinite} + 2H^+ + 2Na^+ + 2\,\text{pyrite/marcasite} + 14O_2 + H_2O \Rightarrow 2\,\text{alunite} + 6SiO_2 + 4Fe^{2+} + 4HSO_4^- \quad (6)$$

(= leading to complex Fe sulphates of the melanterite series).

In samples from the German mines, coal sulphates such as natroalunite, rhomboclase, szomolnokite, paracoquimbite and coquimbite can be identified besides kaolinite, dickite attesting to a pH of below 6 (Dill et al., 1991) (reaction (6)). This has an important bearing on the stability of apatite, which becomes diluted at the expense of APS minerals and on the white mica that is converted into 7-Å phyllosilicates of the kandite group. This mineralization, which bears AS and little APS, represents the passage from epigenetic to supergene alteration of coal. The boundary between the two types of alteration cannot be drawn with certainty. Part of these minerals spontaneously forms during mining when S- and P-enriched coal is exposed to the atmosphere (Dill and Pöllmann, 1999).

Phosphorus may have been introduced by volcanic ashes falling into non-marine coal-bearing environments and later altered to kaolinitic claystones commonly called tonsteins. Apatite occurs in trace

amounts in tonstein. The volcanic ash deposited immediately beneath peat beds is affected by humic and fulvic acids generated from organic matter. These primary occurrences suggest that phosphate replacement occurred soon after burial before the glass could be altered to clay minerals by diagenesis (Rao and Walsh, 1999). Secondary APS mineralization in tonsteins occurred during the formation of andosols (soil on pyroclastic deposits). Under acidic conditions, organic P in soil water reacts rapidly with weathered glass (allophane and alumina) to form insoluble APS minerals (Tan, 1984)—see also Section 4.5.

Crandallite occurs at relatively high values of $[Ca^{2+}]/[H^+]^2$ ($\log[Ca^{2+}]/[H^+]^2 > 9.0$ and $\log [H_3PO_4] > -4.5$ (Vieillard et al., 1979). These conditions can occur in the coal swamp. In an acidic swamp (high-moor) with pH ranging from 3.3 to 4.6 phosphate ions, available from leaching of volcanic ash, could result in the precipitation of crandallite/woodhouseite and alunite as well (Fig. 4). The poorly crystallised predecessors of this sort of APS mineralization are referred to in Section 3.5.

3.5. APS minerals in soils and paleosols

3.5.1. Results

Phosphorus and sulphur are essential for the evolution of living beings. Therefore, the content and the availability of both elements have been studied for decades in soils of different types as well as the plant response to deficiencies or excess amounts of P and S in soils (Scheffer and Schachtschabel, 1976). Soil, which averages 0.08 wt.% P, lie intermediate to continental sediments and marine sediments that average 0.07 and 0.12 wt.% P, respectively (Brinck, 1978). Concern has been expressed over the acid rain. With this in mind, the mineralogy of APS minerals in soils attract growing attention as they are crucial to the retention or mobility of sulphate ions in soils. Mineralogical investigations were focused on sulphate-rich soils (Courchesne and Henderschot, 1990; Shamshuddin and Auxtero, 1991; Van Breemen, 1993; Shamshuddin et al., 1995). Mineral stability relationships, laboratory experiments and field studies of modern soil profiles indicate that the solid phases of concern among APS minerals are alunite and jarosite (see also Section 3.4). The species are poorly crystallised and in places physical evidence for the aforementioned minerals is lacking. At outcrop, APS minerals appear as yellowish mottles occupying voids and/or root channels.

Phosphates of the supergroup under study are able to scavenge heavy metals from the solutions percolating through the soil and cause these pollutants to become immobile as evidenced by the presence of plumbogummite.

In paleosols and silcretes of Cainozoic age in western Portugal Meyer and Pena Dos Reis (1985) have discovered alunite besides clay minerals and siliceous compounds (Table 2). The duricrusts as much as 10 m thick lie atop of a fining-upward sequence.

3.5.2. Interpretation

Fe sulphides in hydromorphic soils or peat bogs are oxidised when they are exposed to the atmosphere during fluctuation of the water level. A mineralogical description of the processes in waterlogged environments taking into account well-crystallised mineral species is given below by reaction (7). APS minerals in these acid sulphate soils form via pseudomorphic replacement of pyrite under oxidising conditions (Shamshuddin et al., 1995). Investigations by Courchesne and Henderschot (1990) on spodosols demonstrated that most data points in a plot of $2\ pH + p\ SO_4$ vs. $p\ Al^{+3} + p\ OH^-$ cluster around the solubility line of natural gibbsite ($pK_s = 33.2$) (Fig. 6). Ion activities of leachates from B horizons are clearly undersaturated with respect to jurbanite; some solutions fall directly on the solubility line of alunite, some show a slight oversaturation. Solutions from the C horizon (open triangles) are all undersaturated with respect to alunite. The formation of APS minerals in acid soils can affect the sulphate retention in these acid soils.

The paleosols under consideration in this paper formed on an alluvial plain (Fig. 7). Swamps are the most favourable environment of deposition for alunite. They represent the waning stages of a fluvial drainage system evolving on a flat alluvial plain (Fig. 7). Alunite is not the final product of chemical weathering (see next section) but was probably introduced by pedological processes when the overlying soil horizons formed. Alunite permeating the top of these silcretes has migrated in from the overlying

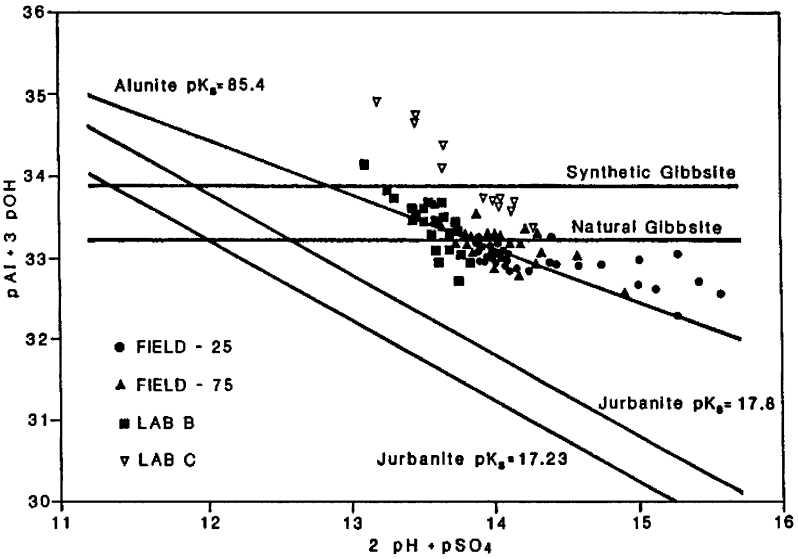

Fig. 6. Solubility diagram for alunite, jurbanite (pK_s of 17.2223 (Van Breemen, 1972) and of 17.8 (Nordstrom, 1982), natural gibbsite ($pK_s = 33.2$) and synthetic gibbsite ($pK_s = 33.9$). Plotted symbols represent the coniferous soil leachates (Courchesne and Hendershot, 1990).

beds. It precipitated in the silcretes because of the relative impermeability to the downward circulating solutions. In such a low-relief environment, chemical conditions may change quickly, primarily with the amount of water available. Sulphides formed in organic-rich sediments and later were destroyed by oxidation, liberating sulphuric acid. Sulphuric acid may directly react with illite to give alunite at a pH as low as 3 to 4. A further drop of pH would have given rise to jarosite instead of alunite (Van Breemen, 1972; Goldbery, 1980) (reaction (5))

$$2\,\text{pyrite} + 7.5O_2 + 13H_2O + 3\,\text{kaolinite} + 2K^+ \Rightarrow \text{alunite} + 6SiO_2 + 4\,\text{goethite} + 2H^+. \quad (7)$$

The various mechanisms mentioned in the text and in reactions (7) and (6) shed some light on the conversion of sulphide into sulphates in peat swamps during the incipient stages of coal formation (see Section 3.4).

3.6. APS minerals in saprolite

3.6.1. Results

Saprolite profiles are well developed on different bedrocks. The most well-known representatives of these saprolites are laterites and bauxites that may host APS minerals in significant amounts (Sehnke, 1996; Seghal, 1998). The mineral assemblages are variegated and prevalently dominated by REE-selective species (Table 2). APS mineralization in saprolites formed throughout the whole geological past on various types of bedrock as exemplified by the following sites: Precambrian dolomites of the Middle Tima, Russia (Yasychenko et al., 1989; Mordberg, 1999), Cretaceous dolomites, Hungary (Maksimovic and Panto, 1995), Cretaceous carbonatites, Brazil (Walter et al., 1995) and basic volcanic rocks (Schwab et al., 1996), Carboniferous pegmatite and granites, Germany and France (Gilg and Frei, 1997), Triassic and Cretaceous siliciclastic sediments, Peru and Germany (Störr et al., 1991; Dill et al., 1997a), Permian and Tertiary siliceous volcanites and tuffs, Germany and Peru (Störr et al., 1991; Dill et al., 1997a). The oldest APS-bearing saprolite under discussion dates back to the Devonian (Mordberg, 1999). Timing of supergene alteration may be constrained based on K/Ar or Ar/Ar dating of alunite present in the saprolite mineral assemblage (Gilg and Frei, 1997), e.g. St. Yrieix, France: 40.8 ± 1.0 (corrosion during late halloysite formation) and 45.5 ± 1.8 Ma (timing of weathering). Among the APS

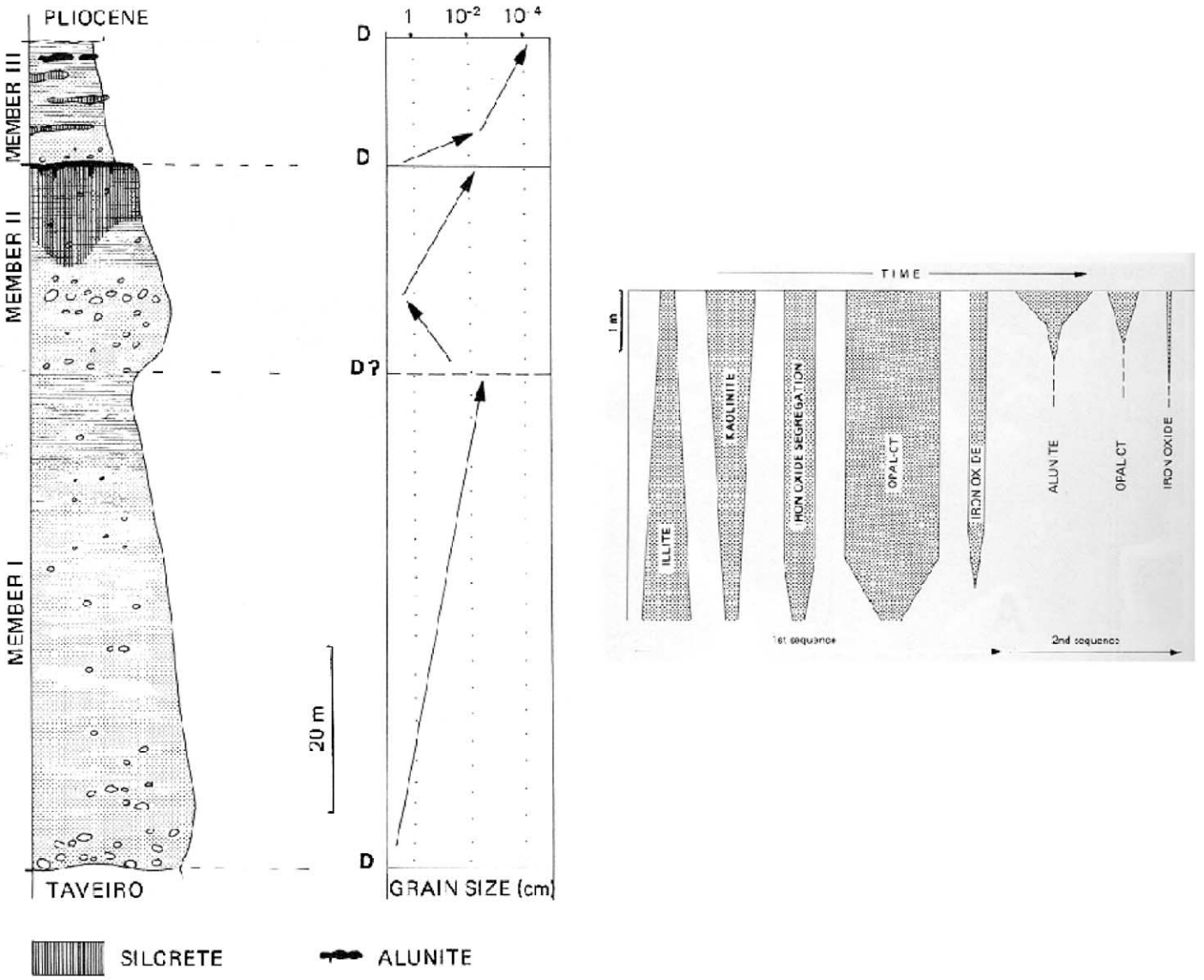

Fig. 7. Composite stratigraphic section (left) illustrating the position of silcretes (ruled) and alunite mineralization (black) together with grain size variation along depth. The sequence of mineralization in the Member II silcrete is given in the diagram on the right (Meyer and Pena dos Reis, 1985).

minerals recorded from saprolites (Table 2), the anion $(XO_4)^{x-}$ is dominated by P rather than S. As far as the larger cations in the A site are concerned, REE stands out among Sr, Ba, Pb and Ca. B sites are mainly occupied by Al and to a lesser extent by Fe.

The variation of APS minerals in a typical saprolite profile as a function of depth is illustrated in the cross-section through the laterite at Trauira, Brazil (Fig. 8). The basic volcanic rock is deprived of its accessory apatite and replaced by wardite and wavellite in the lowermost and middle part of the saprolite section. The maximum quantity of APS minerals with crandallite as the major constituent is achieved in zone B close to present-day surface. The topmost

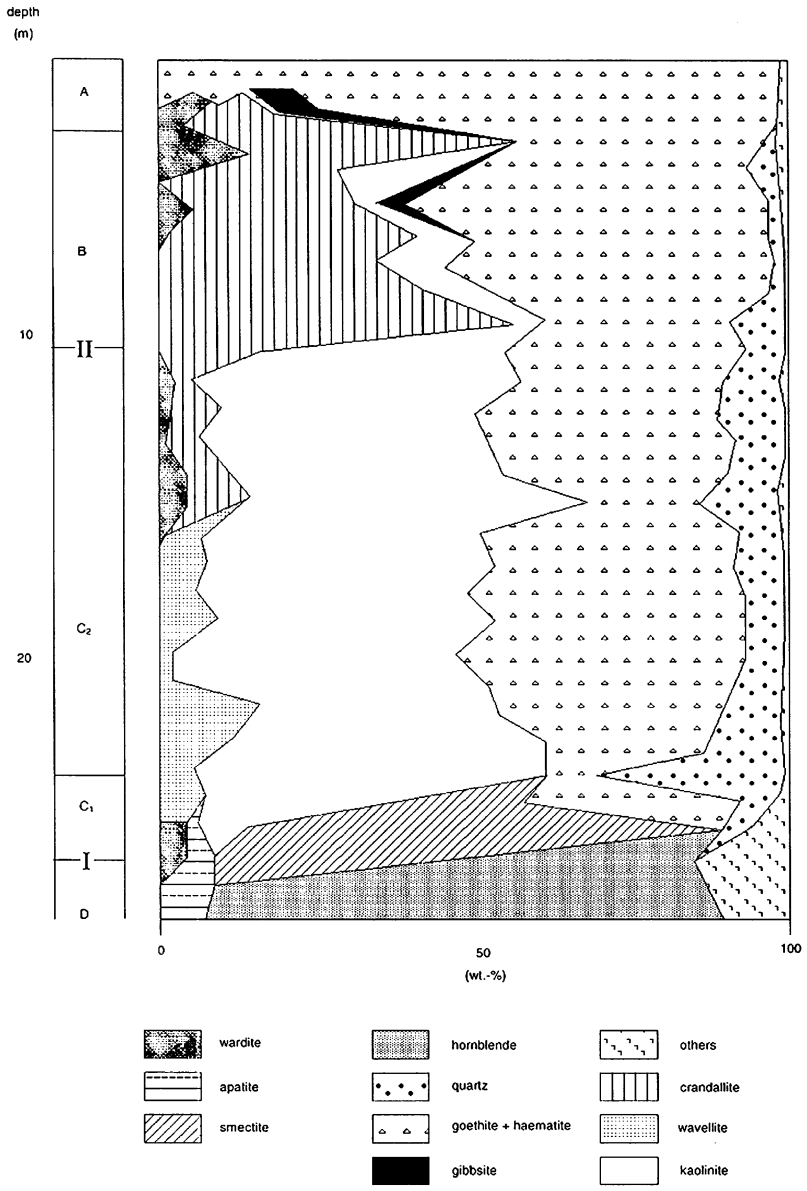

Fig. 8. The mineral assemblages of the Trauira phosphate laterite plotted as a function of depth in the coastal region of Para and Maranhao, Brazil (Schwab et al., 1996).

section is barren as to APS minerals and consists of quartz, exclusively.

3.6.2. Interpretation

The source for K, Ba and Pb is the hydrolysis of feldspar and illite–muscovite. Ca, Sr, and Mg may either have derived from feldspar or leaching of carbonate minerals while sulphuric acid was produced by the oxidation of sulphides, mainly pyrite (reactions (7) and (8)). APS mineralization forms part of so-called saprolitization, which has been discussed at length in textbooks such as these published by Goudie and Pye (1983) or by Cooke et al. (1993). Modifiers others than those mentioned above in the A and B sites of the general formula of $AB_3(XO_4)_2(OH)_6$ may be accommodated in the crystal lattice as it may be the case with AsO_4^{3-}, CO_3^{2-} and SiO_4^{2-} that can proxy for the $(XO_4)^{x-}$ anion complex. Yet they seldom found in nature and gain neither economic value nor can they be used as reliable tool to discriminate these supergene APS mineralization from hypogene equivalents (Hak et al., 1969).

APS minerals prevailing in saprolite profiles may be accounted for using thermodynamical calculations and laboratory trials. In the cross plot of pH vs. log $a\ H_3PO_4$, the stability field of woodhouseite relative to some sulphate-poor and sulphate-free APS minerals is shown to expand with increasing hydrogen sulphate concentration (Fig. 9a). Hydrogen sulphate concentration falls in the range 10^{-4}–10^{-10}. At high H_3PO_4 concentrations, apatite is stable down to a pH of about 6. In this case, crandallite appears first among the APS minerals. Increasing acidity of the pore solution and a lowering of the pH value down to four causes augelite or wavellite to come into existence dependant on the quantity of H_3PO_4 (log $a\ H_3PO_4 = -2.75$). At a very low quantity of H_3PO_4 (e.g. log $a\ H_3PO_4 = -9$), apatite at a pH value of approximately 7 is converted into woodhouseite. Ongoing lowering will lead to gibbsite as the final product of phosphate alteration. In the phase diagram of Fig. 9b, the size of the stability field of the APS minerals woodhouseite is shown as a function of cations in the A site. Ba^{2+} substituting for Ca^{2+} would cause a significant enlargement of the stability field of the APS minerals. A similar relation is portrayed in Fig. 9c. Any substitution of HREE for LREE in the A site will increase the stability field of the APS minerals and account for its predominance in the weathering profile relative to gibbsite, augelite or wavellite. This stability sequences may also be applied in a similar way to crandallite-enriched s.s.s.: $Pb^{2+} > Sr^{2+} > Ba^{2+} > Ca^{2+}$. Sr and Ba have changed their position. Raising the temperatures from 298 to 333 K during their laboratory trials did not lead to pure crandallite even after a period of time of 3 years (Schwab et al., 1993). Only amorphous products, goyazite and gorceixite could be proved. Substitution of arsenate for phosphate enhances the thermodynamic stabilities and arsenocrandallite may become a stable phase at 473 K. Since the stability fields of crandallite are enlarged with falling temperature crandallite may become a widespread stable phase in the saprolites.

Elevated Pb contents found in many kaolinitic saprolites by Störr et al. (1991) may easily be accounted for by the high stability of plumbogummite in view of the experimental trials discussed above.

3.7. APS minerals in arenaceous rocks

3.7.1. Results

Pure sandstones outside the reaches of weathering and hydrothermal alteration rarely contain APS minerals in significant amounts. The mineral assemblages may be based on the presence or absence of alunite subdivided into either monotonous alunite-assemblages or more varied woodhouseite–crandallite mineral associations. A complex APS mineralization containing s.s.s. of the hinsdalite group was recorded from the Late Permian sandstones of the Mitterberg Formation in the Northern Calcareous Alps, Austria (Spötl, 1990). Similar series occur in Australia in sandstones of various ages. They are characterised by ubiquitous florencite and REE-bearing crandallites, gorceixite and goyazite (Birger et al., 1998). From a Mio-Pliocene series in Kuwait which bears sulphate- and calcareous minerals Khalaf (1990) described various types of alunitic APS mineralization, one type mainly composed of hydronium alunite. In a lacustrine clastic series from the Ghor Kabid Area, Jordan Na-bearing alunite was recorded from Khoury (1987). In the Lake Tyrell, Victoria, Australia, alunite associated with jarosite and hydrous iron oxides

is found in a broad spectrum of clastic rocks (Table 2). The APS mineralization mentioned above formed at very shallow depth. Goyazite and gorceixite was reported from the Precambrian Athabascan Formation made up of an alternating sequence of sandstone and siltstones with some intercalated tuffs (Wilson, 1985). An extraordinary site of APS mineralization in arenaceous series is the Bangombe, Gabon natural reactor zone (Eberly et al., 1996) where REE from a natural fission reactor have contributed to the build-up of florencite (Janeczek and Ewing, 1996).

3.7.2. Interpretation

The APS mineralization has much in common with the APS mineralization found in saprolites as far as the sources of elements is concerned. The APS mineralization is, however, different with respect to the timing of its formation and the amount with which APS minerals contribute to the overall mineral association in the sandstone. It is subordinate to other rock-forming minerals, as the Al content of arenites commonly is very low.

The APS mineralization recorded from the sandstone of the Mitterberg Formation pre-dates syntaxial quartz cementation (Spötl, 1990). In the calcretized sandstones from the Arabian Gulf, alunitization forms the final stage of a mineral succession starting out from gypsification through sulphurization and giving way through silicification to alunitization.

The APS mineralization in the Australian sandstones was described as the result of "reverse weath-

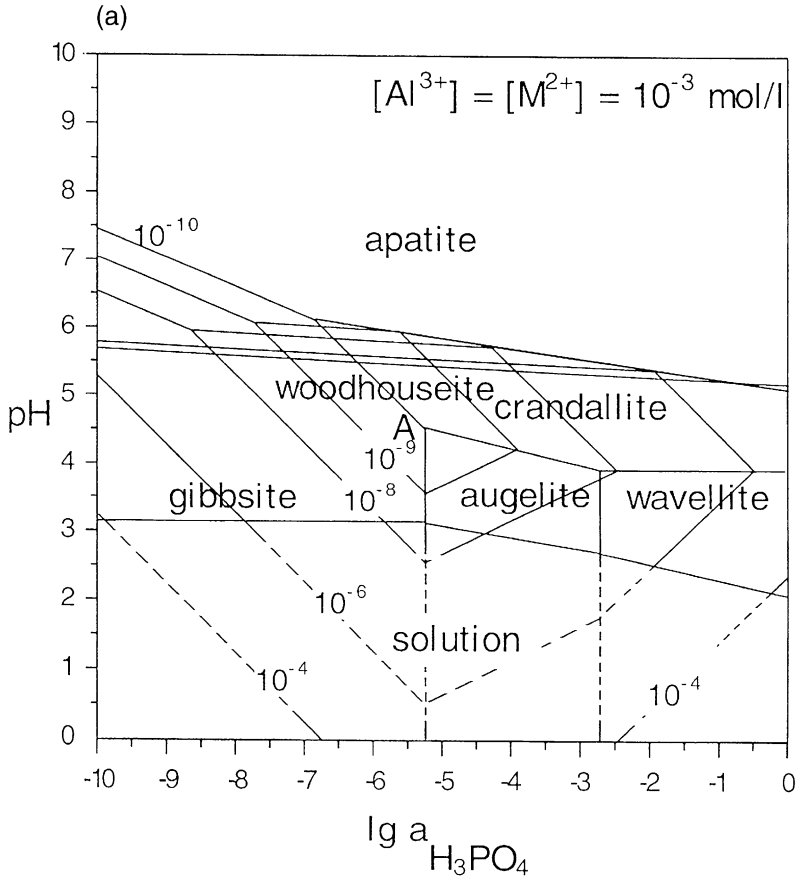

Fig. 9. Phase diagrams to show the pH and log a H_3PO_4 activities of various APS minerals common to laterites (Schwab et al., 1996). (a) Phase diagram for the system CaO-Al_2O_3-P_2O_5-SO_3-H_2O. (b) Phase diagram for the system MO-Al_2O_3-P_2O_5-SO_3-H_2O (M = Ca^{2+}, Sr^{2+}, Ba^{2+}, Pb^{2+}). (c) Phase diagram for the system REE_2O_3-Al_2O_3-P_2O_5-SO_3-H_2O (REE = Ce^{3+}, La^{3+}, Pr^{3+}, Nd^{3+}, Sm^{3+}, Eu^{3+}, Y^{3+}, Bi^{3+}).

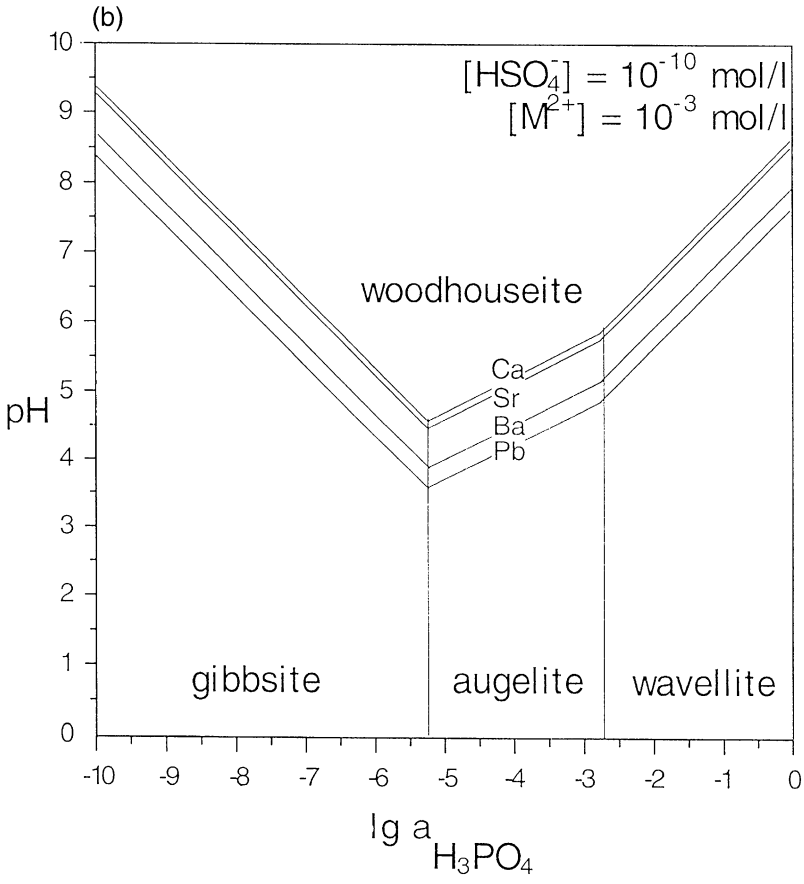

Fig. 9 (*continued*).

ering" after the release of REE and PO_4 by the reduction of Fe–Mn oxyhydroxides and the decomposition of organic material coating detrital particles (Birger et al., 1998). These APS minerals, together with apatite and xenotime precipitated within the zone of sulphate-reduction and methanogenesis. The APS mineralization in the sandstones characterise early diagenetic alteration at a shallow depth in lacustrine, fluvial and shallow marine environments of deposition. They originated from intrastratal solutions that are still in contact with the overlying marine or continental waters as well as touch deep-seated sources such as oil fields. Intrastratal solutions, which migrated through the Lower Proterozoic sandstone around the Bangomne, Gabon natural fission reactor bear nuclides of some REE (Eu 153, Eu 151, Y 89, Sm 152, Gd 152) that were accommodated in the lattice of florencite cement in the pore space of the arenaceous host rocks (Raimbault et al., 1996; Janeczek and Ewing, 1996).

3.8. APS minerals in calcareous–argillaceous sequences hosting Carlin-type SHDG deposits

3.8.1. Results

Limestone and shale sequences have attracted the interest of exploration geologist for their disseminated gold contents, e.g. Vantage gold deposits, Alligator Ridge-Bald Mountain Mining District, NV, USA (Ilchik, 1990). A comprehensive paper on this so-called sediment-hosted disseminated gold (SHDG)- or Carlin-type deposits has been published

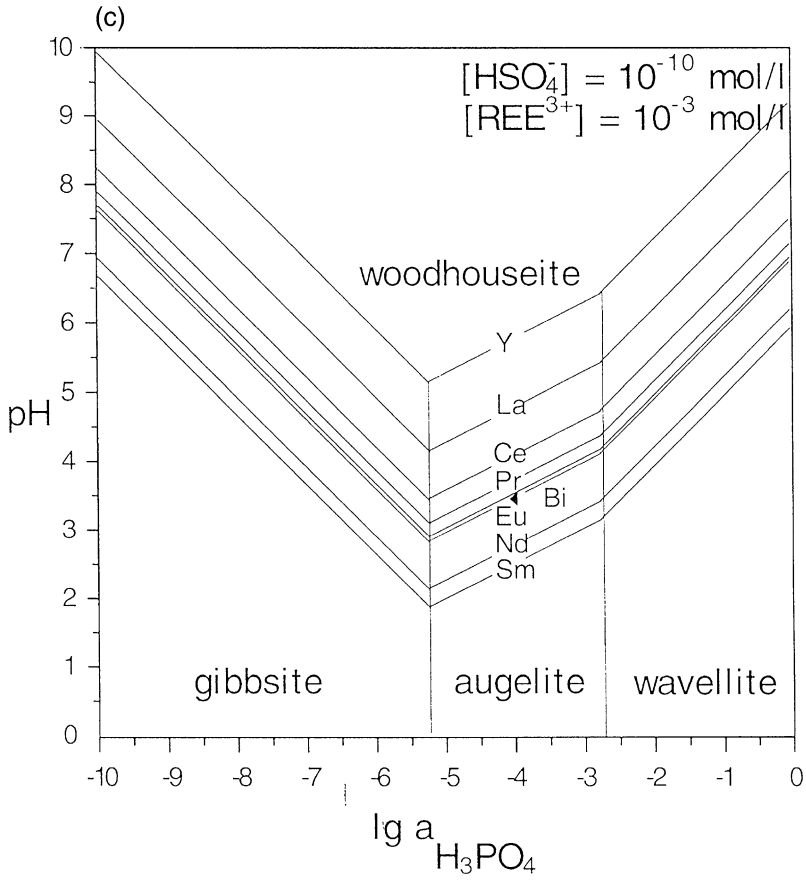

Fig. 9 (*continued*).

by Arehart (1996). The most common rock types are silty carbonates to calcareous siltstones and calcareous shales of Cambrian to Triassic age. A generalised paragenetic sequences shows besides extremely fine-grained gold Fe-, As-, Sb-, Ag-, Tl-, Hg-sulphides, barite, realgar, orpiment, kaolinite, barite, calcareous minerals and some APS minerals mainly jarosite, crandallite and alunite. The APS minerals come up during the latest stages of mineralization. Carlin-type gold mineralization in the Alšar district, Macedonia in a jasperoid dolomite has little jarosite besides dickite and kaolinite (Percival et al., 1993), in the Bau Mining District (Percival et al., 1990; Dill and Horn, 1996) where more or less pure limestones give host to the Au–Sb deposits, APS minerals have not been identified so far.

3.8.2. Interpretation

The depositional mechanisms for the main ore and gangue minerals include fluid mixing, -cooling and oxidation (Arehart, 1996). The ore-forming process involved replacement of host-rock carbonates by quartz. There is little debate that the argillic alteration zones dominated by kaolinite in the core and sericite at the margin are of hypogene origin.

The APS mineralization is, however, under hot debate. Two oxidation events post-date Au mineralization and silicification. The APS mineralization formed throughout the first phase of oxidation. Arehart et al. (1992) interpreted the entire APS mineralization based on isotope studies as supergene (Section 7.2). Ilchik (1990) stressed that APS mineralization derived from two different processes: one

simply called a more intense form of weathering, the other by hydrothermal fluids. The early oxidation is supposed to have taken place in the way shown in reactions (8) and (9):

$$2\,\text{illite} + \text{pyrite} + H_2O + 3.75O_2 \Rightarrow \text{alunite} + \text{kaolinite} + 5\,\text{quartz} + 0.5\,\text{hematite} \quad (8)$$

$$2\,\text{illite} + 3\,\text{pyrite} + 10H_2O + 11.25O_2 \Rightarrow \text{jarosite} + 2.5\,\text{kaolinite} + 2\,\text{quartz} + 4HSO_4^- + 4H^+. \quad (9)$$

The presence or absence of APS minerals also seems controlled by the type of host rock lithology. Pure calcareous host rocks (e.g. Bau, Malaysia) are less favourable for the evolution of APS minerals (see also previous sections on APS minerals in carbonate host rocks). More siliceous or argillaceous wall rocks provide much better conditions for the emplacement of APS.

4. APS minerals in igneous rocks

4.1. APS minerals in slightly altered barren volcanic and subvolcanic rocks

4.1.1. Results

APS minerals occur in a great variety of volcanic, subvolcanic and pyroclastic rocks mostly of Cainozoic age and of acidic to intermediate chemical composition (Table 3). APS form later than the common mafic and sialic minerals in the aftermath of the intrusion or eruption when the various types of igneous rocks undergo hypogene and supergene alteration by S- and P-enriched fluids. S and P are present in unaltered igneous rocks only in subordinate amounts. According to Fisher and Schmincke (1984) sulphur falls in the range 10–1200 ppm S and phosphorus in the range 0.01–1.01 wt.% P_2O_5. Not surprisingly, igneous petrographers have paid little attention to this sort of minerals and only a few papers are available on studies of APS minerals found outside traditional mining areas.

Pons et al. (1989) have reported some alunite and jarosite from Martinique, French Lesser Antilles (Table 3). In the altered latite at Gleichenberg, Austria, Barth-Wirsching et al. (1990) found alunite besides smectite, kaolinite and opal CT. Tomita et al. (1994) investigated the volcanic ashes of the 1980 eruption of the Shin-dake in Kuchinoerabu Island, Japan, where they determined abnormally high quantities of alunite. Takano and Watanuki (1990) detected pyrite, natrolalunite and native sulphur in the material suspended in the water of the Yuguma crater lake, Japan, during their 25 years of monitoring. In the lake shore water, *Thiobacillus thiooxidans* has also been recognised (Takano and Watanuki, 1990).

4.1.2. Interpretation

Most of the above APS mineralizations formed from hydrothermal fluids. Based on the absence of jarosite and on smectite thermometry, the temperatures for the APS alteration in igneous rocks was determined to be as high as 200°C (Barth-Wirsching et al., 1990). The feldspar of the volcanites was converted into kaolinite and smectite, which reacted with acidic solutions dominated by SO_4^{2-} in the way depicted below (reactions (10) and (11)).

$$2\,\text{kaolinite} + 2K^+ + 6H^+ + 4SO_4^{2-} \Rightarrow 2\,\text{alunite} + 6H_4SiO_4(\text{aq}) \quad (10)$$

$$3\,\text{smectite} + 4K^+ + 24H^+ + 14SO_4^{2-} + 66H_2O \Rightarrow 7\,\text{alunite} + 33H_4SiO_4(\text{aq}). \quad (11)$$

At Shin-dake in Kuchinoerabu Island, Japan, the alunite is enriched in K and was formed together with pyrophyllite in a geothermal system at obviously higher temperatures than in Gleichberg, Austria. The presence of pyrophyllite is held to be controlled by the temperature of formation. It derives from kaolinite and quartz when the temperature is increased to as much as 325°C to 375°C (Berman, 1988) (reaction (12)).

Conversely, the absence of andalusite in the alteration zone precludes temperatures greater than 400°C for this sulphate–phyllosilicate assemblage.

$$\text{kaolinite} + 2\,\text{quartz} \Rightarrow \text{pyrophyllite} + H_2O. \quad (12)$$

An alternative reaction path involving muscovite is also possible. In reaction (13), white mica is the predecessor of pyrophyllite and its formation caused by pH variation and silica added to the solution.

$$\text{muscovite} + 4H^+ + H_4SiO_4 \Rightarrow \text{pyrophyllite} + K^+ + Al^{3+} + 4H_2O. \quad (13)$$

Table 3
APS mineralization in various types of igneous environments of formation (m.l. = mixed layer phyllosilicates)

Locality	Reference in the literature and in text	Host rocks	
		Lithology	Age of formation
Martinique, French Lesser Antilles; Gleichenberg, Austria; Yuguma, Japan; Shin-dake in Kuchinoerabu Island, Japan	Pons et al. (1989), Barth-Wirsching et al. (1990), Takano and Watanuki (1990), Tomita et al. (1994)—Section 4.1	latite, dacite, andesite	Tertiary to Quaternary
Maricunga Belt, N Chile	Vila and Sillitoe (1991)—Section 4.2	dacite, andesite, microdiorite	Tertiary
Batu Hijau-SW Sumbawa Island, Indonesia	Simon et al. (1994)—Section 4.2	tonalite, diorite	Tertiary to Quaternary
Tombulilato district, Indonesia	Perelló (1994)—Section 4.2	submarine to subaerial basic to acid volcanic rocks interbedded with marine and continental sedimentary rocks	Tertiary, late Miocene (?) to Pleistocene
Nansatsu-District, Japan	Hedenquist et al. (1994)—Section 4.2	andesite lavas and pyroclastics	Tertiary
Crofoot-Lewis, USA	Ebert and Rye (1997)—Section 4.2	felsic volcanics and pyroclastic rocks, clastic freshwater sediments	Tertiary to Quartenary
Baguio- Northern Luzon, Philippines	Aoki et al. (1993)—Section 4.2	diorite, dacite	Tertiary
Mt. Skukum, Canada	Love et al. (1998)—Section 4.2	rhyolite, andesite	Tertiary
Masupa Ria district-central, Indonesia	Thompson et al. (1994)—Section 4.2	andesite	Tertiary
Rodalquilar, Spain	Arribas et al. (1995)—Section 4.2	rhyolite, andesite (ash flow tuffs)	Tertiary
Cosuño and Milluri, Bolivia	Dill et al. (1997b)—Section 4.3	volcanic and pyroclastic rocks, of rhyolitic to andesitic composition	Tertiary

APS mineralization			
Associated non-APS minerals	Mineral assemblage	Age of formation	Origin
illite, smectite, celadonite, chlorite, pyrophyllite, gypsum, opal CT, cristobalite, kaolinite, halloysite, feldspar, quartz, native sulfur	alunite, jarosite, natroalunite	Tertiary to Quaternary	fumarolic post-volcanic mineralization overprinted by supergene alteration
Fe–Cu–As sulfides, native sulfur, gold, kaolinite, gypsum, anhydrite, chlorite, sericite	alunite, jarosite	Tertiary to Quaternary	transitional hypogene mineralization between porphyry and high sulfidation epithermal Cu–Au-type overprinted by supergene alteration
biotite, magnetite, quartz, chlorite, epidote, sericite, albite, kaolinite, pyrophyllite, gold, Fe–Cu sulfides	alunite	Tertiary to Quaternary	porphyry Cu–Au mineralization
sericite, illite, chlorite, quartz, kaolinite, pyrophyllite, gold	alunite	data not available	transitional hypogene mineralization between porphyry Cu–Au, high sulfidation epithermal Cu–Au–Ag and low-sulfidation epithermal Au–Ag-type
dickite, kaolinite, pyrophyllite, illite, illite–smectite m.l., gold, Cu–As sulfides, zunyite, pyrite, barite, diaspore	alunite	Tertiary to Quaternary	high sulfidation epithermal Cu–Au–Ag mineralization
opal-A, opal-CT, opal-C, cristobalite, kaolinite, smectite, illite, quartz, calcite, Fe sulfides, chlorite, bitumen, mordenite, native sulfur, gypsum, cinnabar, Fe oxide	alunite, natroalunite, jarosite	Tertiary to Quaternary	low-sulfidation epithermal Au–Ag mineralization overlain by a thick high sulfidation epithermal Cu–Au–Ag mineralization
sericite, pyrophyllite, dickite, diaspore, tourmaline chlorite, quartz, adularia, calcite, rhodonite, rhodochrosite, Cu–Pb–Zn sulfides, tellurides, gold	svanbergite, hinsdalite, minamiite, woodhousiete, natroalunite, alunite	Tertiary	high sulfidation epithermal Au mineralization
pyrophyllite, kaolinite	alunite	Tertiary	epithermal Au-bearing quartz-calcite (adularia) vein system caused by high-temperature mixing of S-bearing magmatic and meteoric waters
Fe–Cu–Zn sulfides, gold, quartz, illite, pyrophyllite, diaspore, kaolinite	alunite	data not available	steam-heated, epithermal Au-bearing base metal mineralization
complex Pb–Zn–(Cu–Ag–Au) and Au(Cu–Te–Sn) minerals, diaspore, zunyite, pyrophyllite, hematite, amorphous silica, quartz, kaolinite, dickite, illite, sericite, pyrite, iodide, tellurates	K- and natroalunite, woodhouseite–svanbergite, crandallite, florencite, jarosite,	Tertiary	hypogene low-sulfidation Pb–Zn–(Cu–Ag–Au) and high-sulfidation Au–(Cu–Te–Sn) superimposed by a supergene APS mineralization
Ag–Au–Zn–Bi–As minerals, stibnite, quartz, Fe-sulphides, dickite, kaolinite, nontronite	alunite	Tertiary	hypogene steam-heated, high sulfidation epithermal Sb–(Au) mineralization

(continued on next page)

Table 3 (*continued*)

Locality	Reference in the literature and in text	Host rocks	
		Lithology	Age of formation
Kremnica, Slowakia	Haber et al. (1994)—Section 4.3	pyroxene andesites, rhyolites, dacites, granodiorites, diorites, quartzdiorites	Tertiary
Red Mountain, USA	Bove and Honn (1990)—Section 4.4	dacitic lavas and intrusions	Tertiary
Marysvale Volcanic Field, USA	Cunningham et al. (1984)—Section 4.4	monzonite and rhyolite stocks	Tertiary
Salar de Gorbea Area, Chile	Cornejo (1987)—Section 4.4	andesites, dacites, forming stratovolcanoes, rhyodacites, forming ignimbrite sheets	Tertiary
Sungsan, Korea	Hyean Goo Cho and Soo Jin Kim (1993)—Section 4.4	acid volcaniclastic rocks	Cretaceous
Cerro Blanco and Agua Shuca, El Salvador	Dill et al. (2000)—Section 4.5	andesitic lavas and tuffs	Tertiary (Pliocene) to Quaternary
La Noemia, Sangal, Socosmayo, El Sol 3, La Providencia, El Guitarrero, Peru	Dill et al. (1997a,b)—Section 4.5	rhyolite, andesite, dacite, latite, trachite (lavas and tuffs)	Tertiary
La Vanguardia, Chile	Dill et al. (1995a)—Section 4.5	diorite, andesite	Cretaceous to Paleocene
Desa Toraget, Indonesia	Dill et al. (1995c)—Section 4.5	andesites, trachyandesites (lavas and tuffs)	Tertiary (Pliocene) to Quaternary
Tokaj Mts., Hungary	Mátyás (1974)—Section 4.5	rhyolite stocks and tuffs	Tertiary
Variscan Mts., Germany	Strunz (1974), Mücke et al. (1990)—Section 4.6	S-type granites and pegmatites	Lower Carboniferous to Permian

The logarithmic activity diagrams in the system K_2O-SiO_2-Al_2O_3-H_2O, however, do not display a direct phase boundary between muscovite and pyrophyllite at temperatures below 120°C (Bjorkum et al., 1993) so that this reaction may supposed to have taken place between 120°C and 375°C.

APS mineralization			
Associated non-APS minerals	Mineral assemblage	Age of formation	Origin
quartz, calcite, dolomite, rodochrosite, barite, adularia, Cu–Ag–Fe–Zn–Sb sulfides native gold, tellurides, Pb–Sb sulfosalts	alunite	Tertiary	transitional mineralization between high sulfidation and low sulfidation epithermal base metal-Sb–(Au) types
kaolinite, smectite, sericite/high-Mg muscovite/phengite, pyrite, quartz, topaz, fluorite, pyrophyllite, gypsum, K feldspar, biotite	Sr- and P-enriched alunite	Tertiary (early Miocene)	hypogene hydrothermal alunite replacement deposit atop a moderately high fluorine Mo porphyry system
kaolinite, hematite, pyrite, amorphous silica, quartz	alunite, Na alunite, jarosite	Tertiary (early Miocene)	hypogene hydrothermal and steam heated replacement and vein-type alunite deposit overlying a porphyry-type deposit (?)
kaolinite, limonite, white mica, chlorite, chalcedony, opal, tridymite, cristobalite, pyrite, barite, quartz	alunite, natroalunite, jarosite	Tertiary (early to middle Miocene)	hypogene hydrothermal sulphur deposit linked to a solfataric vent systems in a volcanic environment with supergene alteration
dickite, quartz, barite, kaolinite	alunite	data not available	replacement-type alunite deposit
opal CT, cristobalite, amorphous matter, alunogen, aluminite, kaolinite, goethite, smectite, feldspar	alunite–crandallite s.s.s., alunite–woodhouseite s.s.s, gorceixite, florencite, jarosite, dussertite	Tertiary to Recent	hypogene hydrothermal and steam-heated kaolin deposit linked to a solfataric vent systems
quartz, muscovite, halloysite, metahalloysite, kaolinite, dickite, pyrophyllite, smectite, smectite–illite m.l., pyrophyllite, zunyite, topaz	alunite, svanbergite–woodhouseite s.s.s., P-bearing alunite, REE-bearing woodhouseite–svanbergite-s.s.s., florencite-bearing crandallite–goyazite s.s.s. florencite–goyazite	Tertiary (Miocene)	hypogene hydrothermal and steam-heated kaolin and alunite deposit with a zone of supergene alteration superimposed on them
muscovite, kaolinite	Ca–Pb-bearing alunite, woodhouseite–hinsdalite, K-bearing svanbergite–woodhouseite, K-REE-bearing woodhouseite, Ca–Sr-bearing gorceixite, Ca–Sr-bearing florencite, Ca–Sr-bearing florencite	Tertiary to Quaternary (?)	hypogene hydrothermal kaolin deposit
aluminum sulfates, native sulfur, kaolinite	Pb-bearing alunite, Pb-bearing, alunite–woodhouseite s.s.s.	Tertiary to Quaternary (?)	hypogene steam-heated kaolin deposit
kaolinite, dickite, illite, allevardite, cinnabar, quartz, christobalite	alunite	Tertiary (Miocene)	hypogene steam-heated vein-type to replacement-type alunite-kaolin-allevardite–smectite deposits
Li–Mn–Fe phosphates, quartz, feldspar, muscovite	brazilianite, crandallite	Tertiary to Quaternary (?)	supergene vein-like mineralization

Deposition of APS minerals in a lacustrine environment of the Yugama crater lake, Japan is different from the above mode of emplacement (Takano and Watanuki, 1990). It is mainly a function of the concentration of polythionates (sulphane disulphonates) and sulphate in the lake water. Polythion-

ate ions decrease from 2000 ppm to zero and sulphate ions increase from 2500 to 5000 ppm prior to the eruption. During the eruption, the concentration varied inversely. Aqueous reactions of fumarolic SO_2–H_2S gases, which have been fed into the crater lake form the basis for the sulphate compounds that may be captured on the surface of aluminosilicates of volcaniclastic debris. Alunite is supposed to have formed according to the reaction shown by Eqs. (10) and (11). These reaction can account for the temporary increase in SiO_2 and pH values of the lake water from 1.2 to 1.8. The water is far below the solubility line for jurbanite (Fig. 6) and the crater lake is undersaturated even for the highest SO_4^{2-} and Al^{3+} concentrations so that hydrous aluminium sulphates do not precipitate.

T. thiooxidans has been recognised in the on-shore facies of the lake. It constrains the maximum temperature of formation to approx. 40°C (Leduc and Ferroni, 1994). According to Suzuki and Takeuchi (1992), in *T. thiooxidans*, elemental sulphur may be oxidised according to the following stoichiometry (reaction (14)) and thus may offer an additional source to precipitate APS minerals in volcanic lakes.

$$S^\circ + O_2 + H_2O \Rightarrow H_2SO_3 + 1/2O_2 \Rightarrow H_2SO_4. \quad (14)$$

Another direct bacterial leaching of *T. ferrooxidans* may also contribute to the build up of SO_4^{2+} in aqueous medium like that described above and favour the precipitation of S-enriched APS minerals (Bosecker, 1997). The process may be described according to the following reaction (15). MeS stands for the metal sulphide and may involve a direct interaction of *T. ferrooxidans* on sulphides like covellite, stibnite and galena.

$$MeS + 2O_2 \Rightarrow MeSO_4. \quad (15)$$

4.2. APS minerals in porphyry-type and epithermal Au–Ag-base metal deposits

4.2.1. Results

The most promising target area to study APS minerals in igneous rocks, however, is in pervasively altered volcanic and subvolcanic series in island arcs round the Pacific Ocean (e.g. Andean–Caribean Cordillera) or along the Alpine–Himalayan Mt. Range (e.g. Carpathian Mts.) where predominantly alunite s.s.s. occur in the alteration zones of some well-known Cu, Pb, Zn, Sb, Au and Ag deposits (Mitchell, 1992; Erikson and Cunningham, 1993; Dill et al., 1997b) (Table 3).

The genetic link between porphyry Cu–Au deposits and epithermal precious metal deposits has been a long-held premise of magmatic-hydrothermal models of island-arc metallogenesis (Hedenquist and Lowenstein, 1994). In the Maricunga Belt, Northern Chile, several porphyry-type stockworks are overlain by pyrite- and alunite-rich advanced argillic alteration that carry Ba, Cu and S mineralizations (Vila and Sillitoe, 1991). At some places (e.g. La Pepa), the above authors recorded high-grade vein-type Au mineralization of the so-called high sulphidation, epithermal type sensu Hedenquist (1987). This APS mineral-bearing mineralization was also termed such as "acid-sulphate type" by Heald et al. (1987) and "kaolinite–alunite type" by Berger and Hemley (1989). The transition from Au–Cu-bearing stockworks to advanced argillic alteration and high sulphidation epithermal mineralization at shallow levels is shown in a cross section through the Maricunga belt, northern Chile (Fig. 10). Alunite was observed besides kaolinite, siliceous minerals, pyrite and native sulphur in the ore body. The overlying leaching zone is characterised by the depletion in silicates and sulphides, the hydration of anhydrite to gypsum and the precipitation of jarosite in more pyritic alteration types and the goethite in K silicate-rich assemblages. At the surface, jarosite is associated with chalcanthite, scorodite and wavellite.

A similar geological setting was recorded from the Batu Hijau porphyry copper–gold deposit, Sumbawa Island, Indonesia (Meldrum et al., 1994) where various alteration zones were mapped: (1) potassic alteration, (2) propylitic alteration (chlorite–epidote), with both overprinted by (3) intermediate argillic alteration (sericite–chlorite), (4) phyllic (sericite–pyrite), (5) sodic argillic (sericite–kaolinite) and advanced argillic (kaolinite–alunite–pyrophyllite) assemblages near the surface.

A more complex picture than that presented for the transitional zone of the Maricunga belt has been drawn by Perelló (1994) for the Tombulilato district, North Sulawesi, Indonesia. An island arc-type vol-

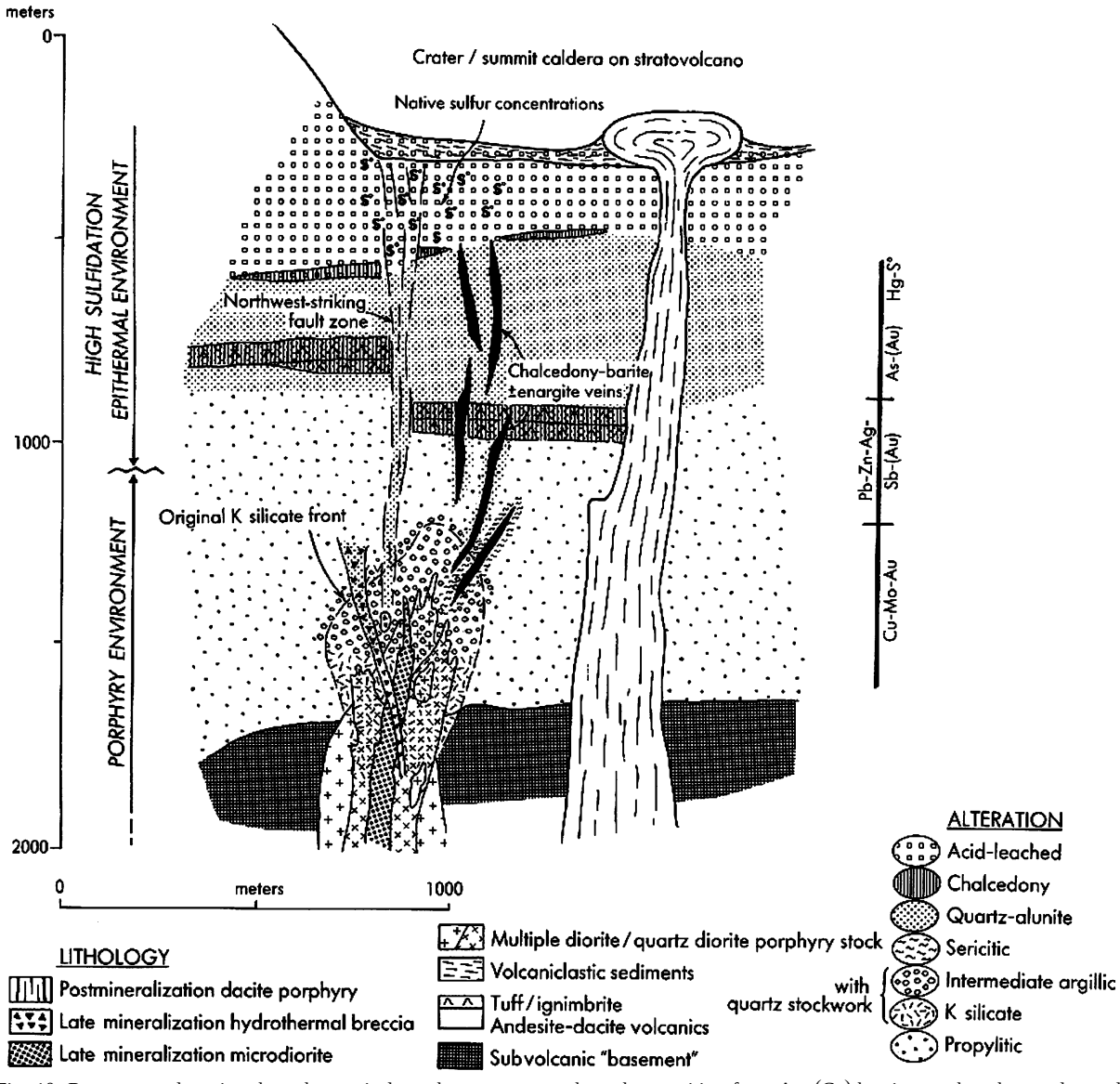

Fig. 10. Reconstructed section through a typical porphyry system to show the transition from Au–(Cu)-bearing stockworks to advanced argillic alteration and high sulphidation epithermal mineralization at shallow levels (Vila and Sillitoe, 1991).

cano-sedimentary pile is intruded by high-level stocks and dikes, and cut by diatreme breccias of late Pliocene and Pleistocene age. Three main mineralization types are present in the district: porphyry Cu–Au; high-sulphidation epithermal Cu–Au–Ag; and low-sulphidation epithermal Au–Ag (Table 3). High-sulphidation epithermal Cu–Au–Ag mineralization displays an alteration pattern consisting of a core of residual (vuggy) silica, bordered outward by zones of quartz-alunite, quartz-kaolinite, and chlorite. Cu–Au–Ag mineralization is contained in the silica core associated with multiphase hydrothermal breccias, which are typically cemented by Fe–Cu–As–Zn–Pb sulphides.

Studies on the "kaolinite–alunite type" precious metal deposits are numerous and have been carried

out in many parts of the world: Summitville, CO, USA, Stoffregen (1987), Baguio, Philippines (Aoki et al., 1993), Masupa Ria, Central Kalimantan, Indonesia, Thompson et al. (1994), Nansatsu-District, Japan (Hedenquist et al., 1994, older examples cited thereunder), Rodalquilar, Spain (Arribas et al., 1995), Crofoot-Lewis, NV, USA (Ebert and Rye, 1997), Spancevo, Macedonia (Kanazirski et al., 1998), Virginia Range, NV, USA, Vikre (1998), Mount Skukum, Yukon Territory, Canada (Love et al., 1998).

The Nansatsu-District, Japan is one of the few sites where APS minerals in precious metal-bearing acid sulphate zones have been investigated in greater detail (Hedenquist et al., 1994). Hypogene alunite includes early formed woodhouseite, which is partly dissolved or replaced by Na- and K-alunite. The P-bearing source mineral apatite is no longer observed in the Nansatsu-District.

The advanced argillic alteration investigated at Baguio, Northern Luzon, Philippines looks quite similar to that from Nansatsu (Aoki et al., 1993). The aforementioned authors outlined the chemical variation of APS s.s.s. throughout epithermal acid sulphate mineralization (Fig. 11). The cores are rich in PO_4 with svanbergite and hinsdalite. Towards the rim, they become richer in Ca leading to minamiite and woodhouseite and eventually gave rise to oscillatory zoned alunite–natroalunite–minamiite s.s.s..

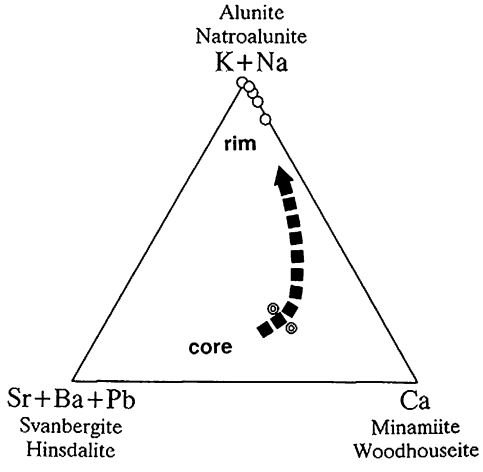

Fig. 11. Chemical variation from core to rim in a crystal of alunite s.s.s. (Aoki et al., 1993).

Alunite associated with some zunyite and oxides occurs in the vuggy silica zone of the Rodalquilar, Spain Au-alunite deposit. In the enclosing advanced argillic zone quartz, alunite I, dickite, illite and pyrophyllite formed. Stage I alunite is chemically heterogeneous and commonly contains turbid core of partially altered woodhouseite–svanbergite, crandallite, and florencite. Its Na/K value is characteristically high (up to 0.4). In the intermediate and sericite zone, alunite is rare. Stage II alunite is fine-grained and has a characteristic pseudomorphic morphology. It forms thin, cryptocrystalline veinlets and is associated with quartz, kaolinite, jarosite, hematite and amorphous silica. Stage II alunite has Na/K values of < 0.05 and is rimmed by bands of Ca- and Sr-APS minerals

4.2.2. Interpretation

Porphyry-type and epithermal ore deposits have overlapping or telescoped alteration patterns but are not contemporaneous. Cu–Au porphyry-type deposits developed in the early stages of igneous activity (Vila and Sillitoe, 1991). Hydrothermal convective cells giving rise to epithermal ore deposits developed later at a more shallow depths. This shift from porphyry-type to epithermal acid-sulphate-type mineralization is accompanied by an increase in APS minerals. APS-bearing, acid-leached rocks are linked to subhorizontal zones of pervasively silicified rocks beneath the paleosurface (Sillitoe, 1991).

Rye et al. (1992) have discussed the systematics of alunite mineralization in these volcanic environments. Magmatic hydrothermal alunite (APS minerals included) are related to intrusion-driven hydrothermal systems which contain magmatic components in the hydrothermal fluids. Steam-heated alunite directly precipitates from the vapour phase. This sort of alunite may be brought about by geothermal systems where ascending H_2S gas is oxidised to give H_2SO_4. Hayba et al. (1986) have called this latter type of APS mineralization "primary supergene". To rule out any confusion when dealing with hydrothermal APS mineralization throughout this review, the following terminology is applied:

- hypogene hydrothermal APS mineralization
- hypogene steam-heated APS mineralization

Fluid inclusion studies in the Nansatsu District gave a mean T_h value of 230°C. The mineralising fluids were relatively oxidising and close to pyrite–alunite coexistence. Hedenquist et al. (1994) have singled out the conditions conducive for high sulphidation or acid-sulphate mineralization: (1) exsolution of fluids from a crystallising magma at depth favour metal fractionation from melt to fluid; (2) the exsolved fluid separates into vapour and saline liquid phase, with the latter being metal rich; (3) the gas-rich vapour (HCl and $SO_2 + H_2S$) ascends to the surface with at least a portion condensed into meteoric water and leaches the host rocks to create a permeable zone; (4) the metal-bearing solutions also ascend into this leached zone and precipitate base metal sulphides and gold. The surface expression of this type of emanation may be called fumaroles or acidic hot springs. In addition to a high geothermal gradient and fractures as conduits a wet climate is held necessary for large-scale convection of meteoric waters in these acid sulphate mineralization (Ebert and Rye, 1997). It favoured the formation of large inland lakes, which provide abundant recharge water for the hydrothermal system. A fluctuating water table controlled by changing climatic conditions enabled steam-heated acid sulphate fluids to overprint lower grade mineralization.

Aoki et al. (1993) found contrasting chemical compositions of APS s.s.s. in hypogene and steam-heated acid sulphate environments. The core of hypogene alunite is commonly enriched in PO_4 and multi-valent cations such as Ca (crandallite, woodhouseite), Sr (svanbergite) and Ba (gorceixite). These complexes are usually rimmed by minamiite and rhythmic bands of alunite s.s.s., alunite and natroalunite. In contrast, alunite formed in a steam-heated acid sulphate environment, overlying boiling neutral pH geothermal waters, lacks the complex core and has a range of composition limited to alunite–natroalunite s.s.s. The sulphur isotopic composition of alunite formed by steam-heated waters is similar to that of coexisting sulphide minerals due to the relatively low temperature of formation and lack of isotopic equilibration. These criteria applied to the Rodalquilar deposit (Arribas et al., 1995) suggest that the APS mineralization is of hypogene magmatic hydrothermal origin. Stage II alunite in this deposit, which has a very low Na/K ratio and rimmed by Ca- and Sr-APS minerals is of supergene origin.

The presence of tourmaline, zunyite, pyrophyllite and dickite constrain the upper limit of the temperature of formation to 375°C (Berman, 1988)—see Eq. (12) (Table 3).

4.3. APS minerals in volcanic-hosted epithermal Au–Sb deposits

4.3.1. Results

In Bolivia several Sb deposits, some of which also abundant in gold, have been under operation since decades (Ahlfeld, 1974). Several of these ore deposits are located in volcanic rocks of Late Tertiary age (Dill et al., 1997b). At Cosuño and Miluri, volcanic edifices made up of a wide spectrum of volcanic and pyroclastic rocks form the host rocks of Au–Sb mineralizations (Fig. 12).

The mineral assemblage at Cosuño and Milluri is extensive. The mineralization consists of a Ag–Au–Zn–Bi–As mineral assemblage with stibnite intergrown with APS minerals. Besides APS minerals quartz, Fe-sulphides, dickite, kaolinite and nontronite may be observed. Acicular crystals of stibnite, are scattered in a yellow earthy matrix made up of euhedral to subhedral crystals of alunite (Fig. 13). This alunite–stibnite mineralization developed in stockworks and small veinlets scattered throughout the apical parts of the pervasively altered Tertiary volcaniclastic rocks (Fig. 12). Massive alunite is the only representative of APS mineralization. Elongated aqueous fluid inclusions of 20–35 μm length in the stibnite, associated with massive alunite mineralization, have been studied by infrared microscopy. Measurements of nine inclusions yielded reproducible temperature values between 85°C and 95°C. Quartz found in a similar position yielded somewhat higher temperatures of up to 102°C, which is assigned also to the APS mineralization as temperature of formation.

In sediment-hosted vein-type Sb–(Au) deposits being located peripheral to the acidic to intermediate volcanic and subvolcanic stocks alunite was observed besides kaolinite, Fe–Sb oxides and Au–Sb oxides at Kharma, Bolivia (Dill et al., 1995d).

In the central Slowak Neogene, volcanic field APS mineralization associated in time and space

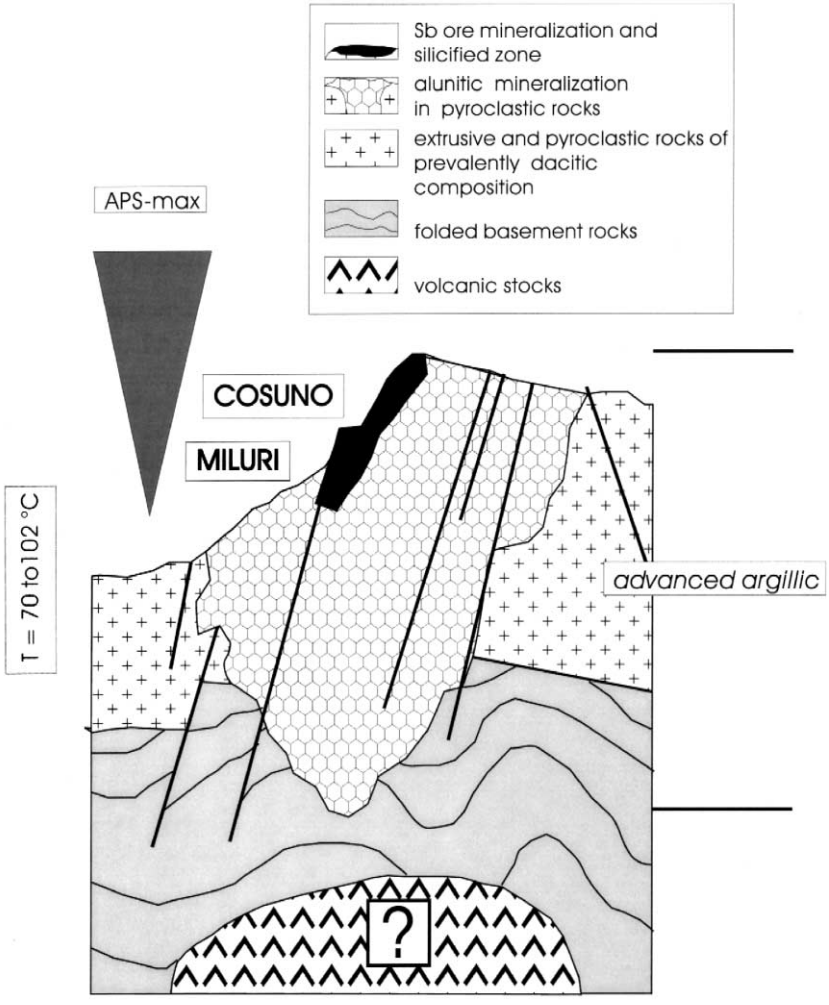

Fig. 12. Diagrammatic section through the APS-bearing volcanic-hosted stibnite deposits in central Bolivia (not to scale).

with Sb mineralization is found in stratovolcanoes near Banska Stiavnica and Kremnica (Haber et al., 1994). According to Pouba and Ilavsky (1986), venting of pyroclastic rocks and lavas took place in the Kremnica Sb deposit during the upper Miocene. The alteration pattern observed at outcrop involves silicification, advanced argillic alteration with alunite, adularia, kaolinite and pyrophyllite as well as sericitisation.

4.3.2. Interpretation

This acid-sulphate-type stibnite mineralization found in and around the dacitic domes indicates hot-spring activity with temperatures below 100°C (first-generation stibnite 85°C to 95°C, second-generation stibnite approximately 70°C, quartz 85°C to 102°C) and a pressure below 300 bar for stibnite deposition. Assuming a hydrostatic pressure gradient this pressure corresponds to a mineralising depth of maximal 3 km and agrees well with an interpretation as hypogene-steam-heated APS mineralization. Hydrothermal activity subsequent to the Tertiary volcanism was responsible for this sort of volcanic-hosted APS mineralization (e.g. Milluri) and for the late-stage alunitic alteration, which affected the shear zone-hosted mesothermal stibnite deposits in the

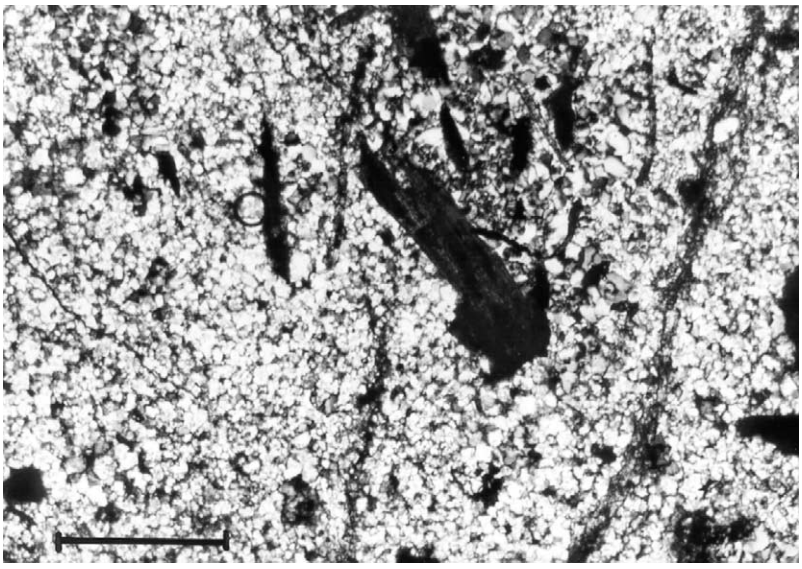

Fig. 13. Micrographs of thin sections from Cosuño, Bolivia acicular crystals of stibnite (black) disseminated in a matrix of equigranular alunite. Fissures penetrating the massive alunitic Sb ore are filled with white mica (subparallel streaks). Crossed polars, scale bar 300 μm.

argillaceous country rocks surrounding the dacitic dome structures. K/Ar dating of alunite from acid-sulphate-type deposits in volcanic domes in Bolivia and Peru yielded a mid-Miocene age of formation (Columba and Cunningham, 1993; Dill et al., 1997a,b).

In Kremnica, precipitation of stibnite in the Sb vein took place in the *T* range 296–156°C. The alunite plays a minor part among the gangue minerals so that this Au–Sb mineralization is considered transitional to what might be called epithermal low-sulphidation or adularia-type mineralization.

4.4. Volcanic-hosted alunite deposits

4.4.1. Results

One of the largest alunite concentrations is located in the western USA in the Red Mountain, Colorado (Bove and Honn, 1990). Alunitized rocks occur in two large conical centres (Fig. 14), grading outward into argillized dacitic rocks and downward through argillic, sericitic, silicic and potassic zones into weakly altered dacitic and brecciated rocks. Various generations of alunite are associated with pyrite and various phyllosilicates (Table 3). First-generation and second-generation alunite derived from fluids having a magmatic source at temperatures between 200°C and 350°C.

The Marysvale volcanic field, Utah, is another volcanic-hosted alunite deposit (Cunningham et al., 1984). The Marysvale deposits in monzonitic lava flows are horizontally zoned outward, from alunitic cores to kaolinitic and propylitic envelopes and are vertically zoned from a lower pyrite-propylitic assemblage upward through assemblages dominated by alunite, jarosite, and hematite to a flooded silica cap.

In the Salar de Gorbea Area (25–26°S latitude), Chile, sulphur deposits evolved together with alunite in the upper parts of stratovolcanoes during the Mio-Pliocene (Table 3) (Cornejo, 1987). Similar to the deposits mentioned above the Salar de Gorbea, volcanoes are also pervasively altered. Two of the alteration zones, argillic and advanced argillic alteration contain APS minerals such as alunite, natroalunite, and jarosite. The zone of silicification with quartz and chalcedony are barren with regard to APS minerals.

Similar to the above deposits in their outward appearance is the Sungsan Mine, Korea (Hyen Goo Cho and Soo Jin Kim, 1993). Alunite is replaced by

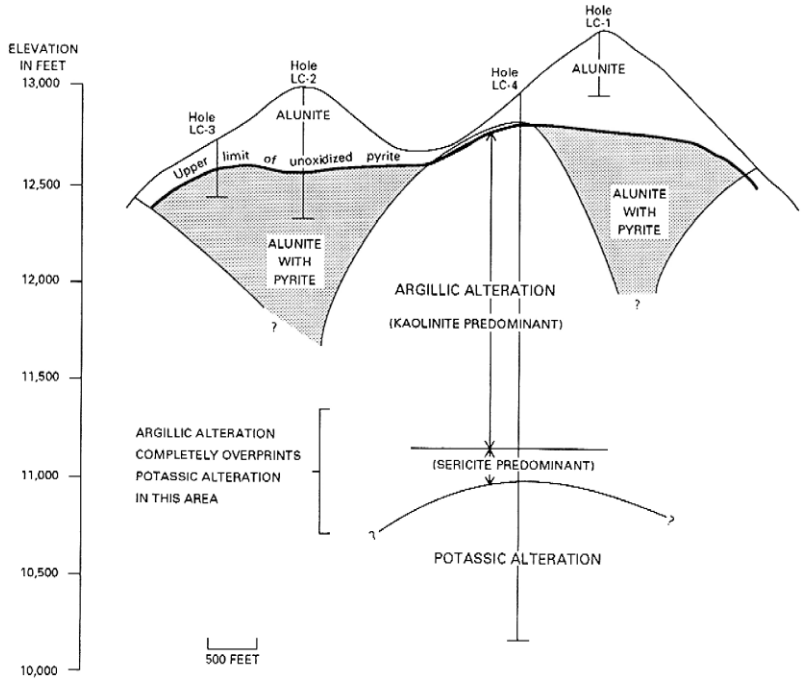

Fig. 14. Cross-section of hydrothermally altered area at the Red Mountain, Lake City caldera, USA (Bove and Honn, 1990).

dickite. The most effective factor for the zoning in alunite is the fluctuation in the composition of mineralising fluids.

4.4.2. Interpretation

Judging by the geological setting and mineralogical textures, the alunite deposit at Red Mountain may be classified as a replacement deposit. Its APS mineralization has formed from a magmatic vapour plume that rose above the level of the meteoric-water-dominated fringe of a weakly mineralised Mo porphyry hydrothermal system at depth (Bove and Honn, 1990). The Sr- and P-content in the alunite point the source material in the parent rock, the feldspar and accessory apatite.

The alunite deposits in the Marysvale volcanic field are of replacement and vein-type (Cunningham et al., 1984). The change from the propylitic zone to kaolinite- and alunite-bearing rocks reflects (1) the boiling or degassing of H_2S and (2) the lower limit of penetration of atmospheric oxygen (Cunningham et al., 1984).

The mode of formation of APS mineralization in the Salar de Gorbea volcanoes is similar to that discussed above for the Marysvale replacement deposit. The fumarolic H_2S gases, which reached the surface of this vent system, were oxidised and caused sublimation of native sulphur.

4.5. Volcanic-hosted APS-bearing argillite deposits

4.5.1. Results

There is no sharp boundary between the alunite deposits mentioned previously and the volcanic-hosted argillaceous deposits that are mined mainly for kaolinite and smectite. Both phyllosilicates are also present, albeit in subordinate amounts, in the mineral assemblages of Red Mountain deposit (Bove and Honn, 1990). Since these deposits are very much attractive for exploration geologists in search of raw materials to produce ceramic goods, fillers and filter material and some of these mineralizations are host of a broad spectrum of APS minerals the volcanic-hosted argillaceous APS mineralization is treated in

a chapter on its own (Leoni and Sartori, 1988; Dill et al., 1997a, 2000). In the following paragraphs, chemical formulae are given in text as it is one of the few studies where the complex APS s.s.s. encountered in nature have precisely been determined.

All case studies in this paper are in volcanic, subvolcanic and volcaniclastic rocks from the circum-Pacific rim: (Ahuachapan geothermal field, W El Salvador (Dill et al. 2000), Cajamarca non-metallic province, W Peru (Dill et al., 1997a), kaolin province Illapel Region, Central Chile (Dill et al., 1995a), kaolin province in the North Arm of Sulawesi, Indonesia (Dill et al., 1995c). The non-APS minerals, which are very diverse in the various deposits, are listed in Table 3.

In El Salvador, in the Agua Shuca kaolin deposit APS minerals make up approximately 12% by volume, whereas in the Cerro Blanco deposit the amount of APS minerals runs up to 7% by volume. The APS minerals are especially widespread in those zones where kaolinite and cristobalite are most abundant.

The intimate intergrowth among APS minerals and their zonation within single crystals can be made visible by means of chemical mapping using TEM-EDX (thickness of APS minerals: 150 Å) (Fig. 15a,b). The APS mineral assemblage at Agua Shuca is enriched in minerals of the alunite group relative to the mineral assemblage of the adjacent Cerro Blanco deposit. Vice versa, minerals of the crandallite-group are more widespread in Cerro Blanco than in Agua Shuca deposits. AS such as alunogen and aluminite are exclusively found in the marginal zone of the Agua Shuca deposits. The amount of jarosite in Agua Shuca is low. Only in microtome sections jarosite crystals may be spotted at the edge of APS minerals. In alunite from the still active fumaroles at Agua Shuca the K/Na ratio has been shifted in favour of K when compared with the K/Na ratio of alunite from Cerro Blanco. Alunite-group minerals and crandallite s.str. precipitated first in the centre of APS minerals. Late-stage jarosite, gorceixite and florencite are responsible for elevated Ba, Ce and P concentrations at the margin of the mineral aggregates.

The results of a joint microchemical and crystallographic study to track down variation in the crystal habit along with chemical changes are shown in the SEM micrographs of (Fig. 16).

Non-metallic deposits operated mainly for kaolin and alunite in the Cajamarca Province in western Peru evolved in Tertiary lavas and pyroclastic rocks (Table 3). The interrelation of the Peruvian mineralizations in space and the variation of APS minerals throughout mineralization in the Cajamarca Province are illustrated in the composite diagram of Fig. 17.

All kandite-group minerals (Weaver, 1989), nacrite excluded, have been determined from the Peruvian kaolin deposits under study: dickite (La Noemia), well-ordered kaolinite (El Sol 3, Socosmayo, Sangal, La Noemia), moderately well to poorly ordered kaolinite (La Providenica, El Guitarrero), halloysite to metahalloysite (El Sol 3, La Providenica). Second in abundance among the non-APS minerals are siliceous compounds such as quartz (El Guitarrero), cristobalite and opal CT (El Sol 3, La Providencia). In La Noemia zunyite, topaz and pyrophyllite occur as rare constituents—see also Section 4.2.

In La Noemia (two different generations of Na- and K-alunite), Sangal, Socosmayo and El Sol 3 deposits alunite is the sole representative of APS mineralization (Fig. 18).

In La Providencia, alunite is associated, in places, with APS minerals belonging to the svanbergite–woodhouseite s.s.s. The APS mineral assemblage at El Guitarrero is depleted in sulphate. The primary APS mineralization is very complex and contains minerals of the woodhouseite–svanbergite s.s.s., which gradually convert into florencite-type minerals at the edge of the mineral aggregates $(Sr_{0.53}, Ca_{0.28}, REE_{0.11}, K_{0.01}, Ba_{0.03})\ Al_3\ [(OH_6)/(PO_4)_{1.37}\ (SO_4)_{0.63}]$. Ongoing addition of REE to the APS mineralization led to an APS mineral whose formula may be calculated to $(Sr_{0.51}, REE_{0.31}, Ca_{0.09}, K_{0.01})\ Al_3\ [(OH_6)/(PO_4)_{1.72}\ (SO_4)_{0.28}]$. Further depletion in sulphur gave rise to a florencite-bearing crandallite–goyazite s.s.s. $(Sr_{0.38}, Ca_{0.25}, REE_{0.21}, K_{0.03}, Ba_{0.07})\ Al_3\ [(OH_6)/(PO_4)_{1.72}\ (SO_4)_{0.28}]$, which formed an intermediate stage.

Near Combarbalá, Chile, a volcano-sedimentary sequence was subject to strong kaolinization (Rivano and Sepulveda, 1991). In the deposit, two different types of alteration may be encountered. Type I that evolved proximal to the fault zone is enriched in quartz (~ 60%) besides some muscovite (35%) and little kaolinite (~ 5%). It is surrounded by the type II

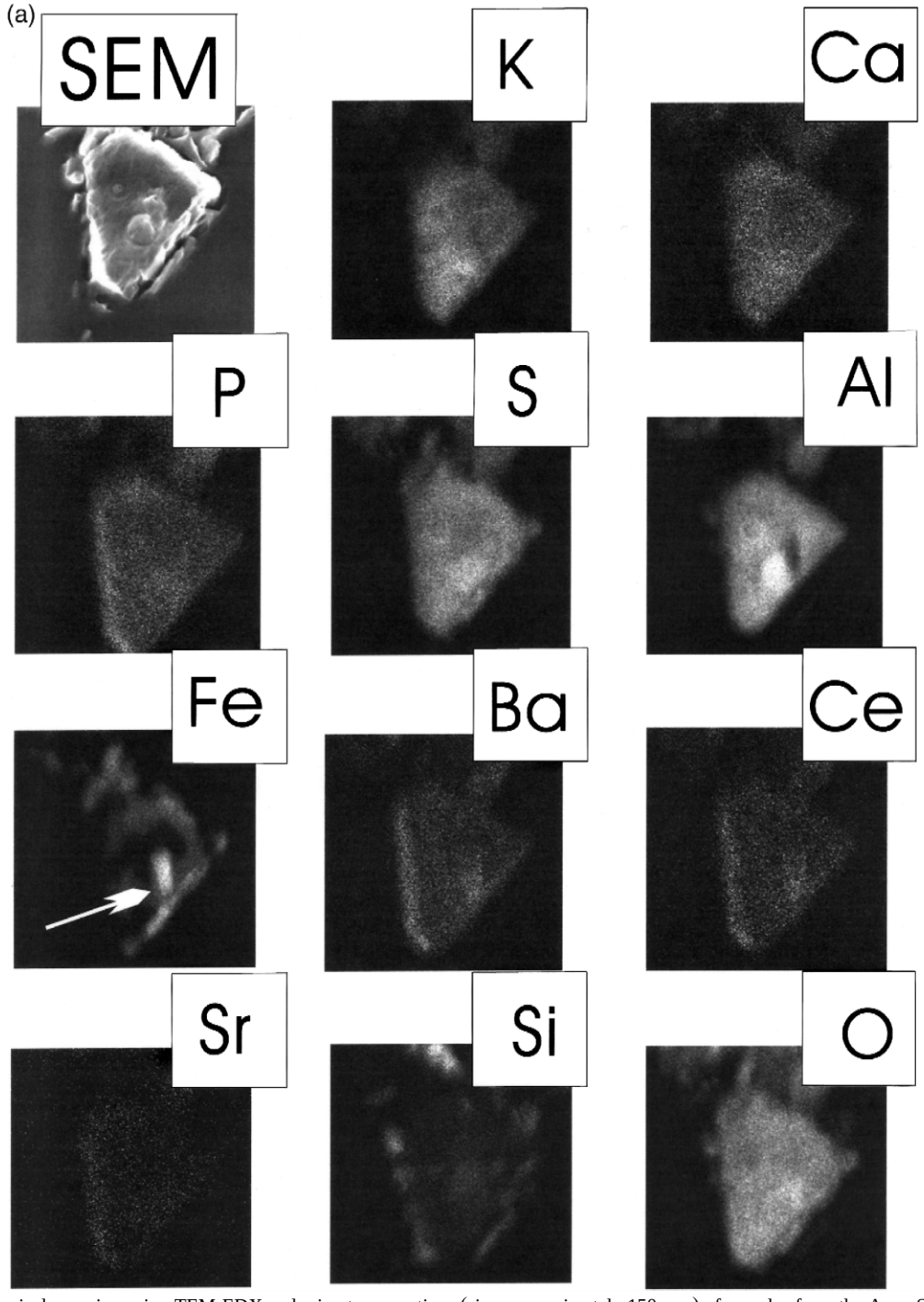

Fig. 15. Chemical mapping using TEM-EDX and microtome sections (size: approximately 150 μm) of samples from the Agua Shuca kaolin deposit, El Salvador. (a) Aluminum-phosphate–sulphate and aluminium-sulphate mineral aggregates. White arrow in "Fe" denotes jarosite overgrowth. (b) Pseudocubic crystals of aluminium-phosphate–sulphate s.s.s.

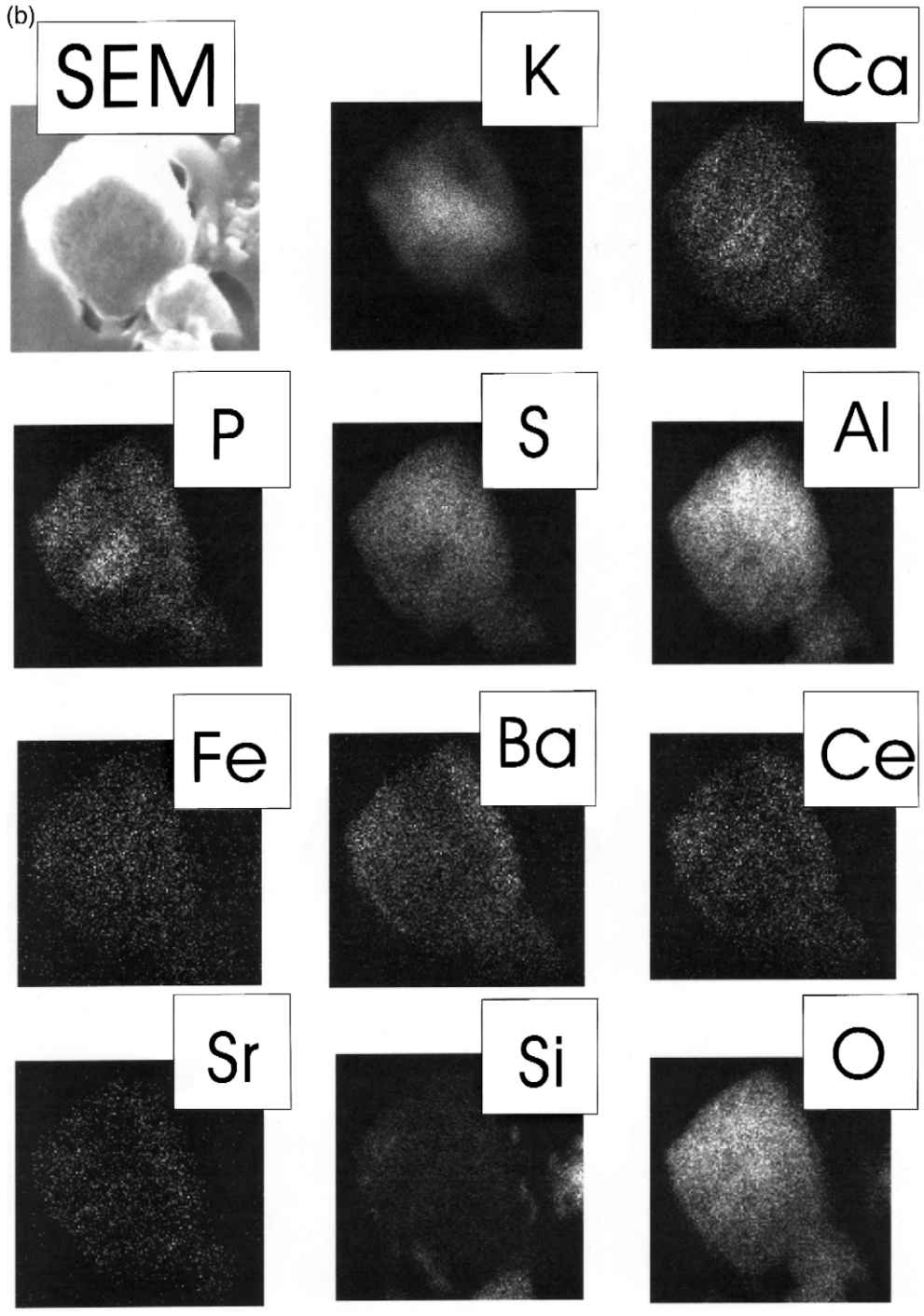

Fig. 15 (*continued*).

alteration zone in which quartz is less abundant (30%) and kaolinite is more abundant than in type I. Type II argillaceous alteration zone is also host to some muscovite (~ 25%). In the silicification/seri-

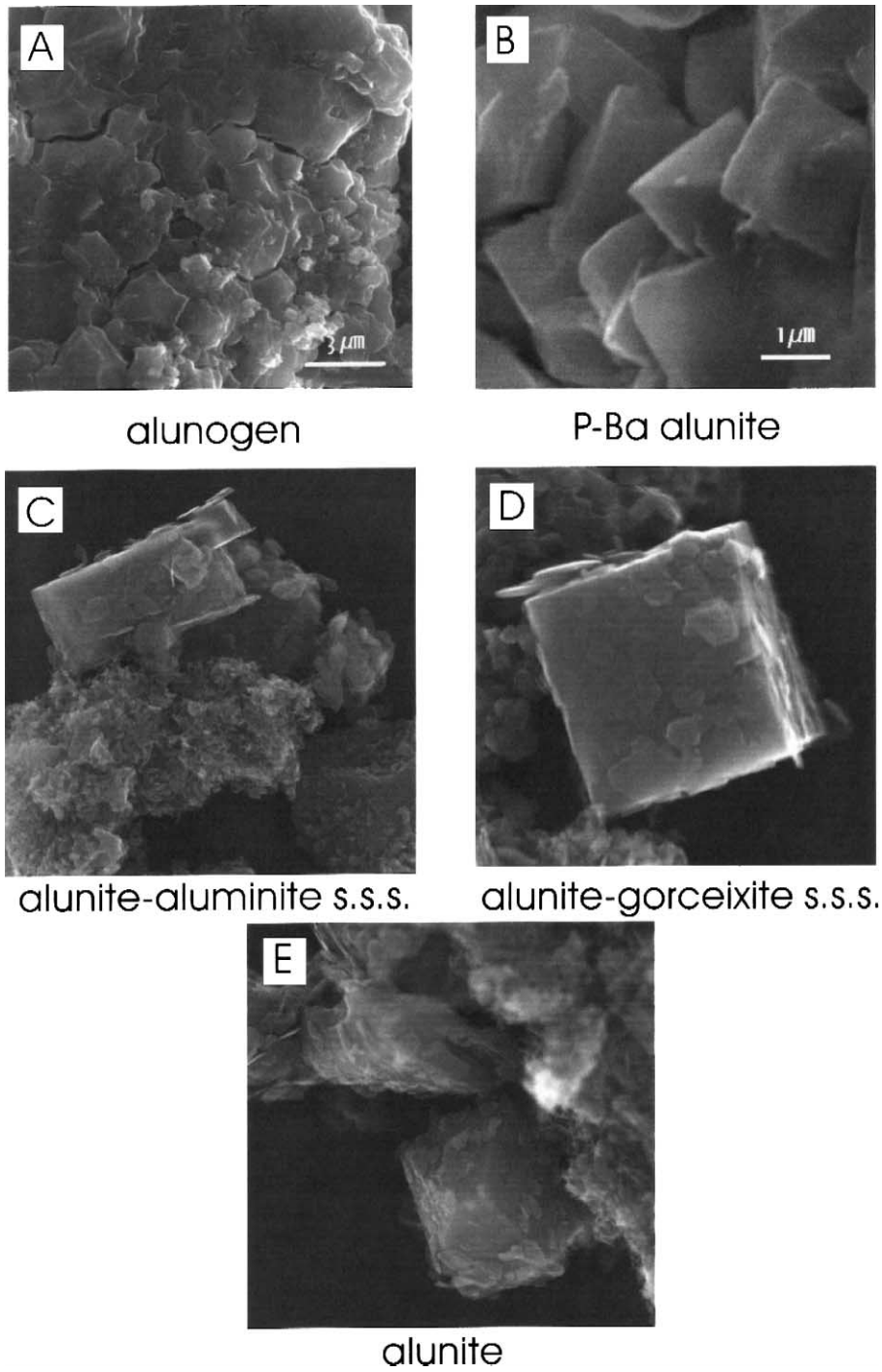

Fig. 16. SEM micrographs to illustrate the variation in the outward appearance of APS/AS aggregates and the crystal habit of s.s.s. along with changes in the chemical composition: (A) alunogen, (B) P–Ba alunite, (C) alunite–aluminite s.s.s. (D) alunite–gorceixite s.s.s. (E) (K-)alunite.

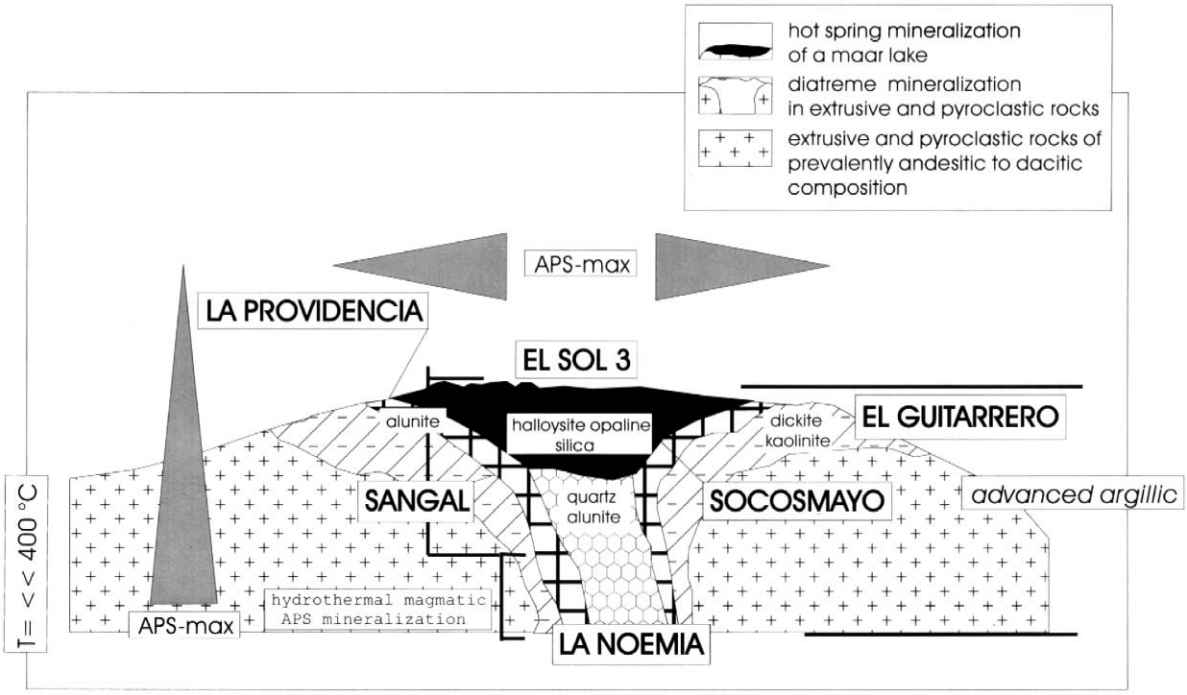

Fig. 17. Diagrammatic section through the APS-bearing kaolin deposits in western Peru (not to scale).

citisation zone, a complex s.s.s. consisting of K-alunite, woodhouseite and hinsdalite predominates among the APS minerals (s.s.s = $(K_{0.63}, Ca_{0.12}, Sr_{0.04}, Ba_{0.03}, REE_{0.01}, Pb_{0.16}, rem._{0.01}) Al_3 [(OH_6)/$

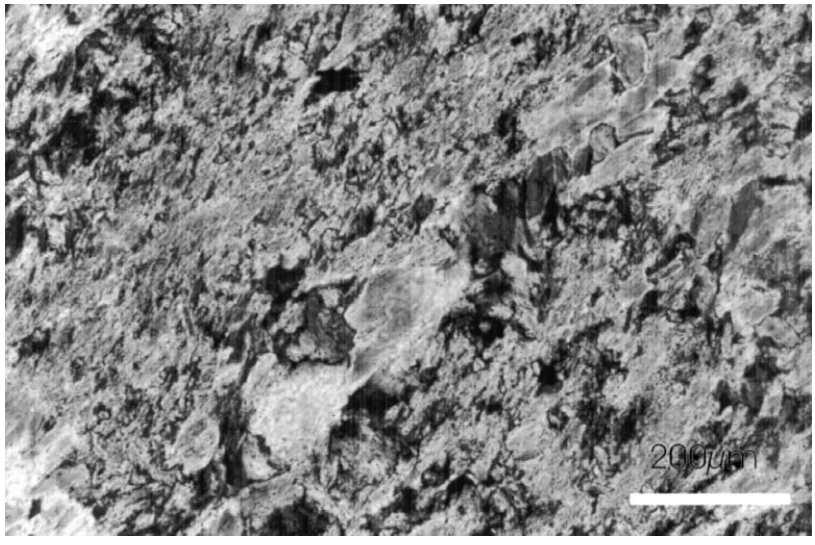

Fig. 18. Minerograph of a thin section displaying structures typical of alunite minerals from Peruvian kaolinite–alunite deposits. Scale bar 200 μm. Crossed polars. High-sulphidation type alteration zone with two generations of P-free alunite. First generation alunite aligned parallel to subparallel to the former bedding of volcaniclastic parent rocks. Phenocrysts of second generation alunite, which crystallised across the layering starting out from fissures. Deposit: La Noemia.

$(SO_4)_{1.59}$ $(PO_4)_{0.41}$]. This complex APS mineral is replaced by a APS mineral, which was identified as K–Sr-bearing woodhouseite ($Ca_{0.50}$, $Sr_{0.17}$, $K_{0.16}$, $Ba_{0.10}$, $Pb_{0.05,}$ $rem._{0.01}$) Al_3 [$(OH_6)/(PO_4)_{1.38}$ $(SO_4)_{0.62}$]. In the type-II alteration zone, the quantity of APS minerals increases by three orders of magnitude relative to type-I alteration. APS mineralization starts out with a woodhouseite–hinsdalite–alunite s.s.s.—($K_{0.72}$, $Pb_{0.19}$, $Ca_{0.13}$, $Sr_{0.04}$, $Ba_{0.01}$, $REE_{0.01}$) Al_3 [$(OH_6)/(SO_4)_{1.73}$ $(PO_4)_{0.27}$]. The APS mineral closely resembles that s.s.s. found in the zone of silicification, yet the amount of alunite has increased in the s.s.s.. This alunite-selective s.s.s. among the APS minerals is accompanied by various APS minerals, which have one thing in common a strong depletion in sulphate: K-REE-bearing woodhouseite ($Ca_{0.51}$, $REE_{0.17}$, $K_{0.14}$, $Sr_{0.10}$, $Ba_{0.01}$, $Pb_{0.06}$) Al_3 [$(OH_6)/(PO_4)_{1.50}$ $(SO_4)_{0.50}$], Ca–Sr-bearing gorceixite ($Ba_{0.61}$, $Ca_{0.16}$, $Sr_{0.14}$, $K_{0.04}$, $Pb_{0.04}$, $REE_{0.02}$) Al_3 [$(OH_6)/(PO_4)_{1.84}$ $(SO_4)_{0.16}$], Ca–Sr-bearing florencite ($REE_{0.44}$, $Sr_{0.25}$, $Ca_{0.24}$, $K_{0.01}$, $Pb_{0.06}$) Al_3 [$(OH_6)/(PO_4)_{1.89}$ $(SO_4)_{0.11}$], crandallite–goyazite ($Sr_{0.41}$, $Ca_{0.38}$, $Ba_{0.06}$, $REE_{0.06}$, $K_{0.05}$, $Pb_{0.03}$) Al_3 [$(OH_6)/(PO_4)_{1.98}$ $(SO_4)_{0.02}$].

The Desa Toraget kaolin deposit, Indonesia, lies in a caldera that is rimmed by Quaternary stratovolcanoes, which make up the Neogene North Sulawesi Volcanic Arc (Kavalieris et al., 1992). The matrix of the APS mineral assemblage consists of 90% kaolinite. Quartz is second most in abundance making up 8% of the claymud. The APS mineralization is dominated by alunite ($K_{0.75}$, $Pb_{0.09}$, $Ca_{0.08}$, $Sr_{0.04}$, $Ba_{0.03}$) Al_3 [$(OH_6)/(SO_4)_{1.79}$ $(PO_4)_{0.21}$], which bears some Pb and Ca. Increasing contents of Ca at the expense of K and of phosphate at the expense of sulphate triggered the precipitation of woodhouseite–alunite s.s.s. ($K_{0.55}$, $Ca_{0.28}$, $Sr_{0.07}$, $Pb_{0.07}$, $Ba_{0.03}$) Al_3 [$(OH_6)/(SO_4)_{1.53}$ $(PO_4)_{0.47}$]. AS minerals and native sulphur are present at the edges of the outcrop.

Similar deposits are being operated for APS and clay minerals in NE Hungary (Mátyás, 1974) (Fig. 1). In the largest deposits in the Tokaj Mts., Hungary, near Mád Királyhegy, allevardite was identified in addition to the common 7, 10 and 14-Å phyllosilicates. The central zone of the deposit contains opal and cristobalite. Towards the margin, the siliceous mineralization gives way through a alunite–dickite–kaolinite mineralization to smectite and the aforementioned allevardite. As a rare constituent, cinnabar has been recorded from this mining site. At Kabutar-Kuh kaolin deposit, E-Iran the mineral association of economic is kaolinite–alunite–pyrophyllite (Golestaneh et al., 1988). On the Isle of Milos, Greece, the above proportion has been shifted in favour of alunite (Marcopoulos and Katerinopoulos, 1986).

4.5.2. Interpretation

The temperature of formation may be constrained based on examination of the paragenetic sequence and direct temperature measurements of the mineralising fluids at outcrop. The analyses of S, O and H isotopes successfully applied by Rye and Stoffregen (1995) and Stoffregen et al. (1994) to temperature determination of the APS elsewhere is hampered in these case studies by the very fine-grained size of APS minerals, their complex zonation and the intimate intergrowth of the different mineral species.

In the argillaceous deposits, which formed from active fumaroles, the fluid temperature of the main stages may directly be obtained through sampling of fluids vented from numerous brine pools in the geothermal field near Ahuachapan; El Salvador—140°C to 250°C (Ripperda et al., 1991)—and the non-indurated claymud of the APS mineralization at northern Sulawesi—approximately 60°C.

The temperature regime operative in main stage of the K–Na alunite–kaolinite deposit La Noemia may be assessed by considering the minerals dickite and pyrophyllite associated with APS. The maximum temperature of formation of the alunite–kaolinite mineralization may be around 325°C to 400°C—see reaction (12). Experimental studies of well-ordered kaolinite, dickite and pyrophyllite lend support to this temperature determination (Winkler, 1976; Shelley, 1993).

The La Noemia, Peru, Cerro Blanco, El Salvador, and La Vanguardia, Chile, non-metallic deposits are grouped among the magmatic hydrothermal APS mineralizations. These vein-like, columnar or cylindrically shaped APS mineralizations display a conspicuous zonation on various scales due to the considerable fractionation of the fluids throughout mineralization with sulphides, mainly Fe disulphides, as a typical marker mineral in the field. A complex core zone is rimmed by rhythmic bands of APS

minerals of various chemical composition. Their mineral assemblages developed at a fairly high temperature. This idea is corroborated also by the presence of minerals like zunyite and topaz in some of these sites.

In these acid sulphate systems, sulphuric acid is produced by the disproportionation of SO_2 with decreasing temperature according to reaction (16) (Holland, 1965; Rye et al., 1992).

$$4SO_2 + H_2O \Rightarrow 3H_2SO_4 + H_2S. \quad (16)$$

The La Noemia mineralization mirrors the incipient stages of a maar volcano or near vent facies. Hypogene APS mineralization at Sangal is younger than the alunite–kaolinite mineralization at La Noemia and certainly formed at a lower temperatures as may be inferred from the lack of pyrophyllite and dickite. By contrast with the early eruptive stages at La Noemia, no hydrofractured breccias or pipelike structures may be encountered. The magma got depleted in H_2S (low-alunite mineralization) and was emplaced off the feeder channels (distal vent facies).

The mineralizations Socosmayo, El Sol 3 and part of La Provindencia pertain to the group of steam-heated alunite mineralizations. The aqueous fluids, which discharged in these depressions gave rise to subaerial siliceous sinter with alunite, cristobalite, opal CT and tridymite. The near-surface silica–alunite–kandite mineralizations resulted from a late stage hydrothermal event within a lacustrine environment, with Socosmayo deposit closest to the feeder channels (kaolinite–alunite). Compared with alunite from previous stages, this alunite is finer-grained and peppered throughout the argillaceous country rocks. Outwards the hypogene, high-alunite mineralization at Socosmayo gives way through low-alunite mineralization at El Sol 3 (halloysite–alunite-silica) to those rich in smectite, kaolinite, halloysite, alunite, silica and APS minerals at the margin of these ephemeral shallow lakes (La Providencia). The most recent hot spring facies of this maar may be accounted for by degassing during periods of volcanotectonic quiescence. H_2S outflows were oxidised near or above the water table resulting in the precipitation of alunite, kaolin and some residual silica.

In the steam-heated environments of Peru, in the geothermal fields of western El Salvador and Desa Toraget sulphuric acid is produced by oxidation of H_2S distilled off an underlying hydrothermal system above the water table according to the reaction (17).

$$H_2S + 2O_2 \Rightarrow H_2SO_4. \quad (17)$$

The steam-heated APS occurrences are less diversified with regard to their mineral associations and mostly show a massive, mushroom-like or layered structure in contrast to the more vertical extension of the magmatic hydrothermal APS mineralizations.

Kaolin deposits with little APS minerals as at El Guitarrero and part of La Providencia being located on a peneplanation resulted from chemical weathering of pyroclastic rocks. Its textures have been interpreted in terms of evolution of a paleosol or saprolite. Precipitation of REE-enriched APS minerals unequivocally formed from per descensum processes (Dill et al., 1997a,b)—see also Section 3.6.

4.6. APS mineralization in granitic and pegmatitic rocks

4.6.1. Results

Many high silica S-type peraluminous plutonic rocks are notably enriched in P (London, 1992). Rare-element pegmatites and compositionally similar granites of western Europe can contain greater than 1.5 wt.% P_2O_5. Despite their rather high-P contents and the close spatial link with alumosilicates, APS mineralization is not very common in granitic and even P-bearing pegmatites. In the central part of an alkali feldspar pegmatite near Hagendorf, Germany, Li–Mn–Fe phosphates formed in the apical parts of a quartz core (Mücke et al., 1990) (Fig. 19). As a rare constituent, secondary brasilianite was observed among the primary phosphates in the Hagendorf pegmatite. Elsewhere in the NE-Bavarian pegmatite province crandallite was spotted, in places, in the gauge of faults (Strunz, 1974).

4.6.2. Interpretation

The primary Li–Fe–Mn phosphates evolved at very high temperature between 600°C and 440°C following the formation of the feldspar–quartz–mica–cleavelandite assemblage (Mücke et al., 1990). Secondary phosphates such as the APS minerals mentioned above came into existence at a much lower temperature 300°C and so (see also the experimental results published by Schreyer (1987),

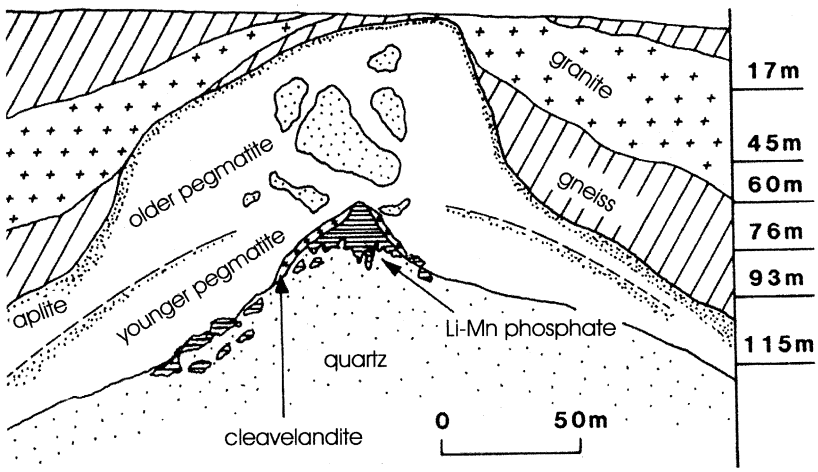

Fig. 19. Cross-section through the Hagendorf pegmatite to show the phosphate-bearing central zone (Mücke, 1991).

Section 5). During these late-stage hydrothermal processes, the alumosilicates were left untouched and the resultant Al-limitation prevented APS minerals to form. Rarely crandallite is observed in fractures and fissures associated with fault gauge that was washed into these cavities from above when these granites were subject to supergene alteration (see Section 3.6). Alunite s.s.s. or woodhouseite e s.s.s. are absent in the zones of late stage hydrothermal granitic alteration as these alteration took place also under conditions of strong S-limitation.

5. APS minerals in metamorphic rocks

5.1. Results

The metamorphic rocks have been subdivided in many different ways based on: parent material, heat source and physicochemical conditions (Winkler, 1976; Shelley, 1993). Among this scenario APS minerals, however, are restricted only to a very peculiar group of metaclastic rocks that were brought about through processes of regional metamorphism.

Lazulite, goyazite, brazilianite and palermonite are found in sandstones and conglomerates of the Verrucano (Brianconnais) near Giogo di Toirano, Italy (Cortesogno et al., 1987). The phosphates constitute the matrix of the metaclastic rocks and occur in veins cutting through metamorphic rocks, which underwent greenschist facies regional metamorphism. At the Passo di Vizzi, NE Italy, a metaquartzite horizon bearing Al phosphates occurs over several kilometres in the Penninic Lower "Schieferhuelle" units of the Tauern window (Morteani and Ackermand, 1996). The horizon contains the following type of mineral associations: (1) lazulite, crandallite–goyazite, apatite, tourmaline, (2) lazulite, svanbergite–goyazite, bearthite, apatite, celestite, (3) staurolite, chlorite, tourmaline. The maximum P–T conditions of the metamorphism were established to be 550°C and 10 kbar.

In the "Fischbach" window NE Styria, Austria, upper Permian to Scythian, metapsammitic and metapsephitic rocks are exposed (Bernhard et al., 1996). Three different types of phosphate-bearing minerals associations have been recorded from these metamorphic rocks: (1) svanbergite, florencite and lazulite phosphate enrichment, (2) augelite, svanbergite, goyazite, lazulite, (3) Ba-free goyazite, Sr-free gorceixite and crandallite. Tremolite present in metacarbonate rocks associated with the metapsammitic and metapsephitic rocks points to greenschist facies conditions.

Studying peraluminous metamorphic rocks Schreyer (1987) found APS minerals making up a considerable proportion of the mineral assemblage as well as metamorphic minerals that may be traced

back to APS parent minerals. In an Archaean greenstone belt at O'Briens, Zimbabwe, part of a volcanic pile containing ultramafic and some more acidic igneous rocks was converted in corundum-fuchsite rocks where andalusite, fuchsite and corundum form pseudomorphs after alunite (trigonal, pseudocubic XX). In the Hillsborough pyrophyllite mine, N Carolina, USA, among the country rocks of the massive pyrophyllite body alunite quartzites were encountered. Under the microscope, these metamorphic rocks show well-oriented elongated blades of alunite after (001). EMP analyses yielded a Na alunite ($K_{0.58}$–$Na_{0.42}$). The alunite contains additional F, which is also present in the associated mineral topaz. Besides alunite and pyrophyllite, the quartzites carry topaz, lazulite and APS minerals of the florencite–woodhouseite–svanbergite s.s.s.

Similar peraluminous APS-bearing metamorphic rocks were recorded from Cuba where andalusite–alunite rocks were described by Velinov et al. (1983) and from Sweden where svanbergite-bearing and lazulite–rutile-bearing rocks were studied by Geijer (1963). Nagy and Ivancsics (1995) recorded florencite from the mica schist belt of the Sopron Mts., Hungary, and Ek and Nysten (1990) florencite together with augelite, berlinite, souzalite and wyllieite from the Håsjöberg and Hökensås kyanite deposits, Sweden.

5.2. Interpretation

The APS mineral associations is, locally, more diverse than in igneous or sedimentary rocks (see, e.g. palermonite that points to Li enrichments). The prerequisite for APS minerals to crystallise during metamorphic process is a peraluminous source rock. It may have originated from temporary lacustrine processes (Cortesogno et al., 1987), coming into existence under sabkha-like conditions with Na leached by flash waters (Morteani and Ackermand, 1996) or derived from postvolcanic hydrothermal processes (Schreyer, 1987). Some kyanite deposits enriched in APS minerals and rutile are likely to have formed from saprolites or bauxites. The unaltered equivalents of these environments of APS deposition are dealt with in Sections 3 and 4, respectively. Premetamorphic alunite may be pseudomorphosed giving rise to the various types of metamorphic minerals:

- alunite ⇒ corundum + fluid
- alunite + quartz ⇒ andalusite + fluid
- alunite + quartz ⇒ muscovite + fluid.

Na-alunite occurs side-by-side with pyrophyllite in the mineral assemblages of the near vent facies of hydrothermally altered volcanic rocks and, not surprisingly, it is also stable under low-grade regional metamorphism (Eqs. (12) and (13)). Pyrophyllite may survive retrograde metamorphism, coexisting andalusite does not, and it becomes partly hydrated. This is also the case in some high-P and high-T peraluminous metamorphic rocks containing primarily kyanite and sillimanite, respectively. APS minerals are produced by retrograde metamorphism (Ek and Nysten, 1990). In the phosphate enrichment in Austria, APS minerals are suggested to have derived from metasomatic reactions. Extensive fluid activity caused mobilisation of sedimentary phosphates and concentration in quartz veins. (Ba-free goyazite, Sr-free gorceixite and crandallite rim around vein lazulite and svanbergite are held to be supergene phosphate minerals. Experimental studies showed that alunite can be stable up to about 400°C at 1 kbar fluid pressure. The reaction during mineral transformation is governed by the activities of H^+, K^+, and SO_4^{2-}, which are likely to decrease as H_2O is released from the enclosing metavolcanics.

6. Manmade APS concentration—acid mine drainage and alum production

6.1. Results

For nearly all pit lakes, SO_4 is the dominant solute (jurbanite and alunite), but is limited by gypsum solubility (Tilley and Gunter, 1988; Böttcher, 1997; Eary, 1999). Fluorite, calcite, and barite are also important solubility controls. One of the most widespread minerals left after alum production and visible in nice dripstones and flowstones in opencast and underground mines operated for alum production is diadochite (Rosendahl and Krause, 1996).

6.2. Interpretation

Trends observed in pit lakes are indicative of sulphide mineral oxidation and evapoconcentration is responsible for acidic conditions. In waste dumps or during the former alum production, organo-mineralogical processes are decisive for the quality of the leachate. The processes resemble supergene alterations mentioned in the previous sections (see reactions (14) and (15)).

7. Discussion

7.1. Supergene vs. hypogene APS mineralization

APS mineralization is formed under oxidising conditions mostly at shallow depth. The question of whether an APS mineralization is of hypogene or supergene origin is often difficult to answer. This question is, however, not only of academic interest. It is essential also to the evaluation of APS minerals in alteration zones when used as a guide to precious metal-bearing ore and it is of importance when an APS mineralization containing REE or radioactive elements is assessed as to its economic potential and its extension towards depth. Discrimination of hypogene and supergene APS mineralization can be performed using the wide spectrum of geological, mineralogical and chemical features typical of these two different types of deposit.

"Supergene s.str." or "secondary supergene" sensu Hayba et al. (1986)—see also Section 4.2—by definition formed from superficial or atmospheric oxidation of primary sulphides in a weathering environment. By contrast, "hypogene" APS mineralization originated from magma-driven hydrothermal or geothermal systems.

Some geological features unequivocally point to an emplacement of APS mineralization by per descensum processes. In La Providencia, Peru, APS-bearing kaolin is extensive in two dimension (Section 4.5) and accumulated on an old peneplain cutting through volcanic rocks (Vidal, 1987). APS and AS minerals found in coal mines along stopes and underground galleries as well as yellow staining and mottles in open casts have, without any doubt, been triggered by the current mining operation (Section 3.4). The same holds true for APS minerals in present-day soil (Section 3.5). The thick argillaceous saprolite gradually evolved from the underlying bedrock leading to a vast blanket of argillaceous material (Section 3.6).

Mineralogical criteria may sometimes help to narrow the space of speculation on supergene or hypogene. Alunite–jarosite mineralization is often characteristically massive, cryptocrystalline and porcelaneous in aspect. Supergene alunite commonly approaches the K end-member composition in the s.s.s.. Frequently, an admixture with or partial replacement by jarosite may be encountered. The question whether vein-like APS mineralization in argillaceous–carbonaceous environments (Section 3.3) is supergene or hypogene cannot in every place be answered with certainty. In those sites, where APS minerals are paragenetically linked to REE phosphates such as monazite, xenotime and U "black ore" (e.g. brannerite, uraninite) hydrothermal solutions may have contributed to the APS mineralization (Rojkovič et al., 1999). In the vein-like deposits from Sudan, the APS minerals are closely linked to a U mineralization in radioactive disequilibrium that points to a supergene mode of formation (Dill et al., 1991).

Chemical investigations using trace elements and isotopes are often the most efficient tool to disentangle this problem of per ascensum vs. per descensum. Jarosite and alunite, which formed together with a variety of oxides in the oxide zone of the ore bodies of Carlin-type deposits are due to weathering (Arehart et al., 1992). Sulphur isotope composition of alunite from several SHDG deposits are virtually identical to those of sulphides, suggesting that alunite sulphur came from quantitative (closed-system) oxidation of primary sulphides during weathering. Sulphur and oxygen isotope composition of barite are markedly different from those of alunite. The O- and H-isotope composition of alunite fall in the supergene alunite field, data for cogenetic kaolinite fall on the kaolinite line, whereas those for hypogene kaolinite do not. K/Ar ages of alunite that sometimes are much younger than the sulphide mineralization may advocate in favour of supergene origin of APS mineralization when these age data are correlative with ages of geomorphologic or hydrologic processes elsewhere in the study area (e.g. age of weathering,

peneplanation) (Arehart et al., 1992; Sillitoe and McKee, 1996).

Detailed chemical and mineralogical studies of weathering profiles bearing REE-enriched APS minerals such as Nd goyazite or florencite proved REE to be an efficient tool to describe the supergene processes operative and to assist in distinction of hypogene and supergene argillaceous alteration zones (Maksimovic and Panto, 1995; Walter et al., 1995; Dill et al., 1997a,b). The REE patterns of these APS mineralization showed that weathering processes may cause an enrichment and also fractionation of LREE and HREE (Banfield and Eggelton, 1989). In Fig. 20, the major REE are plotted vs. Ba + Sr. Those APS-bearing argillaceous zones that formed during supergene processes are significantly enriched in REE relative to hypogene equivalents. There is predominance of some species of APS minerals in saprolites while others are relatively seldom and the REE selectivity of some APS minerals may be explained in terms of their thermodynamic stability (Fig. 9).

7.2. The source of major elements

In igneous rocks, one source of P is phosphate accommodated in the lattice of accessory minerals such as apatite, monazite and xenotime, which appear during the later stages of magma differentiation (see also Section 4.6). During unroofing and denudation of the crystalline rocks, these accessory P minerals may survive when the chemical weathering was moderate and they re-appear together with other heavy mineral in clastic rocks (Dill, 1998). In Ca-poor peraluminous intrusives or S-type igneous rocks, which often form the parent material of supergene and hypogene APS mineralization alkali feldspar constitutes another reservoir of P (alkali feldspar in pegmatite: > 0.3 wt.% P_2O_5, granites > 0.6 wt.% P_2O_5, individual values > 1 wt.% P_2O_5) (London, 1992). Incorporation of P in alkali feldspar occurs along a vector represented by the exchange operator $AlPSi_{-2}$. Which source has contributed most to the P-budget of secondary APS mineralization can hardly be determined for rocks that contain both sorts of P-bearing minerals. In environments of formation where organic material is a major constituent, the sources of P are much more diverse than in pure siliceous rocks.

There is not a unique organic or inorganic source of P to produce APS minerals in coal. Swaine (1990) regarded P in coal as a trace element mostly lying below 1000 ppm P and concluded that it is likely present in phosphates, with an uncertain proportion

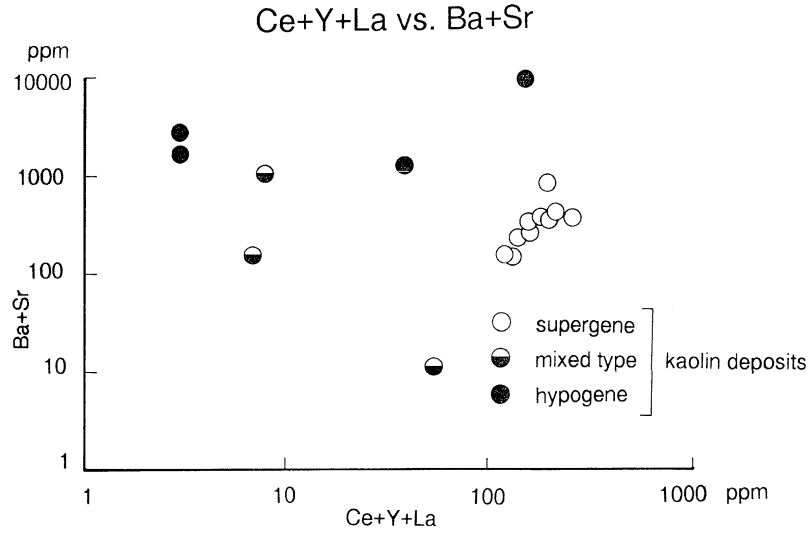

Fig. 20. Cross plot of Ce + Y + La vs. Ba + Sr to distinguish between supergene and hypogene APS-bearing kaolin deposits (Dill et al., 1997a,b).

of organically bound P. In the organic material, lycopods reportedly contain up to 7.4 wt.%.

Phosphate minerals in the parent rock of APS mineralization not only deliver the phosphate necessary to the built-up of APS minerals but they may also form the source of the REE accommodated in the APS s.s.s.. The chemical results derived from investigation of carbonaceous sedimentary rocks and coal suggest that REE elements share in two different groups of host minerals. Phosphates are LREE-selective accumulating prevalently Ce, Pr, Nd, Sm, Eu, Gd, Tb and Dy. Fe-bearing minerals preferentially concentrate Ho, Er, Tm, Yb and Lu. This pattern of REE selectivity in the parent rock is a mirror image of what has been observed during investigations of APS mineralization, which evolved on Precambrian metabiolites (Dill et al., 1991). Notably, LREE from Ce to Er are linked with ferricretes, whereas the remaining HREE are concentrated in phosphates of the crandallite–woodhouseite s.s.s, a group of minerals that may locally become abundant in coal as well (Ward, 1978; Triplehorn and Bohor, 1983; Rao and Walsh, 1997).

In addition to the REE held in the lattice of phosphates and loosely bound to oxides, the absorption of REE onto organic compounds has to be envisaged when the fractionation of LREE and HREE in coal is concerned. Laboratory experiments suggest the ability of HREE to form strong complexes with organic compounds (Eskenazy, 1998). The maximum quantity of REE was absorbed on organic matter in the pH range of pH 3–5 according to the laboratory trials by Eskenazy (1998). This is also the range in which the APS minerals used to form.

In contrast to P which is a true trace element in coal sulphur acts as a major element in many coal seams. Low-sulphur coal ($\leq 1\%$ S) is derived primarily from plant material. Medium- (>1 to $<3\%$ S) and high-sulphur coal ($\geq 3\%$ S) mainly received their total sulphur content from seawater that flooded peat swamps (Chou, 1990). The presence of S-enriched or S-poor APS species or alunite and jarosite during alteration of the coal may be taken as a clear-cut evidence on whether there was a marine flooding of the peat swamp or not.

The derivation of sulphur in APS minerals may much be better tracked down to the source than the aforementioned elements such as P and REE, because of significant isotope fractionation of sulphur during natural redox processes.

The issue is coupled with the question whether the APS minerals under consideration formed from descending or ascending fluids, which was addressed in Section 7.1. The compilation of sulphur isotopes of SHDG deposits in Fig. 21 shows that the spread of $\delta^{34}S_{CDT}$ of sulphides and APS minerals are overlapping, whereas a contrast may be recognised in the isotopic signature between bedded and vein barite and APS minerals (Section 3.8). All of these data are consistent with a derivation of S in APS minerals from decomposition of primary sulphides (Arehart et al., 1992).

Bird et al. (1990) have studied the S isotope variation of superficial APS minerals, which are representative of APS in regolith, duricrusts and arenaceous host rocks (Section 3.6) and concluded two different types of S. One source of sulphur of supergene alunite and jarosite is the primary sulphide mineralization at depth. The range of isotope values of sulphate (sulphate: $\delta^{34}S_{CDT} + 1.5‰$ to $6.9‰$) is similar to the range of isotope values of sulphides (sulphide: $+1.1‰$ to $+4.6‰$). The second source is very much different from the source mentioned before. $\delta^{34}S$ values of APS minerals in Australian inland salt-lakes (playas) indicate that the sulphate is derived predominantly from marine cyclic sulphate rather than from weathering. Much of the sulphate has blown onto the continent in particulate form by prevailing southwesterly windstream. The $\delta^{34}S$ val-

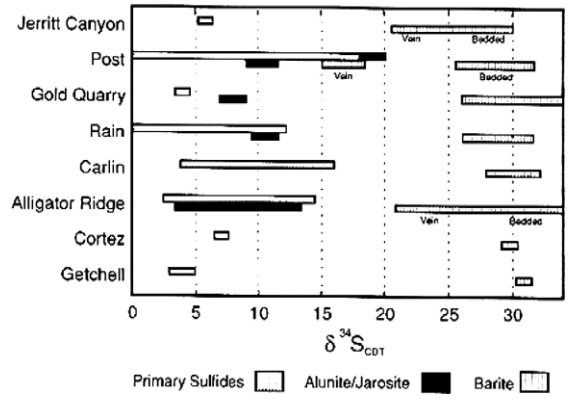

Fig. 21. Compilation of sulphur isotope data of sulphates and sulphides from various sediment-hosted gold deposits (Arehart et al., 1992).

ues of APS from acid salt lakes, a conspicuous feature of semiarid environments, are as high as +18.0‰. Their range of values overlaps with that of gypsum from the same sort of lakes (gypsum: +15.1‰ to +21.0‰).

In the Carlsbad and Lechuguilla limestone cavern, New Mexico, USA, the S isotopes—$\delta^{34}S = +0.1‰$ to −28.9‰—of the APS minerals (Polyak and Guven, 1996) are isotopically much lighter than the APS minerals recorded from the SHDG deposits (Section 3.1). The S isotopes are comparable to the cave gypsum and native sulphur values. Isotopically light sulphur as H_2S was generated from sulphur-reducing bacteria—see also Section 4.1. The caves were partly developed by H_2SO_4 formed by oxidation/hydrolysis of H_2S escaping from spring water.

Sulphur isotope variation in APS mineralization that evolved in black shales (Section 3.3) cluster around $\delta^{34}S = 0$ (Dill et al., 1991). Along a vertical section through the APS mineralization, $\delta^{34}S$ values of $1.55 \pm 0.15‰$ at the bottom of the trench shift to $\delta^{34}S$ values of $0.62 \pm 0.15‰$. Samples taken at outcrop gave much lighter S isotope values of as low as −6.6‰. The studies of the isotopic composition reveal that the sulphate sulphur towards the present-day surface approaches values typical of meteoric sulphur. The isotopically heavier APS minerals at a depth of several meters below ground yield isotope values similar to those of primary sulphides in the (meta) argillites—see, e.g. Cambel and Kantor (1976). The primary source of S in the APS minerals of carbonaceous–argillaceous rocks is held to be biogenic sulphur concentrated by redox processes under continental or marine euxinic conditions.

An unconventional source for S in APS was suspected for sandstone-hosted alunite. The sulphuric acid was produced by the oxidation of hydrogen sulphide that seeped in from the oil field of the area (Khalaf, 1990). The source of sulphur in APS minerals contained in sedimentary rocks are mostly primary sulphides formed during diagenetic processes, their $\delta^{34}S$ data are virtually identical to the precursor sulphides. Bacteriogenic reduction of aqueous sulphate, however, may modify this isotope signature.

In volcanic and subvolcanic rocks, the source of sulphur in APS minerals is pertinent to two principal category. One source is the primary sulphide mineralization, which is subject to atmospheric oxidation. The approach taken during isotopic studies is the same as that taken for SHDG deposits (Arehart et al., 1992) and APS minerals in regolith (Bird et al., 1990). The second source of S lies in the hydrothermal system and the issue is immediately linked to the question where the fluids came from (Rye et al., 1992).

The investigations centred around this question are manifold and successfully carried out when using hydrogen and oxygen isotopes in context with S isotope variation. Most alunites of steam-heated origin have $\delta^{34}S$ values the same as those of precursor H_2S and δD values similar to that of local meteoric water. The isotope values mirror the degree of exchange of meteoric fluids with wall rocks. Magmatic hydrothermal alunite have $\delta^{34}S$ values 16‰ to 28‰ larger than that of associated pyrite, reflecting equilibrium between aqueous H_2S and SO_4 formed by the disproportion of magmatically derived SO_2 (Rye et al., 1992) as recorded by Arribas et al. (1995) for the Rodalquilar deposit ($\delta^{34}S_{\text{alunite 1}} = +22.3‰$ to 31.0‰, $\delta^{34}S_{\text{pyrite}} = 0.3$ to 8.0). Second generation alunite ($\delta^{34}S_{\text{alunite 2}} = +4.1‰$ to 10.4‰) is significantly different and of supergene origin (see previous section). In Baguio, Philippines, the isotopic composition of hydrothermal alunite falls in the range $\delta^{34}S$ +15.0‰ to +24.0‰. (Aoki et al., 1993).

Isotopes at Red Mountain alunite deposit have proven that stages I and II alunites were derived from sulphate having a magmatic source at temperatures between 200°C and 350°C. Stages III and IV alunites were formed from local oxidation of H_2S from the magmatically derived hydrothermal plume as atmospheric oxygen was drawn into the upper levels of the late-stage hydrothermal system (Bove and Honn, 1990). The major portion of APS mineralization derived from a magmatic hydrothermal system, the proportion of steam-heated alunite, which derived from the vapour phase is of minor importance.

The S of replacement alunite in the Marysvale volcanic field derived from underlying Mesozoic evaporites based on S isotopes ($\delta^{34}S_{\text{alunite replacement}} = +11.5‰$ to 15.4‰, $\delta^{34}S_{\text{Na-alunite}} = -5.5‰$ to −0.7‰, $\delta^{34}S_{\text{alunite vein}} =$ near 0‰). Na alunite superimposed on the replacement alunite deposit is distinctly lower in its S isotopic composition and indicates a nonevaporitic source of sulphur. It is

significantly younger than the replacement alunite and related to a separate thermal event. The source for the high Na/K in solutions, which is required to form Na alunite may have been halite-rich evaporites in the underlying Mesozoic sedimentary rocks. The vein-type alunite, which formed in extension fractures above a concealed stock has a magmatic source of S and crystallised in a wet-stream geothermal system (Cunningham et al., 1984). This is also the case in the Mount Skukum epithermal gold deposit, Yukon Territory, Canada where alunite is similar to the Marysvale vein alunite with $\delta^{34}S$ values ranging from -1.75 to $+2.93$ (Love et al., 1998).

The APS mineral association and the silicate mineralization in the same alteration zone may locally have different sources of fluids. Stable isotope results of $\delta^{18}O = 7 \pm 2‰$ and $\delta D = -25 \pm 5‰$ indicate that alunite from Nansatsu, Japan formed from a mixture of magmatic and local meteoric fluids (Hedenquist et al., 1994), whereas the clays in the marginal halo have isotopic composition indicative of a $\delta^{18}O$ shift of 6‰ to 8‰ from local meteoric water.

7.3. Minerostratigraphy of volcanic-hosted APS mineralization and the temperature of formation

Despite many studies focused on porphyry-type and epithermal ore deposits, a precise identification of the various APS species as well as investigations of their evolution in time and space are missing (Aoki et al., 1993; Hedenquist et al., 1994; Arribas et al., 1995; Dill et al., 1995a,b,c, 1997a,b, 2000) In the volcanic rocks under consideration, the APS mineralization may be subdivided into four stages (Table 4). The temperature of formation for the hypogene mineral assemblages of the mineralization has been concluded from paragenetic investigations and is based on fluid inclusion studies dealt with in each case in the previous sections under the heading "Interpretation".

Stage I is a low-sulphate and Ca-enriched prestage prior to the main alunite mineralization (stage II). Acidic hydrothermal solutions percolating through the volcanic edifice decomposed magmatic apatite and provided phosphate and part of the Ca to form APS minerals of the woodhouseite and crandallite s.s.s (reaction (18)). Alunite, if already present in this stage, is enriched in Na. Destruction of alkali feldspar led to the release of aluminium, earth alkaline and alkaline elements necessary for the build-up of APS minerals (Nriagu and Moore, 1984) (reaction (19)). This process of feldspar replacement may also add to the P and Ca budget (London, 1992).

$$\text{apatite} + 3Al(OH)_4 + 9H^+ \Rightarrow \text{crandallite} + 4Ca^{2+} + HPO_4^{2+} + 7H_2O \quad (18)$$

$$3AlO(OH) + (K,Na)^+ + 3H^+ + 2SO_4^{2-} \Rightarrow \text{alunite}. \quad (19)$$

During stage II, alunite became the main sulphate-bearing mineral through the SO_4^{2-} bearing solution, which reacted with kaolinite and smectite (reactions (10) and (11)). Stage II alunite is normally enriched in Na relative to K as it is the case with alunite from low grade regionally metamorphosed rocks (Section 5). Plumbian alunite and hinsdalite–woodhouseite s.s.s. appear very early in sites where volcanic host rocks or mineralizations abundant in Pb were percolated through by hydrothermal solutions (e.g. Baguio, Desa Toraget).

P-bearing alunite appears rather late during formation of stage II as a consequence of coupled substitution of $(Ca, Sr)^{2+} + (PO_4)^{3-}$ for $K^+ + SO_4^{2-}$. This substitution in the alunite lattice heralds the passage from alunite into alunite woodhouseite–svanbergite s.s.s., which is secondmost in abundance relative to alunite minerals in stage II. It reflects a depletion of the aqueous solutions in sulphate. According to Stoffregen and Alpers (1987), only a few thermodynamical constraints can be placed upon the stability field of this sort of APS mineral s.s.s. Woodhouseite–svanbergite s.s.s. can coexist with alunite, kaolinite and muscovite (Fig. 4). This APS mineral s.s.s. becomes thereby the most typical s.s.s. among the APS minerals as far as the advanced argillic alteration is concerned.

The temperature of formation determined for the APS mineralization of stages I and II shows a very wide spread from 330°C determined for alunite associated with pyrophyllite and zunyite in alteration zones of hydrothermal magmatic mineralizations (Rodalquilar, Baguio, Cajamarca Province) down to temperatures of less than 60°C that were measured in steam-heated mineralizations at the rim of brine pools

Table 4
Minerostratigraphy and temperature of formation of APS mineral assemblages in volcanic and subvolcanic rocks: Rodalquilar, Spain (Arribas et al., 1995), Baguio District, Philippines (Aoki et al., 1993), Nansatsu-District, Japan (Hedenquist et al., 1994), Northern Sulawesi, Indonesia (Dill et al., 1995c), Western El Salvador (Dill et al., 2000), Cajamarca Province, Western Peru (Dill et al., 1997a), Illapel Province, Chile (Dill et al., 1995a). The mineral formulae are given in an abridged form showing only their major components

Stages	Interpretation	Rodalquilar, Spain	Baguio District, Philippines	Nansastu, District Japan	Northern Sulawesi, Indonesia	Western El Salvador		Cajamarca Province, Western Peru	Illapel Province, Central Chile
I	hypogene sulfate-phosphate	woodhouseite-svanbergite, crandallite – florencite (Ca, Sr, Ce) (SO_4, PO_4)	svanbergite-hinsdalite (Sr, Ba,Pb) (SO_4, PO_4)	woodhouseite s.s.s (Ca) (PO_4 >>SO_4,)		alunite- crandallite s.s.s. (Na >>K) (SO_4) - (Ca) (PO_4)			
	Temperatures of formation of stages I + II	***230 to 330°C***	***200 to 300 °C***	***approx. 230°C***	***< 60 °C***	***150° – 250 °C***		***< 325 °C***	***< 200 °C***
II	hypogene sulfate	Na-bearing alunite (Na>K)(SO_4)	minamiite-woodhouseite s.s.s (Ca>>K, Na) (SO_4) - (Ca) (SO_4, PO_4) Na-bearing alunite (Na>K)(SO_4)	alunite-woodhouseite s.s.s (K, Na) (SO_4) - (Ca) (SO_4, PO_4)	Pb-bearing alunite (Pb, K, Na)(SO_4) Pb-bearing alunite-woodhouseite s.s.s. (Pb, K, Na) (SO_4) - (Ca) (SO_4, PO_4)	alunite-woodhouseite s.s.s. (K, Na) (SO_4) - (Ca) (SO_4,PO_4)		alunite (Na>>K) (SO_4) svanbergite-woodhouseite s.s.s. (Sr,Ca) (SO_4,PO_4) P-bearing alunite (K)(PO_4 << SO_4)	woodhouseite-hinsdalite-alunite (Ca, Pb, K)(SO_4>>PO_4) K-bearing svanbergite-woodhouseite s.s.s. (K, Sr, Ca)(SO_4, PO_4)
III	hypogene-supergene transition	alunite (K > Na)(SO_4) svanbergite-woodhouseite s.s.s. (Sr,Ca) (SO_4,PO_4)			(aluminum sulfates + native sulfur)	aluminite+ alunogen Al_2 SO_4 $(OH)_4$ .7 H_2O Al_2 SO_3 $(OH)_3$ .17 H_2O	gorceixite + florencite Ba (PO_4) +Ce (PO_4)	REE-bearing woodhouseite- svanbergite-s.s.s. (Ce, Ca, Sr) (SO_4, PO_4) florencite-bearing crandallite-goyazite s.s.s. (Ce, Ca, Sr)(PO_4>>>SO_4) florencite-goyazite (Ce, Sr)(PO_4>>>SO_4)	K-REE-bearing woodhouseite- (K, Ce, Ca)(SO_4, PO_4) Ca-Sr-bearing gorceixite (Ca, Sr, Ba)(PO_4) Ca-Sr-bearing florencite (Ca, Sr, Ce)(PO_4>>>SO_4) crandallite-goyazite (Ca, Sr) (PO_4)
IV	supergene alteration	jarosite (K, Na) Fe (SO_4)			jarosite+dussertite (K, Na) Fe (SO_4) Ba Fe (PO_4)				

of active fumaroles (Desa Toraget) where alunite was precipitated together with AS and native sulphur.

During stage III, the pathway of APS mineralization ramifies. One branch of the mineralization becomes enriched in $(PO_4)^{3-}$ while being depleted in $(SO_4)^{2-}$ (e.g. western El Salvador). The other branch is characterised by $(SO_4)^{2-}$ as the only anion complex (e.g. western El Salvador, Rodalquilar, Desa Toraget). Alunite in Chilean porphyry copper deposits, which came into existence during supergene activity in the timespan ranging from 34 to 14 Ma and K-enriched alunite from Rodalquilar may be grouped into stage III (Arribas et al., 1995; Sillitoe and McKee, 1996).

At the edge of the Agua Shuca fumaroles, AS are being precipitated. A similar situation may also be observed in Northern Sulawesi, where AS minerals together with native sulphur may be encountered in outcrops adjacent to the Desa Toraget kaolin deposit. Alunogen and aluminite mirror a peculiar pathway of mineralization as compared to other APS mineralizations under study. The reactive fluids have been drastically depleted in phosphate, alkaline and earth alkaline elements under strongly oxidising conditions. Aluminium sulphate minerals can only form when the activity of H_2SO_4 is persistently high so that pedogenetic processes under whatever climate are impeded and no re-phosphatization can take place (see also Section 4.5). This is the case close to the vents of active or extinct fumaroles or where seasonal migration of phosphate is hampered by special climatic conditions such as under permafrost conditions (Apollonov et al., 1994). Many of the AS mineral assemblages recorded together with poorly crystallised alunite from coal seams belong to stage III mineralization reflecting the transition from the hypogene to the supergene APS mineralization (Dill and Pöllmann, 1999) (Section 3.4). The same holds true for that what was categorised by Ilchik (1990) in SHDG deposits as an APS mineralization caused at the verge of hydrothermal activity to a more intense form of weathering.

As a consequence of rephosphatisation, crandallite group minerals formed in stage III instead of woodhouseite–svanbergite s.s.s. that dominate at the end of stage II. Ba and REE are the most typical cations that occupy the A-site of formula $AB_3(XO_4)_2(OH)_6$. Experimental studies by Schwab et al. (1993) suggest that the stability field of crandallite becomes enlarged with falling temperature and that the structure of crandallite s.s.s. is stabilised by the incorporation of bivalent ions larger than Ca^{2+} such as Ba^{2+}, Sr^{2+} or trivalent cation such as Ce^{3+} (Fig. 9). The occurrence of gorceixite, goyazite and florencite in the crandallite s.s.s. of stage III is a direct response to falling temperature throughout APS mineralization and introduction of the above elements. The re-introduction of $(PO_4)^{3-}$ may plausibly be explained by admixing of phosphate derived from pedogenetic and weathering processes to hydrothermal solutions. The amount of $(PO_4)^{3-}$ in APS s.s.s. increases during waning phases of stage III and towards the present-day surface.

Trivalent Fe accommodated in the lattice of the APS mineral in stage IV may have derived from decomposition of Fe-sulphides and FeOOH. There is an antithetic trend between sulphides and APS minerals present in the Salvadorian kaolin deposits. San Isidro, which is barren as to APS minerals, contains pyrite instead. Apart from this decomposition of Fe disulphides, jarosite may have also result from goethite or lepidocrocite, which both are present in the Cerro Blanco and Agua Shuca kaolin deposits in El Salvador.

Judging by the log ΣSO_4 vs. pH diagram elaborated by Stoffregen (1987) when studying the superficial jarosite mineralization at Summitville, Colorado, jarosite–goethite mineral assemblages need a relatively high sulphur molality and a very low pH. Stage IV mineralization with jarosite prevailing over dussertite is fostered by fumarolic processes where aluminium sulphates dominate among the minerals of precursor stages.

7.4. Minerostratigraphic correlation of APS mineralization in sedimentary environments

The evolution of APS mineralization in sedimentary rocks is much more complex than in volcanic and subvolcanic rocks due to the variety of parent rocks that may undergo such supergene alteration and the diversity of climatic conditions (Table 5).

When the supergene alteration is still moderate, primary apatite gives way through secondary apatite to APS minerals. This intracrystalline conversion or

Table 5
Minerostratigraphy of APS mineral assemblages in sedimentary rocks and their correlation with equivalent alteration processes in volcanic and subvolcanic rocks and throughout mineral dressing Western Senegal (Flicoteaux, 1982), Lohrheim, Germany (Dill et al., 1991), Nuba Mts., Sudan (Dill et al., 1991), Coal Measures, Germany (Dill and Pöllmann, 1999), Trauira, Brazil (Schwab et al., 1996), Mitterberg, Austria (Spötl, 1990). The mineral formulae are given in an abridged form showing only their major components

Stages	Interpretation	Equivalent processes and alteration in igneous rocks and mineral dressing	Western Senegal	Lohrheim, Germany	Nuba Mts., Sudan	Coal Measures, Germany	Trauira, Brazil	Mitterberg, Austria
parent material			phosphorite, limestone, claystone	altered basic volcanics, limestones, bituminous shales	graphite schists, chert	lignitic to anthracitic coal	basic volcanics	fine- to coarse-grained sandstone
transition zone			apatite recrystallization	secondary apatite in limestones	apatite recrystallization			
Ia	aluminium-phosphate-sulfate mineralization	advanced argillic alteration/ alum production			crandallite Ca Al (PO_4>> SO_4)	Na-alunite, (Na >K) (SO_4) -		crandallite-svanbergite-goyazite s.s.s. (Sr>Ca) (SO_4,PO_4)
Ib		supergene alteration	Ca-millisite (Ca>Na, K) Al (PO_4)	gorceixite, Ce Al (PO_4) florencite Ba Al (PO_4)				svanbergite-woodhouseite s.s.s. (Ca>Sr) (SO_4,PO_4)
IIa	aluminium-phosphate-mineralization						wardite Na Al (PO_4)	
IIb			crandallite, Ca Al (PO_4) wavellite Al (PO_4)	goyazite Sr Al (PO_4)	wavellite, variscite, Al (PO_4)		wavellite, Al (PO_4) crandallite, Ca Al (PO_4) wardite Na Al (PO_4)	
III	gossan mineralization	supergene alteration and acid mine drainage	Fe –millisite (Ca, Na, K) Fe Al (PO_4)		faustite (Zn turquoise (Zn, Cu) Al (PO_4)	Fe oxide sulfates Fe (SO_4) .x H_2O		

recrystallization mirrors a gradual adjustment of the primary phosphates to the changing near ambient conditions. This transitional stage is similar to stage I illustrated in Table 4. The alteration works, however, in the volcanic environment much faster than in the sedimentary environments so that APS minerals appear much earlier whereas apatite only survives as some kind of ghost structures in the nuclei of the first-stage APS minerals (Table 4). The meteoric waters, which during pre-stage triggered intracrystalline processes in apatite, are neutral to moderately alkaline and to not allow for the precipitation of APS minerals. In the S-rich Coal Measures, such a pre-stage is missing since acidic conditions are sustained throughout most of the time of coalification (see Sections 3.4 and 3.5).

Sulphates play a minor part during formation of APS minerals in sedimentary rocks (stage Ia). They occur only in those parent rocks that have a high total sulphur content such as coal, biolites and some fine-grained clastic rocks (Table 5). On the other hand, based on the elevated contents of sulphate in these sedimentary environments, one cannot rule out that hydrothermal solutions have caused alteration of the pre-existing rock-forming minerals. This can be proven only by isotope studies, which are often hampered by the disseminated nature of this sort of mineralization. Under semiarid conditions, most of the rocks under consideration directly convert into the common APS minerals enriched in Ca, Na, REE, Ba and Sr (Stage Ib). In those sites where a more detailed study into the variation of APS minerals in

space and time has been performed, a second stage may be observed that is characterised by aluminium phosphates (AP) mainly wavellite and variscite. The predominance of AP over APS in saprolites (Section 3.6) and argillaceous sediments (Section 3.3) is controlled by the chemical composition of the source rock that is dominated by Al and P contents exceeding those of S. The most recent stage overlying stage II is called herein "gossan stage" (stage III). It contains mostly Fe-bearing APS and AS minerals together with some exotic members that are common also to gossans atop of ore deposits of various type. Scott (1987a,b) has given a summary of the complete s.s.s. of APS minerals in the gossan overlying the Pb–Zn mineralization of Mount Isa, NW Queensland. It is prevalently minerals enriched in Fe and sulphate such as Fe jarosite–alunite minerals, which are particularly good accumulators of Ag, Pb, Ba, Sb, PO_4 and SO_4. These minerals are associated with APS minerals such as hinsdalite, plumbogummite and florencite–crandallite.

Minerals found in stages I a and III are the natural equivalence of those chemical compounds that were brought about during former alum production or may precipitate from solution of acid mine drainage (Tilley and Gunter, 1988; Böttcher, 1997; Eary, 1999).

7.5. Climatic conditions and the age of formation of supergene APS mineralization

The APS minerals in the near-surface part of phosphorite-bearing series (e.g. western Senegal) evolve independent of topography. Their presence is exclusively controlled by the availability of water during rainfall and the leaching of groundwater. These conditions are well developed during the wet seasons of semiarid and tropical climates. The Quaternary Sudanese APS mineralization formed during pervasive weathering under semi-arid climatic conditions. The APS-bearing bauxites mentioned herein were emplaced mostly under subtropical to tropical climates.

The climatic conditions favourable to bring about APS minerals are best developed close to the present-day equator. The climatic zone is terminated by the northern and southern tropic. Several geochronological data of supergene APS mineralization have been obtained from K/Ar and Ar/Ar dating as well as U disequilibrium analyses (Dill et al., 1991; Andrew et al., 1992; Arehart et al., 1992; Vasconcelos et al., 1994; Sillitoe and McKee, 1996). The more distant from the present-day equator the APS mineralization is located, the older is its age of formation.

Fig. 22. Cartoon to demonstrate the relationship between APS minerals in metamorphic, igneous and sedimentary rocks and APS concentration in waste dumps and during alum production. Stippled bold face line = pyrophyllite isograde, stippled thin line = water table/sea level. The numbers in the cartoon refer to the various case histories discussed in text.

3. SEDIMENTARY ROCKS
   - 3.1 APS minerals in calcareous environments
   - 3.2 APS minerals in phosphorite-bearing environments
   - 3.3 APS minerals in argillaceous–carbonaceous environments
   - 3.4 APS minerals in coal-bearing environments
   - 3.5 APS minerals in soils and paleosols
   - 3.6 APS minerals in saprolite
   - 3.7 APS minerals in arenaceous environments
   - 3.8 APS minerals in calcareous–argillaceous sequences hosting Carlin-type SHDG deposits
4. IGNEOUS ROCKS
   - 4.1 APS minerals in slightly altered barren volcanic and subvolcanic rocks
   - 4.2 APS minerals in porphyry-type and epithermal Au–Ag-base metal deposits
   - 4.3 APS minerals in volcanic-hosted epithermal Au–Sb deposits
   - 4.4 Volcanic-hosted alunite deposits
   - 4.5 Volcanic-hosted APS-bearing argillite deposits
   - 4.6 APS mineralization in granitic and pegmatitic rocks
5. Metamorphic rocks
6. Manmade APS concentration—acid mine drainage vs. alum production

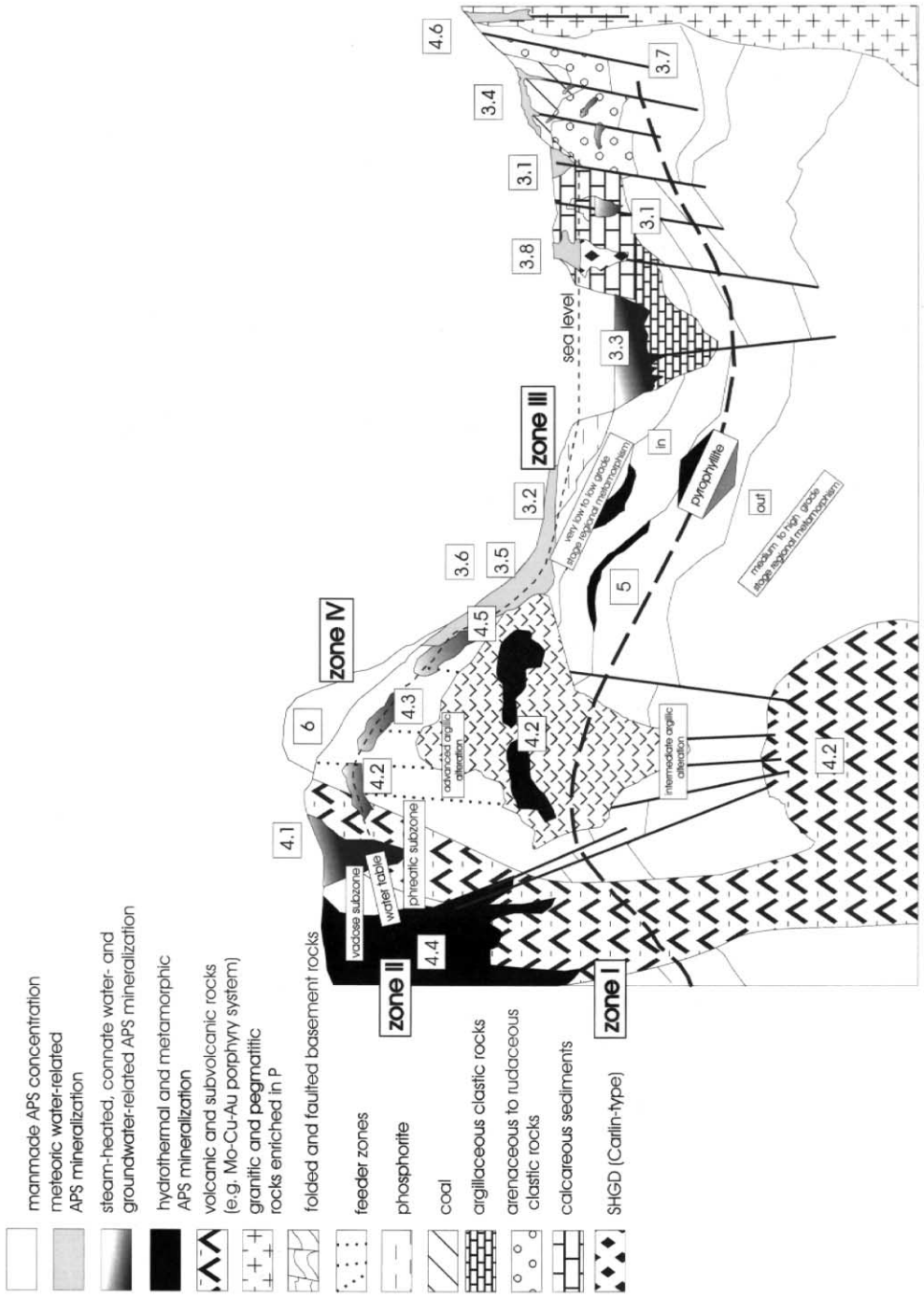
manmade APS concentration
meteoric water-related APS mineralization
steam-heated, connate water- and groundwater-related APS mineralization
hydrothermal and metamorphic APS mineralization
volcanic and subvolcanic rocks (e.g. Mo-Cu-Au porphyry system)
granitic and pegmatitic rocks enriched in P
folded and faulted basement rocks
feeder zones
phosphorite
coal
argillaceous clastic rocks
arenaceous to rudaceous clastic rocks
calcareous sediments
SHGD (Carlin-type)
zone I
zone II
zone III
zone IV
vadose subzone
water table
phreatic subzone
advanced argillic alteration
intermediate argillic alteration
sea level
pyrophyllite
in
out
very low to low grade stage regional metamorphism
medium to high grade stage regional metamorphism
4.1
4.2
4.3
4.4
4.5
4.6
3.1
3.2
3.3
3.4
3.5
3.6
3.7
3.8
5
6

Supergene alunite from Chile fall in the timespan early Oligocene to middle Miocene (Sillitoe and McKee, 1996). From the late Oligocene through the late Miocene, alunite formed in western USA (Arehart et al., 1992; Vasconcelos et al., 1994). In Australia and the Sudan, APS mineralization was emplaced during the Pli-Pleistocene and the Quaternary, respectively (Andrew et al., 1992; Dill et al., 1991). From the late Oligocene through the late Miocene, climatic conditions were conducive to a world-wide development of deep weathering sequences in a climate zone covering that what today is called the subtropical zone. During the recent geological past, this zone has moved closer towards the present-day equator where currently APS mineralization is still being formed and the most extensive weathering is recorded from deep-seated saprolite and laterite profiles.

8. Synopsis—overview of APS mineralization in geology

APS mineralization in the upper part of the earth crust may be subdivided into four zones that are correlative with distinct hydrological levels (Fig. 22). Zone I is characterised by hydrothermal and metamorphic fluids. Na-enriched alunite is stable in regionally metamorphosed peraluminous rocks abundant in phosphate and sulphate in the low grade stage (Winkler, 1976; Shelley, 1993) (Fig. 22, 5). The isograde pyrophyllite-in/out terminates the stability field of APS minerals towards higher temperatures (Winkler, 1976). The coexistence of APS minerals and Al_2SiO_5 modifications such as kyanite in metamorphic rocks attests to retrograde overprinting and furnish evidence of disequilibrium conditions. The pyrophyllite-in/out isograde may be traced through to the field of volcanic and subvolcanic APS mineralization where the isograde is correlative with the boundary between intermediate argillic and advanced argillic alteration. During advanced argillic alteration, magmatic hydrothermal high-sulfidation-type Cu–Au–Ag mineralization (Fig. 22, 4.2) comes into being and replacement and vein-type alunite deposits (Fig. 22, 4.4) are emplaced both reflecting the "smoking guns" of deep-seated Mo–Cu–Au porphyry systems (Fig. 22, 4.2). Stages I and II mineralization is characterised by Na-enriched alunites coexisting, which various other APS minerals (Table 4).

Vertically upward in the earth crust, the water table separating the phreatic from the vadose hydraulic zone is another boundary that separates APS mineralization of different origin. Steam-heated acid sulphate or high sulphidation-type precious and base metal deposits (Fig. 22, 4.2), Au–Sb mineralization (Fig. 22, 4.3) and argillaceous deposits producing mainly kandite- and smectite-group phyllosilicates (Fig. 22, 4.5) formed close to the ground water table in geothermal systems. Only part of the APS mineralization studied in samples taken from crater lakes may be attributed to the APS mineralization of zone II (Fig. 22, 4.1). The off-shore crater lake or near-vent phases formed at more elevated temperatures and have brought about minerals such as pyrophyllite common to the stage of argillic alteration or low grade regional metamorphism. Proximal-vent or onshore facies APS mineralization are characterised by minerals of lower temperatures and the occurrence of microorganisms such as *Thiobacillus* sp. (Suzuki and Takeuchi, 1992; Leduc and Ferroni, 1994).

In the sedimentary realm, the boundary between both hydraulic stockworks the phreatic zone of saturation and the vadose zone of aeration is a significant base level for APS mineralization. Perched water tables and connate/formation waters are of control of APS mineralization in karst cavities (Fig. 22, 3.1), disseminated in arenaceous (Fig. 22, 3.7), argillaceous (Fig. 22, 3.3) and coal-bearing series (Fig. 22, 3.4) that were brought about by hot sulphuric brines. Microorganisms are likely to have a mediating effect on the aforementioned sediment-hosted APS mineralization as it is the case with *Thiobacillus* sp. in geothermal fields (Fig. 22, 4.1) directly related to volcanic activity.

Supergene alteration of the mineralization mentioned above, weathering of phosphorite deposits (Fig. 22, 3.2), APS minerals in soils, paleosols (Fig. 22, 3.5) and the various types of saprolite (Fig. 22, 3.6) are confined to the topmost section of the vadose hydraulic or infiltration zone. This sort of APS mineralization has been derived from pure per-descensum processes and is related to meteoric waters. APS mineralization in cavities and solution pipes (Fig. 22, 3.1), the alteration of SHGD (Fig. 22, 3.8) and part of the APS mineralization encountered

in coal measures (Fig. 22, 3.4) also belongs to the zone III mineralization. The hydraulic conditions and last not least APS mineralization is governed by the existing climate or paleoclimate. The rare APS mineralization in phosphate-bearing peraluminous granites and pegmatites also form part of supergene zone III mineralization (Fig. 22, 4.6). Pressure and temperature during the later stages of plutonic processes are too high to allow for precipitation of APS minerals.

Results obtained from the study of supergene zone III APS mineralization may also form the basis of investigations concerned with the APS enrichment and the pathways of mobilisation in waste dumps, tailings, slag heaps and acid mine drainage or during the processing of alum shales—zone IV (Fig. 22, 6) (Tilley and Gunter, 1988; Böttcher, 1997; Eary, 1999).

The review outlines that APS mineralization is overall present in the topmost part of the earth crust provided their are no limitations as to the S, P and Al availability. APS minerals may bridge the gap between mineralization in nature (Fig. 22, 3, 4 and 5) and compounds obtained by man made processes (Fig. 22, 6).

Acknowledgements

I am indebted to U. Siewers and J. Lodziak who have performed chemical analyses (laboratories of the Federal Institute for Geosciences and Natural Resources, Hannover). H. Rösch and I. Meyer have contributed by XRD analyses to this study. Their assistance is kindly acknowledged. I am grateful for the support of K.-H. Henning, F. Kassbohm, (Greifswald University). Helpful comments concerning microbiology by K. Bosecker are kindly acknowledged. The manuscript benefitted from the suggestions made by A. Pring and another anonymous “Earth-Science Reviews” reviewer.

References

Abed, A.M., Kraishan, G.M., 1991. Evidence for shallow marine origin of a Monterey-Formation-Type chert phosphorite dolomite sequence: Amman Formation (Late Cretaceous) central Jordan. Facies 24, 25–38.

Ahlfeld, F., 1974. Neue Beobachtungen über die Tektonik und die Antimonitlagerstätten Boliviens. Mineralium Deposita 9, 125–131.

Andrew, A.S., Morrison, G.W., Whiford, D.J., Bird, M.I., Scott, K.M., 1992. Origin of alunite- and jarosite-group minerals in the Mt. Leyshon epithermal gold deposit, Northeast Queensland, Australia (discussion and reply). American Mineralogist 77, 857–862.

Aoki, M., Comsti, E.C., Lazo, F.B., 1993. Advanced argillic alteration and geochemistry of alunite in an evolving hydrothermal system at Baguio, Northern Luzon, Philippines. Resource Geology 43, 155–164.

Apollonov, V.N., Dolinina, Yu.V., Ogorodova, L.P., Sokolov, V.N., Shlykov, V.G., 1994. Aluminite from the oxidation zone of low-sulphide silver deposit. Moscow University Geological Bulletin 49, 55–58.

Arehart, G.B., 1996. Characteristics and origin of sediment-hosted disseminated gold deposits: a review. Ore Geology Reviews 11, 383–403.

Arehart, G.B., Kesler, S.E., O’Neil, J.R., Foland, K.A., 1992. Evidence for the supergene origin of alunite in sediment-hosted micron gold deposits, Nevada. Economic Geology 87, 263–270.

Arribas Jr., A., Cunningham, C.G., Rytuba, J.J., Rye, R.O., Kelly, W.C., Podwysocki, M.H., McKee, E.H., Tosdal, R.M., 1995. Geology, geochronology, fluid inclusions and isotope geochemistry of the Rodalquilar gold alunite deposit, Spain. Economic Geology 90, 795–822.

Banfield, J.F., Eggelton, R.A., 1989. Apatite replacement and rare earth mobilization, fractionation and fixation during weathering. Clays and Clay Minerals 37, 113–127.

Barth-Wirsching, U., Ehn, R., Höller, H., Klammer, D., Sitte, W., 1990. Studies of hydrothermal alteration by acid solutions dominated by SO_4^{2-}: formation of the alteration products of the Gleichenberg latitic rock (Styria, Austria)—experimental evidence. Mineralogy and Petrology 41, 81–103.

Berger, B.R., Hemley, R.W., 1989. Advances in the understanding of epithermal gold–silver deposits, with special reference to the western United States. Economic Geology Monograph 6, 405–423.

Berman, R.G., 1988. Internally consistent thermodynamic data for stoichiometric minerals in the system Na_2O-K_2O-CaO-MgO-FeO-Fe_2O_3-Al_2O_3-SiO_2-TiO_2-H_2O-CO_2. Journal of Petrology 29, 445–522.

Bernhard, F., Hoinkes, G., Mogessie, A., Postl, W., Taucher, J., 1996. Phosphate parageneses in the “Semmeringquarzit” and related quartz veins of the lower Austroalpine “Fischbach” window, north-eastern Styria, Austria. Mitteilungen der Oesterreichischen Mineralogischen Gesellschaft 141, 66–67.

Birch, D.W.D., Pring, A., Gatehouse, B.M., 1992. Segnitite $PbFe_3H(AsO_4)_2(OH)_6$, a new mineral in the lusungite group from Broken Hill, New South Wales, Australia. American Mineralogist 77, 656–659.

Bird, M.I., Chivas, A.R., McDougall, I., 1990. An isotope study of surficial alunite in Australia: 2. Potassium–argon geochronolgy. Chemical Geology 80, 133–145.

Birger, R., Buick, R., Taylor, W.R., 1998. Removal of oceanic

REE by authigenic precipitation of phosphatic minerals. Earth and Planetary Science Letters 164 (1–2), 135–149.
Bjorkum, P.A., Walderhaug, O., 1993. A model for the effect of illitization on porosity and quartz cementation of sandstones. Journal of Sedimentary Petrology 63, 1089–1091.
Bohor, B.F., Triplehorn, D.M., 1993. Tonsteins: altered volcanic-ash layers in coal-bearing sequences. Special Paper-Geological Society of America 285, 1–5.
Bosecker, K., 1997. Bioleaching: metal solubilization by microorganisms. FEMS Microbiology Reviews 20, 591–604.
Böttcher, H.-J., 1997. Alaun- und Vitriolwerke in der Dübener Heide. Anschnitt 3, 73–81.
Boujo, A., 1976. Contribution à l'étude du gisement de phosphate Crétace'-Eocène des Ganntour (Maroc Occidental). Sciences Geologiques, Memoire 43, 227.
Bove, D.J., Honn, K., 1990. Compositional changes induced by hydrothermal alteration at the Red Mountain alunite deposit. U.S. Geological Survey Bulletin 1936, 1–21.
Brinck, J.W., 1978. World resources of phosphorus. CIBA Foundation Symposium 57, Phosphorus in the Environment: Its Chemistry and Biochemistry. Elsevier, Amsterdam, pp. 23–48.
Cambel, B., Kantor, J., 1976. Comparison of isotope and geochemical investigations of sulphides from syngenetic pyrite deposits in the western Carpathians. In: Tugarinov, A.I. (Ed.), Recent Contributions to Geochemistry and Analytical Chemistry. Wiley, New York, pp. 424–437.
Chou, C.L., 1990. Geochemistry of sulphur in coal. In: Orr, W.L., White, C.M. (Eds.), Geochemistry of Sulphur in Fossil Fuels. Americ. Chem. Soc., Washington, pp. 30–52.
Columba, M.C., Cunningham, C.C., 1993. Geologic model for the mineral deposits of the La Joya District, Oruru, Bolivia. Economic Geology 88, 701–708.
Cooke, R., Warren, A., Goudie, A., 1993. Desert Geomorphology. UCL Press, London, 400 pp.
Cornejo, P., 1987. Hydrothermal alteration zones and sulphur deposits in upper cenozoic volcanoes of Salar de Gorbea, Andes of northern Chile. Pacific Rim Congress 87, 877–885.
Cortesogno, L., Gaggero, L., Lucchetti, G., 1987. Phosphate mineralizations in a Permo-Triassic sequence (Giogo di Toirano, Italy). N. Jb. Miner. Mh. Jg. 1987, 305–313.
Courchesne, F., Henderschot, W.H., 1990. The role of basic aluminum sulphate minerals incontrolling sulphate retention in the mineral horizons of two spodosols. Soil science 150, 571–578.
Cunningham, C.G., Rye, R.O., Steven, T.A., Mehnert, H.H., 1984. Origins and exploration significance of replacement and vein-type alunite deposits in the Marysvale volcanic field, West Central Utah. Economic Geology 79, 50–71.
Dill, H.G., 1986. Metallogenesis of the Early Paleozoic Graptolite Shales from the Graefenthal Horst. Economic Geology 81, 889–903.
Dill, H.G., 1996. Vulkanitgebundene Industriemineral-Vorkommen in der karpato-pannonischen Region (Nordungarn). Bergbau 47, 497–501.
Dill, H.G., 1998. A review of heavy minerals in clastic sediments with case studies from the alluvial-fan through the nearshore-marine environments. Earth Science Reviews 45, 103–132.
Dill, H.G., Horn, E.E., 1996. The origin of a hypogene sarabauite–calcite mineralization at the Lucky Hill Au–Sb mine Sarawak, Malaysia. Journal of Southeast Asian Earth Siences 14, 29–35.
Dill, H.G., Kantor, W., 1997. Depositional environment, geochemical facies, and a tentative classification system of selected types of phosphate occurrences. Geologisches Jahrbuch, Reihe D 105, 3–43.
Dill, H.G., Pöllmann, H., 1999. Phasenanalytische Untersuchungen des anorganischen Mineralbestandes von Kohlen verschiedener Inkohlungsgrade und Bildungsräume (Deutschland). Glückauf 60, 92–98.
Dill, H.G., Busch, K., Blum, N., 1991. Chemistry and origin of veinlike phosphate mineralization, Nuba Mts. (Sudan). Ore Geology Reviews 6, 9–24.
Dill, H.G., Fricke, A., Henning, K.-H., Theune, C.H., 1995a. An aluminium-phosphate mineralization from the hypogene La Vanguardia kaolin deposit (Chile). Clay Minerals 30, 249–256.
Dill, H.G., Fricke, A., Henning, K.-H., 1995b. The origin of Ba- and REE-bearing aluminium-phosphate–sulphate minerals from the Lohrheim kaolinitic clay deposit (Rheinisches Schiefergebirge, Germany). Applied Clay Science 10, 231–245.
Dill, H.G., Fricke, A., Henning, K.-H., Gebert, H., 1995c. An APS mineralization in the kaolin deposit Desa Toraget from northern Sulawesi/Indonesia. Journal of Southeast Asian Earth Siences 11, 289–293.
Dill, H.G., Weiser, T., Bernhardt, I.R., Riera Kilibarda, C., 1995d. The composite gold-antimony vein deposit at Kharma (Bolivia). Economic Geology 90, 51–66.
Dill, H.G., Bosse, H.-R., Henning, K.-H., Fricke, A., Ahrend, H., 1997a. Mineralogical and chemical variations in hypogene and supergene kaolin deposits in a mobile fold belt—the Central Andes of northwestern Peru. Mineralium Deposita 32, 149–163.
Dill, H.G., Pertold, Z., Riera Kilibarda, C., 1997b. Sediment-hosted and volcanic-hosted Sb vein mineralization in the Potosi region (Central Bolivia). Economic Geology 92, 623–632.
Dill, H.G., Bosse, H.-R., Kassbohm, J., 2000. Mineralogical and chemical studies of volcanic-related argillaceous industrial minerals of the Central American Cordillera (western El Salvador). Economic Geology 95, 517–538.
Eary, L.E., 1999. Geochemical and equilibrium trends in mine pit lakes. Applied Geochemistry 14 (8), 963–987.
Eberly, P.O., Ewing, R., Janeczek, J., Furlano, A., 1996. Clays at the natural nuclear reactor at Bangombe, Gabon migration of actinides. International Conference on Chemistry and Migration Behaviour of Actinides and Fission Products in the Geosphere, 10.09.95–15.09.95, Saint-Malo, France. pp. 271–275.
Ebert, S.W., Rye, R.O., 1997. Secondary pecious metal enrichment by steam-heated fluids in the Crofoot-Lewis Hot Spring Gold–Silver deposit and relation to paleoclimate. Economic Geology 92, 578–600.
Ek, R., Nysten, P., 1990. Phosphate mineralogy of the Håsjöberg and Hökensås kyanite deposits. Geologiska Foereningens i Stockholm Foerhandlingar 112, 9–18.

El Mountassir, M., 1977. La zone rubéfiée de Sidi Daoui, alteration météorique du phosphate de chaux des Ouled Abdoun (maroc). Thèse de 3èècycle, Univer. Louis Pasteur, Strasbourg, 126 pp.

Erikson, G.E., Cunningham, C.G., 1993. Epithermal precious-metal deposits hosted by the Neogene and Quaternary volcanic complex in the Central Andes. Geological Association of Canada Special Paper 40, 419–431.

Eskenazy, G.M., 1998. Aspects of the geochemistry of rare earth elements in coal: an experimental approach. International Journal of Coal Geology 38, 285–295.

Fisher, R.V., Schmincke, H.-U., 1984. Pyroclastic Rocks. Springer, Heidelberg, 472 pp.

Flicoteaux, R., 1982. Genese des phosphates alumineux du Senegal occidental, etapes et guides de l'alteration. Sciences Geologiques, Memoire 67, 1–249.

Flicoteaux, R., Lucas, J., 1984. Weathering of phosphate minerals. In: Nriagu, J.O., Moore, P.B. (Eds.), Phosphate Minerals. Springer, Berlin, pp. 292–317.

Föllmi, K.B., 1996. The phosphorus cycle, phosphogenesis and marine phosphate-rich deposits. Earth Science Reviews 40, 55–124.

Geijer, P., 1963. Genetic relationships of the paragenesis Al_2SiO_5-lazulite–rutile. Akiv Mineral Geology 3, 423–464.

Germann, H., Pagel, J.-M., Parekh, P.P., 1981. Eigenschaften und und Entstehung der Lahn-Phosphorite. Zeitschrift fuer Geologische Wissenschaften 25, 305–323.

Gilg, H.A., Frei, R., 1997. Isotope dating of residual kaolin deposits in Europe (Tirschenreuth, Germany and St. Yrieix, France). In: Rongfu, P. (Ed.), Energy and Mineral Resources for the 21th Century, Geology of Mineral Deposits, Mineral Economics. pp. 123–132, Utrecht.

Girault, J., 1980. Caractères Optiques des Minéraux Transparents-Tables de Détermination. Masson, Paris, 199 pp.

Goldbery, R., 1980. Early diagenetic, na alunites in Miocene algal mat intertidal facies, Ras Sudar, Sinai. Sedimentology 27, 189–198.

Golestaneh, F., Hakim, M., Newesely, H., 1988. Die Mineralparagenese der Kaolinvorkommen von Kabutar-Kuh, E-Iran. Fortschritte der Mineralogie, Beiheft 66, 42.

Goudie, A., Pye, K., 1983. Chemical Sediments and Geomorphology: Precipitates and Residual in the Near Surface Environment. Academic Press, London, 439 pp.

Haber, M., Jelen, S., Kovalenker, V., 1994. Modelling of the epithermal mineralization process at Bianska Stiavnica deposit, Western Carpathians (Slovak Republic). 9th Symposium of International Association on the Genesis of ore Deposits, Abstracts. pp. 581–582, Peking.

Hak, J., Johan, Z., Kvacek, M., Liebscher, W., 1969. Kemmlitzite a new mineral of the woodhouseite group. N. Jb. Mineral. Mh. 1969, 201–212.

Hayba, D.c., Foley, N.K., Heald-Wetlaufer, P., 1986. Characteristics that distinguis zypes of epithermal deposits. Journal of Geochemical Exploration 25, 231.

Heald, P., Foley, N.K., Hyaba, D.O., 1987. Comparative anatomy of volcanic-hosted epithermal deposits: acid-sulphate and adularia-sulphate types. Economic Geology 82, 11–26.

Hedenquist, J.W., 1987. Mineralization associated with volcanic-related hydrothermal systems in the circum-Pacific basin. Circum-Pacific Energy and Mineral Resources Conference, 4th Singapore Trans. pp. 513–524.

Hedenquist, J.W., Lowenstein, J.B., 1994. The role of magmas in the formation of hydrothermal ore deposits. Nature 370, 519–526.

Hedenquist, J.W., Matsuhisa, Y., Izawa, E., White, N.C., Giggenbach, W.F., Aoki, M., 1994. Geology, geochemistry, and origin of high sulphidation Cu–Au mineralization in the Nansatsu District, Japan. Economic Geology 89, 1–30.

Herold, H., 1987. Zur Kristallchemie und Thermodynamik der Phosphate und Arsenate vom Crandallit-Typ. PhD Thesis Erlangen University, 109 pp.

Holland, H.D., 1965. Some applications of thermochemical data to problems of ore deposits: II. Mineral assemblages and the composition of ore-forming fluids. Economic Geology 60, 1101–1166.

Hyen Goo Cho, Soo Jin Kim, 1993. Oscillatory zoning in alunite from the Sungsan mine, Korea. Neues Jahrbuch fuer Mineralogie, Monatshefte, 185–192.

Ilchik, R.P., 1990. Geology and geochemistry of the Vantage gold deposits, Alligator Ridge-Bald Mountain Mining District, Nevada. Economic Geology 85, 50–75.

Jambor, J.L., 1999. Nomenclature of the alunite supergroup. Canadian Mineralogist 37, 1323–1341.

Janeczek, J., Ewing, R., 1996. Florencite-(La) with fissiogenic REEs from a natural fission reactor at Bangombe, Gabon. American Mineralogist 81, 1263–1269.

Kanazirski, M., Velinov, I., Nokov, S., Serafimovski, T., Sandev, B., Queralt, I., 1998. Acid-sulphate alteration of the Opalite mine at Spancevo deposits, Republic of Macedonia. Geochimija, Mineralogija i Petrologija 33, 49–60.

Kassbohm, J., Henning, K.-H., Herbert, H.-J., 1998. Transmissionselektronenmikroskopische Untersuchung am Bentonit MX80. In: Henning, K.-H., Kassbohm, J. (Eds.), Beiträge zur Jahrestagung Greifswald, DTTG, 1998, vol. 6, pp. 228–236.

Kato, T., Radoslovich, E.W., 1968. Crystal structure of soil phosphates. Transactions of the 9th International Congress of Soil Science, Adelaide 2, 725–731.

Kavalieris, I., von Leeuwn, T.M., Wilson, M., 1992. Geological setting and styles of mineralization, north arm of Sulawesi, Indonesia. Journal of SE Asian Earth Sciences 7, 113–129.

Khalaf, F.I., 1990. Diagenetic alunite in clastic sequences, Kuwait, Arabian Gulf. Sedimentology 37, 155–164.

Khoury, H.N., 1987. Alunite from Jordan. N. Jb. Miner. Mh. 1987, 426–432.

Leduc, L.G., Ferroni, G.D., 1994. The chemolithotrophic bacterium *Thiobacillus ferrooxidans*. FEMS Microbiology Reviews 14, 103–120.

Leoni, L., Sartori, F., 1988. Le mineralizzazioni ad alunite e caolino della conca di Frasine (Grosseto, Italia Centrale). Atti della Società Toscana di Scienze Naturali residente in Pisa, Memorie 95, 35–49.

Li, G., Peacor, D.R., Essene, E.J., Broshahan, D.R., Beane, R.E., 1992. Waltherite $Ba_{0.5}[\ ]_{0.5}Al_3(SO_4)_2(OH)_6$ and huangite $Ca_{0.5}[\ ]_{0.5}Al_3(SO_4)_2(OH)_6$ two new minerals of the alunite

group from the Coquimbo region, Chile. American Mineralogist 77, 1275–1278.
Lindsay, W.L., 1979. Chamical Equilibria in Soils. Wiley, New York, NY, 449 pp.
London, D., 1992. Phosphorus in S-type magmas: the P_2O_5 content of feldspar from granites, pegmatites and rhyolites. American Mineralogist 77, 126–145.
Love, D.A., Clark, A.H., Hodgon, C.J., Mortensen, J.K., Archibald, D.A., Farrar, E., 1998. The timing of adularia-sericite-type mineralization and alunite–kaolinite-type alteration, Mount Skukum epithermal gold deposit, Yuikon Territory, Canada, $^{40}Ar/^{39}Ar$ and U–Pb geochronology. Economic Geology 93, 437–462.
Lucas, J., Prevot, L., Ataman, G., Gündogu, N., 1980a. Mineralogical and geochemical studies of the phosphate formations in southeastern Turkey (Mazidagi-Mardin). SEPM Special Publication 29, 148–152.
Lucas, J., Flicoteaux, R., Yaacov, N., Prévot, L., Yacoov, S., 1980b. Different aspects of phosphorite weathering. SEPM Special Publication 29, 41–51.
Maksimovic, Z., Panto, G.Y., 1995. Authigenic rare earth minerals in karstic bauxites and karstic nickel deposits. Romanian Journal of mineralogy 77, 26.
Marcopoulos, T., Katerinopoulos, A., 1986. Die Alunit-Vorkommen von Milos (Griechenland): Mineralbestand und Genese. Chemie der Erde 45, 105–112.
Mátyás, E., 1974. Volcanic and postvolcanic processes in the Tokaj Mountains on the basis of geological data of raw material prospecting. Acta Geologica Hungarica 18, 421–455.
Meireles, C., Ferreira, N., De-Lourdes-Reis, M., 1987. Varsicite occurrence in Silurian formations from Northern Portugal. Comuniccoes dos Servicos Geologicos de Portugal 16, 455–464.
Meldrum, S.J., Aquino, R.S., Gonzales, R.I., Burke, R.J., Suyadi, A., Irianto, B., Clarke, D.S., 1994. The Batu Hijau porphyry copper–gold deposit, Sumbawa Island, Indonesia. Journal of Geochemical Exploration 50 (1–3), 203–220.
Meyer, R., Pena dos Reis, R.B., 1985. Paleosols and alunite silcretes in continental Cenozoic series of western Portugal. Journal of Sedimentary Petrology 55, 76–85.
Michel, F.A., Van Everding, R.O., 1987. Formation of a jarosite deposit on Cretaceous shales in the Fort Norman Area, Northwest Territories. Canadian Mineralogist 25, 221–226.
Mitchell, A.H.G., 1992. Andesitic arcs, epithermal gold and porphyry-type mineralization in the western Pacific and eastern Europe. Transactions of the Institution of Mining and Metallurgy, Section B: Applied Earth Science 101, B125–B138.
Mordberg, L.E., 1999. Geochemical evolution of a Devonian diaspore-crandallite–svanbergite-bearing weathering profile in the Middle Timan, Russia. Journal of Geochemical Exploration 66, 353–361.
Morrison, S.J., Parry, W.T., 1988. Age and formation conditions of alteration associated with a collapse structure, Temple Mountain uranium district, Utah. Bulletin of the Geological Society of America 100, 1069–1077.
Morteani, G., Ackermand, D., 1996. Aluminium phosphates in muscovite–kyanite metaquartzites from Passo di Vizze (Alto Adige, NE Italy). European Journal of Mineralogy 8, 853–869.
Mücke, A., 1991. Sekundäre Phosphatmineralien (Perloffit, Brasilianit, Mineralien der Kingsmountit-Gruppe) sowie Brochantit und die Zwieselit-Muschketoffit-Stilpnomelan-Pyrosmalith-Paragenese der 115-m-Sohle des Hagendorfer Pegmatits. Aufschluss 38, 5–28.
Mücke, A., Keck, E., Haase, J., 1990. Die genetisch Entwicklung des Pegmatits von Hagendorf-Süd/Oberpfalz. Aufschluss 41, 33–51.
Nagy, G., Ivancsics, J., 1995. Florencite from Sopron aera (W-Hungary) re-examined by EMPA. Romanian Journal of Mineralogy 77, 31–32.
Nordstrom, D.K., 1982. The effect of sulfate on aluminum concentrations in natural waters: some stability relations in the system $Al_2O_3–SO_3–H_2O$ at 298 K. Geochimica et Cosmochimica Acta 46, 681–692.
Nriagu, J.O., 1976. Phosphate-clay mineral relations in soils and sediments. Canadian Journal of Earth Science 13, 717–736.
Nriagu, J.O., Moore, P.B., 1984. Phosphate Minerals. Springer, Berlin, 442 pp.
Ossaka, J., Hirabayashi, J.-I., Okada, K., Kobayashi, R., 1982. Crystal structure of minamiite a new mineral of the alunite group. American Mineralogist 67, 114–119.
Ossaka, J., Otsuka, N., Hirabayashi, J.I., Okada, K., Soga, H., 1987. Synthesis of minamiite $Ca_{0.5}Al_3(SO_4)_2(OH)_6$. N. Jb. Miner. Mh. 1987, 49–63.
Pabst, A., 1947. Computations on svanbergite, woodhouseite and alunite. American Mineralogist 32, 16–30.
Palache, C., Berman, H., Frondel, C., 1951. Dana's System of Mineralogy, 2 vol. 7th edn. Wiley, New York, 831 pp.
Parron, C., Nahon, D., 1980. Red bed genesis by laterite weathering of glauconitic sediments. Journal of the Geological Society of London 137, 689–693.
Percival, T.J., Radtke, A.S., Bagby, W.C., 1990. Relationships among carbonate-replacement gold deposits, gold skarns, and intrusive rocks, Bau Mining district, Sarawak, Malaysia. Mining Geology 40, 1–16.
Percival, T.J., Radtke, A.S., Jankovic, S.R., Dickson, F.W., 1993. Gold mineralization of the Carlin-type in the Alšar district, SR Macedonia, Yugoslavia. Proceedings of the 8th Quadrennial IAGOD Symposium. Schweizerbart'sche Verlagsbuchhandlung, Stuttgart.
Perelló, J.A., 1994. Geology, porphyry Cu–Au, and epithermal Cu–Au–Ag mineralization of the Tombulilato district, North Sulawesi, Indonesia. Journal of Geochemical Exploration 50, 221–256.
Polyak, V.W.C., Guven, N., 1996. Alunite, natroalunite, and hydrated halloysite in Carlsbad Cavern. Clays and Clay Minerals 44, 843–850.
Polyak, V., McIntosh, W.C., Guven, N., Provencio, P., 1998. Age and origins of Carlsbad Cavern and related caves from $^{40}Ar/^{39}Ar$ alunite. Science 279, 1919–1922.
Pons, J.-C., Parrra, M., Ferragne, A., Latouche, C., 1989. Caracetristiques des argiles hydrothermales de la Martinique-Petites Antilles Francaises. Applied Clay Science 4, 307–325.

Pouba, Z., Ilavsky, I., 1986. Czechoslovakia. In: Institute of Mining and Metallurgy (Eds.), Mineral deposits of Europe, 3, Blackwell, London, pp. 117–173.

Pouliot, A., Hofmann, H.J., 1981. Florencite: first occurrence in Canada. Canadian Mineralogist 19, 535–540.

Pring, A., Birch, W.D., Dawe, J., Taylor, M., Deliens, M., Walenta, K., 1995. Kintoreite, $(PbFe_3(PO_4)_2(OH, H_2O)_6$ a new mineral of the jarosite–alunite family, and lusungite discredited. Mineralogical Magazine 59, 143–148.

Radoslovich, E.W., Slade, P.G., 1980. Pseudotrigonal symmetry and the structure of gorceixite. N. Jb. Miner. Mh. 1980, 157–170.

Raimbault, L., Peycelon, H., Blanc, P.-L., 1996. Characterization of near- to far-field ancient migrations around Oklo reaction zones (Gabon) using minerals as geochemical tracers. International Conference on Chemistry and Migration Behaviour of Actinides and Fission Products in the Geosphere, 10.09.95–15.09.95, Saint-Malo, France, pp. 283–287.

Rao, P.D., Walsh, D.E., 1997. Nature and distribution of phosphorus in Cook Inlet coals, Alaska. International Journal of Coal Geology 33, 19–42.

Rao, P.D., Walsh, D.E., 1999. Influence of environments of coal deposition on phosphorous accumulation in ahigh latitude, northern Alaska, coal seam. International Journal of Coal Geology 33, 19–42.

Rattray, K.J., Taylor, M.R., Bevan, D.J.M., Pring, A., 1996. Compositional segregation and solid solution in the lead-dominant alunite-type minerals from Broken Hill, N.S.W. Mineralogical Magazine 60, 779–785.

Reinink-Smith, L.M., 1990. Mineral assemblages of volcanic and detrital partings in tertiary coal beds, Kenai Peninsula, Alaska. Clay and Clay Minerals 38, 97–108.

Ripperda, M., Bodvarsson, G.S., Lippmann, M.J., Cuellar, G., Escobar, C., 1991. An exploration model and performance predictions for the Ahuachapán geothermal field, El Salvador. Geothermics 20, 181–196.

Rivano, G.S., Sepulveda, H.P., 1991. Carta Geologica de Chile Hoja Illapel—escala 1:250 000. Serv. Nac. de Geologia y Mineria, Santiago, 107 p.

Rojkovič, I., Konečŷ, P., Novotnŷ, L., Puškelová, L., Streško, V., 1999. Quartz-apatite-REE vein mineralization in early Paleozoic rocks of the Gemeric Superunit, Slovakia. Geologica Carpathica 50, 215–227.

Rosendahl, W., Krause, E.-B., 1996. Im Reich der Dunkelheit. Höhlen und Höhlenforschung in Deutschland. Edition Archaea, Gelsenkirchen, 159 pp.

Ruppert, H., 1980. Fixation of metals on hydrous manganese and iron oxide phase in marine Mn–Fe-nodules and sediments. Chemie der Erde 39, 97–132.

Rye, R.O., Stoffregen, R., 1995. Jarosite-water oxygen and hydrogen isotope fractionations: preliminary experimental data. Economic Geology 90, 2336–2342.

Rye, R.O., Bethke, P.M., Wasserman, M.D., 1992. The stable isotope geochemistry of acid sulphate alteration. Economic Geology 87, 225–262.

Rye, R.O., Bethke, P.M., Lanphere, M.A., Steven, T.A., 1993. Age and stable isotope systematics of supergene alunite and jarosite from the Creede mining district, Colorado: implications for supergene processes and Neogene geomorphic evolution and climate of the southern Rock Mountains (abs.). Geological Society of America Abstracts with Programs 25, A-274.

Scheffer, F., Schachtschabel, P., 1976. Lehrbuch der Bodenkunde. 9th edn. Enke, Stuttgart, 394 pp.

Schmetzer, K., Tremmel, G., Medenbach, O., 1982. Philippsbornit, $PbAl_3H[(OH)_6/(AsO_4)_2]$, aus Tsumeb, Namibia-ein zweites Vorkommen. N. Jb. Miner. Mh. 1982, 248–254.

Schreyer, W., 1987. Pre- and synmetamorphic metasomatism in peraluminous metamorphic rocks. Mathematical and Physical Science 218, 265–296.

Schwab, R.G., Götz, C., Herold, H., Pinto de Oliveira, P., 1993. Compounds of the crandallite type: thermodynamic properties of Ca-, Sr-, Ba-, Pb-, La-, Ce- to Gd-phosphate and arsenates. N. Jb. Miner. Mh. 1993, 551–568.

Schwab, R.G., Mohr, J., Pimpl, T.H., Schukow, H., 1996. About the fixation of alkali- and earth-alkali-elements in laterites. Geosciências 10, 89–112.

Scott, K.M., 1987a. Solid solution in, and classification of gossan-derived members of the alunite–jarosite family, Northwest Queensland, Australia. American Mineralogist 72, 178–187.

Scott, K.M., 1987b. The mineralogical distribution of pathfinder elements in gossans derived from dolomitic shale-hosted Pb–Zn deposits, Northwest Queensland, Australia. Chemical Geology 64, 295–306.

Scott, K.M., 1990. Origin of alunite- and jarosite-group minerals in the Mt. Leyshon epithermal gold deposit, Northeast Queensland. American Mineralogist 75, 1176–1181.

Seghal, J., 1998. Red and Lateritic Soils. Balkema, Rotterdam, 453 pp.

Sehnke, E.D., 1996. Refractory grade bauxite an overview. ICSOBA, 22.06.1992–26.06.1992, Balatonalmadi, pp. 66–73.

Shamshuddin, J., Auxtero, E.A., 1991. Soil solution compositions and mineralogy of some active acid sulphate soils in Malaysia as affected by laboratory incubation with lime. Soil Science 152, 365–376.

Shamshuddin, J., Jamilah, I., Ogunwale, J.A., 1995. Formation of hydroxy-sulphates from pyrite in coastal acid sulphate soil environments in Malaysia. Communications in Soil Science and Plant Analysis 26, 2769–2782.

Shelley, D., 1993. Igneous and Metamorphic Rocks under the Microscope; Classification, Textures, Microstructures and Mineral Preferred-Orientation. Chapman & Hall, London, 445 pp.

Sillitoe, R.H., 1991. Gold metallogeny of Chile—an indroduction. Economic Geology 86, 1187–1203.

Sillitoe, R., McKee, E.H., 1996. Age and supergene oxidation and enrichement in the Chilean porphyry copper province. Economic Geology 91, 164–179.

Slansky, M., 1980. Géologie des phosphates sedimentaires. Bureau de Recherches Geologiques et Minieres, Memoire 114, 1–92.

Slansky, M., 1986. Geology of Sedimentary Phosphates. Academy Press, London, 210 pp.

Spötl, C., 1990. Authigenic aluminium posphate–sulphates in sandstones of the Mitterberg Formation, Northern Calcareous Alps, Austria. Sedimentology 37, 837–840.

Stanislav, V.V., Yossifova, M.G., Vassileva, C.G., 1994. Mineralogy and geochemistry of Bobov Dol coals, Bulgaria. International Journal of Coal Geology 26, 185–214.

Stoffregen, R.E., 1987. Genesis of acid-sulphate alteration and Au–Cu–Ag mineralization at Summitville, Colorado. Economic Geology 82, 1575–1591.

Stoffregen, R.E., 1993. Stability relations of jarosite and natroalunite at 100–250°C. Geochimica et Cosmochimica Acta 58, 903–916.

Stoffregen, R.E., Alpers, C.N., 1987. Woodhouseite and svanbergite in hydrothermal ore deposits: products of apatite destruction during advanced argillic alteration. Canadian Mineralogist 25, 201–211.

Stoffregen, R.E., Rye, R.O., Wasserman, M.D., 1994. Experimental studies of alunite: I ^{18}O and D–H fractionation factors between alunite and water at 250–450°C. Geochimica et Cosmochimica Acta 58, 903–916.

Störr, M., Köster, H.M., Kromer, H., Hilz, M., 1991. Minerale der Crandallit-Reihe im Kaolin von Hirschau-Schnaittenbach, Oberpfalz. Zeitschrift fuer Geologische Wissenschaften 19, 677–683.

Strunz, H., 1970. Mineralogische Tabellen. Akademische Verlagsgesellschaft Geest and Portig K.-G., Leipzig.

Strunz, H., 1974. Granites and pegmatites in Eastern Bavaria. Fortschritte der Mineralogie 52, 1–32.

Strunz, H., Tennyson, C., 1982. Mineralogische Tabellen. Akademische Verlagsgesellschaft Geest and Portig, Leipzig, 621 pp.

Suzuki, I., Takeuchi, T.L., 1992. Oxidation of elemental sulphur to sulphite by *Thiobacillus thiooxidans* cells. Applied and Environmental Microbiology 58, 3767–3769.

Swaine, D.J., 1990. Trace Elements in Coal. Butterworth, London, 278 pp.

Switzer, G., 1949. Svanbergite from Nevada. American Mineralogist 34, 104–108.

Takano, B., Watanuki, K., 1990. Monitoring of volcanic eruptions at Yuguma crater lake by aqueous sulphur oxyanions. Journal of Volcanology and Geothermal Research 40, 71–87.

Tan, K., 1984. Andosols. Van Nostrand-Reinhold, New York, 418 pp.

Thompson, J.F.H., Abidin, H.Z., Both, R.A., Martosuroyo, S., Rafferty, W.J., Thompson, A.J.B., 1994. Alteration and epithermal mineralization in the Masupa Ria volcanic center, Central Kalimantan, Indonesia. Journal of Geochemical Exploration 50 (1–3), 429–455.

Tilley, B.J., Gunter, W.D., 1988. Mineralogy and Water Chemistry of the Burnt Zone from a wet combustion pilot in Alberta. Bulletin of Canadian Petroleum Geology 36, 25–38.

Tomita, K., Kawano, M., Kobayashi, T., 1994. Minerals in the volcanic ash erupted from Shin-dake in Kuchinoerabu Island in 1980. Report of the Faculty of Science, Kagoshima University. Earth Science and Biology 27, 1–10.

Trappe, J., 1991. Stratigraphy, facies distinction and paleogeography of the marine Paleogene from the western High Atlas, Morocco. Neues Jahrbuch fuer Geologie und Palaeontologie, Abhandlungen 180, 279–321.

Triplehorn, D.M., Bohor, B.F., 1983. Goyazite in kaolinite altered tuff beds of Cretaceous age near Denver, Colorado. Clays and Clay Minerals 31, 299–304.

Vieillard, P., Tardy, Y., Nahon, D., 1979. Stability fields of clays and alumium phosphates: parageneses in lateritic weathering of argillaceous phosphatic sediments. American Mineralogist 64, 626–634.

Van Breemen, N.J., 1972. Soil forming processes in acid-sulphate soils. In: Dost, H. (Ed.), Acid-Sulphate Soils. Elsevier, New York, pp. 66–130.

Van Breemen, H., 1993. Mineral reactions in acid-sulphate soils. Transactions of the 15th World Congress of Soil Science, July 10–16, 1994, Acapulco, Mexico, vol. 8a, pp. 15–16.

Vasconcelos, P.M., Brimhall, G.H., Becker, T.A., Renne, P.R., 1994. $^{40}Ar/^{39}Ar$ analysis of supergene jarosite and alunite; implications to the paleoweathering history of the wetsren USA and West Africa. Geochimica et Cosmochimica Acta 58, 401–420.

Velinov, I., Gorova, M., Tcholakov, P., Tchounev, D., Ianeva, I., 1983. Secondary quartzites developed after Cretaceous volcanics from Zaza Zone, Cuba. Geologica Balcanica 13, 53–68.

Vidal, C.C.E., 1987. Kuroko-type deposits in the Middle Cretaceous Marginal Basin of Central Peru. Economic Geology 82, 1409–1430.

Vikre, P.G., 1998. Quartz-alunite alteration in the western part of the Virginia Range, Washoe and Storey counties, Nevada. Economic Geology 93, 338–346.

Vila, T., Sillitoe, R.H., 1991. Gold-rich porphyry systems in the Maricunga Belt, Northern Chile. Economic Geology 86, 1238–1260.

Walenta, K., 1966. Beiträge zur Kenntnis seltener Arsenatminerale unter besonderer Berücksichtigung von Vorkommen des Schwarzwaldes. Tschermaks Mineralogische und Petrographische Mitteilungen 11, 121–164.

Walenta, K., 1981. Mineralien der Beudantit-Crandallitgruppe aus dem Schwarzwald: Arsenocrandallit und sulfatfreier Weilerit. Schweizerische Mineralogische und Petrographische Mitteilungen 61, 23–35.

Walter, A.-V., Nahon, D., Flicoteaux, R., Girard, J.P., Melfi, A., 1995. Behaviour of major and trace elements and fractionation of REE under tropical weathering of a typical apatite-rich carbonatite from Brazil. Earth and Planetary Science Letters 136 (3–4), 591–602.

Ward, C.R., 1978. Mineral matter in Australian bituminous coal. Proceedings of the Australian Institute of Mineralogy and Metallurgy 267, 7–25.

Wasserman, M.D., Rye, R.O., Bethke, P.M., Arribas, A., 1990. Methods for separation of alunite from associated minerals and subsequen analysis of D, $^{18}O_{OH}$, $^{18}OSO_4$ and ^{34}S. Geological Society of America, Abstract of Program 22, A135.

Weaver, C.E., 1989. Clays, Muds, and Shales. Elsevier, Amsterdam, 819 pp.

Wilson, J.A., 1985. Crandallite group minerals in the Helikian Athabsaca Group in Alberta, Canada. Canadian Journal of Earth Sciences 22, 637–641.

Winkler, H.G.F., 1976. Petrogenesis of Metamorphic Rocks. Springer, Heidelberg, 334 pp.

Wipki, M., German, K., Schwarz, T., 1993. Alunitic caolins of the Gedaref region (NE-Sudan). In: Thorweihe, U., Schandelmeier, H. (Eds.), Geoscientific Research in Northeast Africa. Balkema, Rotterdam, pp. 509–514.

Yasychenko, S.Yu., Repina, M.N., Sidorenko, G.A., Yudin, R.N., 1989. Alumophosphates in bauxites of the middle Timan. Lithology and Mineral Resources 23, 330–336.

Zohar, E., Moshkovitz, Z., 1984. A Campanian–Maastrichtian unconformity in the Arad Basin, NE Negev, Israel. Geological Survey of Israel Current Research 1983–1984, 56–59.